MOLECULAR SIGNALING MECHANISMS AT THE μ-OPIOID RECEPTOR

MOLEKULARE SIGNALMECHANISMEN AM μ-OPIOIDREZEPTOR

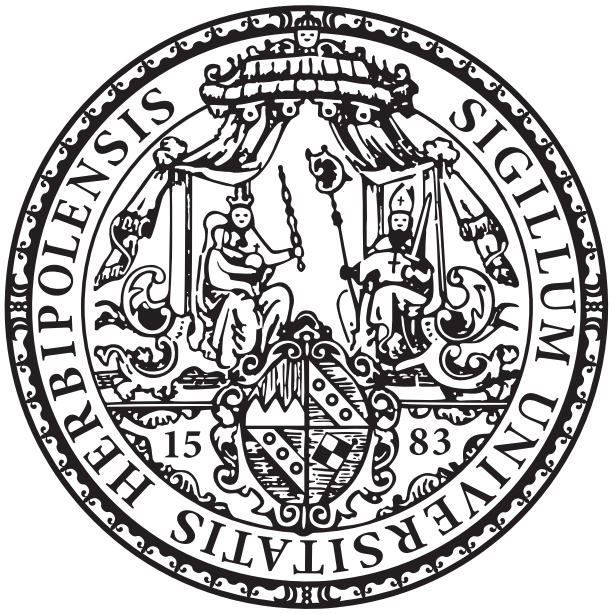

Doctoral Thesis for a Doctoral Degree at the Graduate School of Life Sciences

Julius-Maximilians-Universität Würzburg

Section Biomedicine

submitted by

DR. MED. BENEDIKT SCHMID

from

DACHAU

Würzburg 2018

MOLECULAR SIGNALING MECHANISMS AT THE μ-OPIOID RECEPTOR

MOLEKULARE SIGNALMECHANISMEN AM μ-OPIOIDREZEPTOR

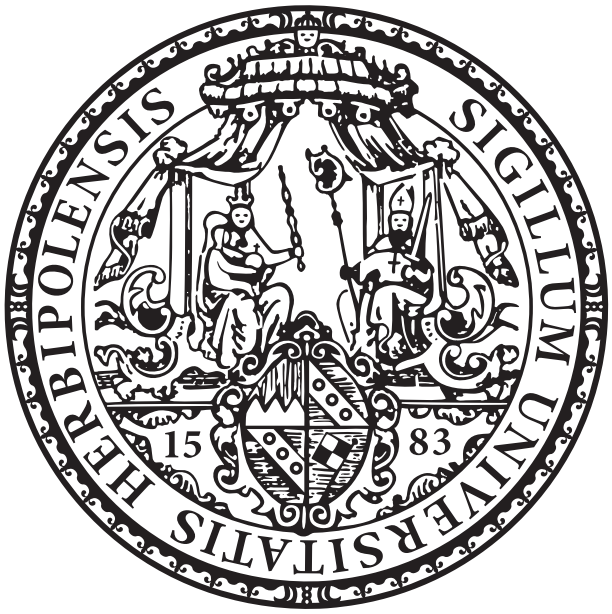

Doctoral Thesis for a Doctoral Degree at the Graduate School of Life Sciences

Julius-Maximilians-Universität Würzburg

Section Biomedicine

submitted by

DR. MED. BENEDIKT SCHMID

from

DACHAU

Würzburg 2018

Submitted on: September 30, 2018

MEMBERS OF THE COMMITTEE

Chairperson:	Prof. Matthias Gamer
Primary Supervisor:	Prof. Carsten Hoffmann
Supervisor (second):	Prof. Christoph Sotriffer
Supervisor (third):	Priv.-Doz. Elmarc-Marc Brede

Date of Public Defence:	February 14, 2019
Date of Receipt of Certificates:	.....

CONTENTS

LIST OF FIGURES

LIST OF TABLES

ACRONYMS

APS	ammonium persulfate
AT_{1A}-R	angiotensin II receptor type 1A
β_2-AR	β_2-adrenergic receptor
BRET	bioluminescence resonance energy transfer
BSA	bovine serum albumin
β-arr	β-arrestin
$CaCl_2$	calcium chloride
cAMP	cyclic adenosine monophosphate
CFP	cyan fluorescent protein
CI	confidence interval
CMV	cytomegalovirus
CO_2	carbon dioxide
DAMGO	[D-Ala^2, N-MePhe^4, Gly-ol]-enkephalin
DMEM	Dulbecco's modified Eagle's medium
DMSO	dimethyl sulfoxide
DNA	deoxyribonucleic acid
DPBS	Dulbecco's phosphate buffered saline
ECL	extracellular loop
EDTA	ethylenediaminetetraacetic acid
Eluc	enhanced click beetle luciferase
FCS	fetal calf serum
FRET	Förster resonance energy transfer
G418	Geneticin sulphate
GDP	guanosine diphosphate
GFP	green fluorescent protein
G_i	inhibitory G protein

GPCR	G protein-coupled receptor
GRK	G protein-coupled receptor kinase
GTP	guanosine triphosphate
[^{35}S]GTPγS	[^{35}S]guanosine-5′-O-(3-thio)triphosphate
H_2O	water
HCl	hydrogen chloride
HEK	human embryonic kidney
HEPES	4-(2-hydroxyethyl)-1-piperazineethanesulfonic acid
ICL	intracellular loop
KCl	potassium chloride
LAL	limulus amebocyte lysate
LB	lysogeny broth
LPS	lipopolysaccharide
M-6-G	morphine-6-glucuronide
$MgCl_2$	magnesium chloride
μ receptor	μ-opioid receptor (protein)
mTq2	modified Turquoise 2 fluorescent protein
NaCl	sodium chloride
NaN_3	sodium azide
NaOH	sodium hydroxide
$Na_4P_7O_2$	sodium pyrophosphate
Na_3VO_4	sodium orthovanadate
NMDA	N-methyl-D-aspartate
Nluc	NanoLuciferase
OPRM	μ-opioid receptor (gene)
PAMP	pathogen-associated molecular pattern
PCR	polymerase chain reaction
PEG	polyethylene glycol
PMSF	phenylmethylsulfonyl fluoride

SD	standard deviation
SDS	sodium dodecyl sulfate
SEAP	secreted embryonic alkaline phosphatase
SEM	standard error of the mean
T4	bacteriophage T4
TAE	Tris base, acetic acid, EDTA
Taq	Thermus aquaticus
TEMED	Tetramethylethylenediamine
TLR4	toll-like receptor 4
TM	transmembrane domain
Tris	Tris(hydroxymethyl)aminomethane
WHO	World Health Organization
YFP	yellow fluorescent protein

1 INTRODUCTION

> *"Et profecto non hic mihi tempero quin gratulabundus animadvertertam, DEUM Omnipotentem, ..., non aliud remedium quod vel pluribus malis debellandis par sit, vel eadem efficacius extirpet, humano generi in miseriarum solamen concessisse, quam sunt opiata [...]."*
>
> Thomas Sydenham (1624-1689) [1, p. 174]

1.1 OPIUM, OPIATES, AND OPIOIDS

TAXONOMY AND GENERAL PRINCIPLES Parts and products of the opium poppy (Papaver somniferum) have been used for many centuries as a remedy to cure all kinds of disorders. The exact point in time when it was first used as a drug and/or remedy is not entirely agreed upon, but literature suggests the use of opium in ancient times already [2]. As the opening quote shows, English doctor and scientist Thomas Sydenham in 1680 reflected on the importance of opiates approximately as follows:

"And indeed I shall not hesitate to complimentingly declare here that it pleased Almighty God to bestow upon mankind in its suffering a remedy unlike any other in its versatility and efficacy, and that is opium."

The dried latex from the opium poppy is referred to as opium. It contains a variety of alkaloids, of which morphine, codein, thebaine, papaverine, and noscapine are of the most pharmaceutical relevance [3]. The alkaloids are contained in the latex to various extents. They are used as drugs themselves or serve as the basis for further modified substances. The terminus *opiate* is not used uniformly in the literature. It can either refer only to alkaloids actually contained in natural opium (like the aforementioned) or also include semi-synthetic drugs, which are derived from the natural alkaloids [4]. *Opioids* is used as the generic term for all opiates or opiate-derived analgesic substances, including fully synthetic opioid drugs. This very basic classification is, among others, also used to categorize opioid drugs.

OPIOIDS IN THIS WORK The opioids used in this work group into the mentioned categories as follows (references to structural formulae in the appendix):

- *Opium alkaloids (figure 29)*
  Morphine is the one opium alkaloid used in this work. Although it can be chemically synthesized completely [5], it is usually extracted from the poppy plant for economic reasons. morphine-6-glucuronide (M-6-G) is is the main metabolite of morphine in the human organism.

- *Semi-synthetic alkaloid derivatives (figure 30)*
  - Buprenorphine is synthesized from the opium alkaloid thebaine [6]. It acts as a mixed partial agonist / antagonist at various opioid receptors. As such, it has nanomolar affinities for the μ, κ, δ, and nociceptin receptor, with intrisic activity only at the μ and nociceptin receptor [7].
  - Hydromorphone is synthesized from native morphine [8] and generally has similar properties as its parent substance.
  - Oxycodone is another thebaine derivative [9, 10] with confirmed μ-opioid receptor (μ receptor) and disputed κ receptor affinities [11].

- *Synthetic opioids*
  - *Anilidopiperidines (figure 31)*
    * Fentanyl is a high-affinity, high-potency μ receptor ligand [12]. Like several other neurotropic drugs, it was first synthesized by Paul Janssen [13].
    * Remifentanil is a high-affinity, highly potent, and ultra-short acting opioid analgesic [14]. It is distinct from all the others in so far as it is degraded by unspecific esterases rather rather than organ-specific metabolic systems.
    * Sufentanil [15] is the most potent opioid used in humans.
  - *Diphenylpropylamine derivatives (figure 32)*
    * Piritramide was first synthesized by Janssen [16] and is approved for use in patients only in certain European countries, including Germany.
    * Methadone is a potent μ receptor activator. It occurs in R- and S-enantiomeric form. The opioid analgesic effects are mostly attributed to R-methadone (Levomethadone), whereas the racemate is said to also show N-methyl-D-aspartate (NMDA) receptor activity [17].
  - *Phenylpiperidines (figure 33)*
    * Pethidine is also one of the early opioids [18], but in many countries including the U.S. is not in use anymore. This is due to its undesired effects, which are

mainly caused by the neurotoxic metabolite norpethidine [19].

– *Others* (chemically less similar to the other opioids, but with distinct μ receptor affinity, figure 34)
  * TILIDINE was described in 1970 by Herrmann et al. [20]. It is metabolized rapidly, therefore its effects are mainly mediated by (1S,2R)-tilidine (dextilidine) and metabolites thereof [21]. Tilidine is used medically only in a few countries, including Germany, where it comes as a fixed combination with the μ receptor antagonist naloxone.
  * TRAMADOL is a μ receptor agonist [22], but also acts on various other receptors/neurotransmitter systems: serotonin release and reuptake inhibition [23, 24], norepinephrine reuptake inhibition [25], NMDA antagonism [26], and more. Tramadol is used as a racemate of the (1R,2R)- and (1S,2S)-isomers, since it turned out to be more effective in humans than either enantiomer alone [27].
  * TAPENTADOL has been developed only recently and, like Tramadol, has norepinephrine reuptake inhibition properities in addition to being an opioid analgesic [28].

- *Synthetic peptides (figure 35)* All the endogenous ligands of opioid recpetors are peptides. [D-ALA^2, N-MEPHE^4, GLY-OL]-ENKEPHALIN (DAMGO) is a synthetic, μ receptor-specific peptide agonist [29]. It is widely used as a reference compound in the literature.

EFFECTS AND UNDESIRED SIDE-EFFECTS Opioids to this day still represent the gold standard in the treatment of mild to severe cancer pain [32, 33]. Morphine, methadone, and codeine are in the WHO's Model List of Essential Medicines [34]. In a clinical context, opioids are often characterized as weak or strong opioids, with a relative observed potency normalized to the morphine effect. Also, pharmacokinetics of opioids differ substantially and need to be taken into consideration. The opioids used in this work range from relative potencies of $^1/_{10}$ (tramadol, tapentadol) to $\sim$1,000 (sufentanil) [35] (for details, see table 1). The indication for the use of opioids in pain other than tumor-related is rather weak. Some authors doubt the usefulness of opioids in non-cancer pain [36–38]. Eventually, a recent Cochrane review found opioids to be effective also in non-cancer pain patients [39].

Much of the concern with the broad usage of opioids originates from their wide range of undesired side-effects. First and foremost,

OPIOID	RELATIVE POTENCY
DAMGO	n/a (synthetic peptide)
Buprenorphine	25
Fentanyl	100
Hydromorphone	5
Methadone	1
Morphine	1
M-6-G	n/a (no approved drug)
Naloxone	n/a (antagonist)
Naltrexone	n/a (antagonist)
Oxycodone	1
Pethidine	0.1
Piritramide	0.7
Remifentanil	300
Sufentanil	1,000
Tapentadol [30]	0.33-0.5*
Tilidine	0.1
Tramadol	0.1

Table 1: Clinical potencies of opioids used in this work relative to morphine. Adapted from Graefe et al. [31]. * Data from animal testing; no data from randomized clinical trials available.

tolerance to the analgesic effects is often observed in patients and leads to dose escalation which in turn can cause additional undesired effects to occur [40]. Among those are sedation, dizziness, nausea, vomiting, constipation, physical dependence, tolerance, and respiratory depression [41]. Respiratory depression certainly poses the most severe threat to patients and, although it is relatively rare, it can be treatment-limiting [42]. Yet still, in 2007 unintentional lethal opioid overdoses were estimated at nearly 12,000 in the United States [43]. Constipation occurs markedly more often and has substantial influence on quality of life [44]. As such, obstipation is a major reason for patients to discontinue opioid therapy [45]. When it comes to recreational use, the United Nations Office on Drugs and Crime estimated the number of global illicit opioid users at around 30 million, or 0.6-0.8 % global prevalence (out of 5.2% total prevalence of all illegal drug use) in 2013 [46]. But also within legal boundaries, opioid use is high: there were 238 million prescriptions of opioid analgesics in 2011 in the United States alone [47].

1.2 THE SIGNALOME OF G PROTEIN-COUPLED RECEPTORS

G protein-coupled receptors (GPCRs) are a superfamily of membrane receptors, whose members are characterized by (1) seven helices spanning the cell membrane (seven-transmembrane domain receptors) and (2) at the same time binding to so called G proteins (guanosine nucleotide-binding proteins) as their main effector molecules. This superfamily comprises more than 800 receptors in the human genome, of which around 350 to 400 are functional non-olfactory receptors [48, 49]. Of those, another 140 are so called orphan receptors [50], i.e. no specific transmitter has yet been found for these receptors. Still, GPCRs are the largest entity of established drug targets so far [51]. More than half of the prescription medicines worldwide directly target GPCRs [52].

G PROTEIN-COUPLED RECEPTORS

The idea of receptors as a concept probably dates back to 1905, when Langley [53], while working on nervous stimulation, hypothesized the existence of a "receptive substance", which should be "capable of affecting the metabolism". However, at that time this idea was more than controversial. It was not until the 1970s, when work from the laboratory of R. Lefkowitz could show the existence of α-adrenergic [54] and β-adrenergic [55] receptors by means of the then modern method of radioligand binding. This continued work eventually culminated in the Nobel Prize in Chemistry awarded to Robert Lefkowitz and Brian Kobilka in 2012 for their work on GPCRs [56].

There are several classification systems in place to bring order into the plethora of GPCRs. Commonly, GPCRs are grouped into six classes based on genetic sequence and function as follows [57]:

- Class A: Rhodopsin-like receptor family
- Class B: Secretin receptor family
- Class C: Metabotropic glutamate receptor family
- Class D and E receptors are not found in humans
- Class F: Frizzeled/smoothened receptor family

The rhodopsin family represents the largest of all families, which are in turn grouped into several subfamilies. A more recent phylogenetic approach to GPCR-classification established the GRAFS (glutamate, rhodopsin, adhesion, frizzled/taste2, secretion) families [48]. The μ receptor, on which this work mainly focuses, belongs to class A of GPCRs (or the rhodopsin familiy, respectively).

STRUCTURAL AND FUNCTIONAL PROPERTIES OF GPCRS

In all GPCRs, the N-terminus lies on the extracellular side of the plasma

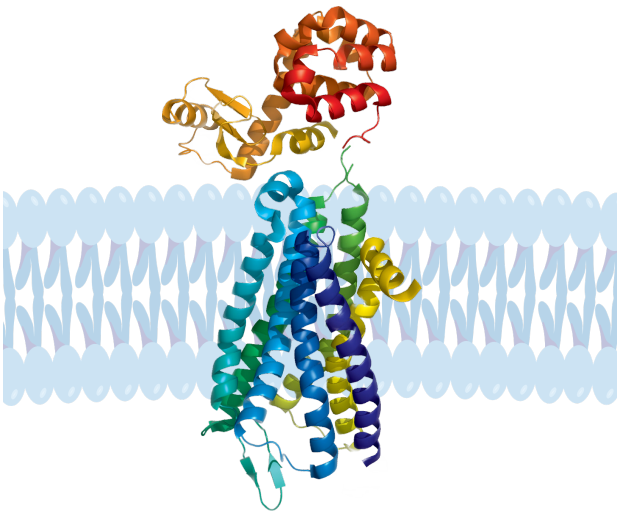

Figure 1: Cartoon rendering of a 2.8 Å resolution crystal structure of a murine μ receptor (class A) [58]. It shows the seven helical TMs in rainbow colors, with intra- and extracellular loops connecting the helices. The receptor is oriented with its extracellular parts facing up. Image rendered using PyMol from PDB ID 4DKL.

membrane. The linear protein then spans the membrane seven times, therefore there are three intracellular loops (ICLs) and three extracellular loops (ECLs). The C-terminus of the receptor is inside the cell. An exemplary GPCR structure is shown in figure 1.

Ligand binding is facilitated in most class A receptors by equivalent residues in TMs 3, 6, and 7 forming the ligand-binding pocket. Variations in this region of the receptor are thought to be responsible for ligand specificity. Binding of a ligand to the receptor and, thus, receptor activation leads to several conformational changes, mainly small changes to the distortion of TM5, relocation of TM3 and TM7, and rotation of TM5 and TM6 [59]. In general, these processes are nowadays thought to occur in a stochastic rather than a deterministic manner, i.e. active, inactive, and intermediate conformations exist throughout; ligand binding merely moves the equilibrium towards the active conformation. Furthermore, the presence of an agonist is believed to "increase structural heterogeneity in ... cytoplasmatic domains", thereby enabling binding of the G protein [60]. After all, complete activation of the receptor requires a G protein. The activation of a GPCR after ligand binding occurs rapidly (e.g. 40 ms for the α_{2A} adrenergic receptor; 1 s for the parathyroid hormone receptor [61]).

G PROTEINS G proteins are a family of signal transduction proteins. Their immediate biochemical function is that of a GTPase and they are activated by GPCRs. A G protein is considered active when guanosine triphosphate (GTP) is bound and inactive when guanosine diphosphate (GDP) is bound. G proteins exist in two major classes:

monomeric, "small" G proteins and heterotrimeric, "large" G proteins. The latter consist of three different subunits denoted as α, β, and γ [62]. The γ subunit bears the actual GTPase activity. The β and γ subunits usually form a stable dimeric complex. The former are monomeric GTPases, analogous to the α subunit of heterotrimeric G proteins. They were not of primary interest in this work. A trimeric G_s protein bound to the β2-adrenergic recptor is shown in figure 2.

When a GPCR is activated by an agonistic ligand, it binds a G protein and by that causes conformational change therein. The change in conformation allows for the GDP bound to the α subunit of the so far inactive G protein to be exchanged for a GTP, thus activating the G protein [63]. Whether this activation of the G protein manifests merely in relative movement of the subunits against each other or whether the α subunit and the $\beta\gamma$ complex dissociate is subject to ongoing debate [64, 65]. The activated G protein facilitates further signalling into the inside of the cell until its intrinsic GTPase activity hydrolizes the GTP to a GDP, thereby reconstituting the original state.

Several subtypes of G protein subunits exist, whereas the type of the α subunit is primarily responsible for immediate further signaling. The principal G_α subunit families are:

- $G_{\alpha i}$ family
- G_s family
- G_q family and
- $G_{12/13}$ family

The $G_{\alpha i}$ family consists of various subtypes, most importantly $G_{\alpha i1-3}$ and $G_{\alpha 0}$. $G_{\alpha t}$ or transducin is the respective G_α protein subunit of the rhodopsin receptor [66]. The *i* stands for *inhibitory*, because most members of the $G_{\alpha i}$ family inhibit an enzyme called adenocyclase, which produces cyclic adenosine monophosphate (cAMP) [67]. cAMP is an important second messenger, causing, among others, elevated Ca^{2+} levels in the cytosol.
There are two major members of the $G_{\alpha s}$ family: $G_{\alpha s}$ and $G_{\alpha olf}$, the latter coupling to olfactory receptors. Both activate adenylyl cyclases, resulting in increased levels of cAMP. Accordingly, the *s* stands for *stimulating*.
The $G_{\alpha q}$ family mainly consists of $G_{\alpha q}$ and $G_{\alpha 11}$, although the subtypes 14, 15, and 16 have been described to belong to this family, too. Their main function is to couple the receptor to an enzyme called phospholipase C (PLC) [68]. PLC cleaves phosphatidylinositol 4,5-bisphosphate into diacyl gylcerol and inositol 1,4,5-trisphosphate, both of which are signaling effectors in the cell.
One major effect of Gα12/13 proteins is the activation of GTPases of the Rho family [69].

The $G_{\beta\gamma}$ complex can be made up of a variety of β and γ subtypes. There seems to be no selectivity of certain α subtypes for specific $\beta\gamma$ combinations. However, certain combinations of $\beta\gamma$ subunits were shown to influence the extent of G protein activation by the α_{2A} adrenergic receptor [70]. The $\beta\gamma$ complex works and occurs only as a dimer [71] and has two main functions. First, it acts as a negative modulator of the α subunit. When in the heterotrimer (or when the G protein is inactive, that is), it increases the affinity of G_α for GDP, thus stabilizing the inactive form [72]. Second, the $\beta\gamma$ complex functions as a signaling molecule itself: it can regulate ion channels [73, 74] or interfere with adenylyl cyclases [75] as some α subunits do.

Many GPCRs can couple to more than one G_α subtype. For each receptor there is distinct selectivity for the types of G proteins it couples to. However, the mechanistics of this selectivity are poorly understood so far. The interaction between receptor and G protein is fast. Förster resonance energy transfer (FRET) studies with the α_{2A} adrenergic receptor and G_i showed interaction kinetics faster than 100 ms [76]. The activation of the G protein itself, i.e. the conformational change it undergoes, was found to take place within 400-500 ms for the same receptor and G protein [76].

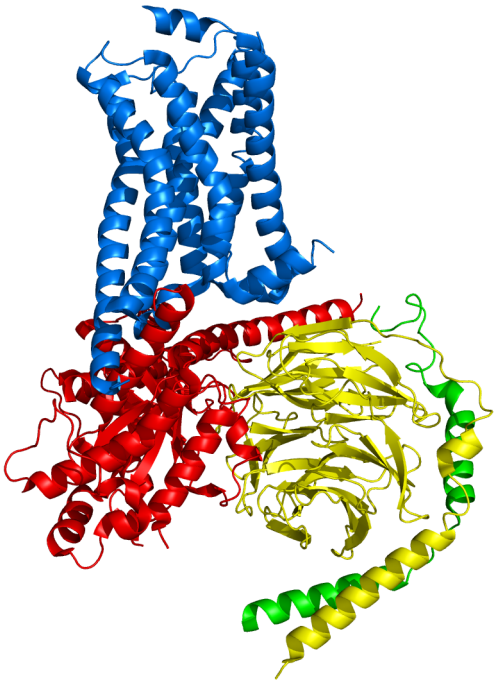

Figure 2: Cartoon rendering of a 3.2 Å crystal structure of the β_2-AR-G_s complex [77]. blue: receptor, red: Gα, yellow: Gβ, green: Gγ. Image rendered from PDB ID 3SN6 and adapted using PyMol.

ARRESTINS Arrestins are, next to G proteins, another family of proteins known to interact directly with GPCRs. Currently, there are four

known arrestins. The first one was found in 1986 by Wilden et al. [78] as a protein which deactivated signaling of the rhodopsin receptor. The second arrestin was first described by Lohse et al. [79] and termed β-arrestin (β-arr), because they found it to interact with the β_2-AR. By that time it was not clear that indeed arrestin 2 would interact with hundreds of GPCRs. Current terminology lists arrestins 1-4, where arrestins 1 and 4 are the so-called visual arrestins. Arrestins 2 and 3 are the ones interacting with many of the known GPCRs. In the literature they are commonly referred to as β-arrestin 1 and β-arrestin 2, respectively, which is prone to cause some confusion. Particularly β-arr 1 and 2, but all four arrestins in general, show high structural homology. In this work, the interaction of β-arrs 1 and 2 (i.e. arrestins 2 and 3) with the μ receptor was under investigation.

The function of β-arrs which was described initially is the promotion of receptor internalization [80]. Herein, β-arr links the receptor to clathrin [81], the clathrin adaptor AP2 [82], and several more proteins which eventually lead to the formation of a vesicle containing the receptor via so called clathrin-coated pits [83]. Moreover, after activation of a GPCR (and phosphorylation thereof, see next paragraph), β-arr binds with high affinity to the receptor and as a consequence terminates receptor signaling to the cell by sterically preventing further G protein coupling to the receptor [83]. Further direct interaction partners of β-arr are, among others, components of the mitogen-activated protein kinases (MAPK) pathway [84]. It was shown that β-arr interacts simultaneously with ERK, MEK1, and Raf, all of which form a signaling complex activating several transcription factors in the nucleus [85]. Often, β-arr1 and β-arr2 serve similar purposes within a cell, however β-arr2 has higher affinity for class A GPCRs [86], to which also the μ receptor belongs.

G PROTEIN-COUPLED RECEPTOR KINASES G protein-coupled receptor kinases (GRKs) are a family of serine/threonine kinases, which phosphorylate residues at the intracellular C-terminal end and the third intracellular loop of GPCRs [87]. The family comprises seven members to this date (GRKs 1-7) [88, 89]. Expression of GRK1 (retina [52]), GRK4 (testes [90]) and GRK7 (retina [89]) is restricted to certain tissues, the other GRKs are expressed ubiquitously in humans. GRKs are grouped into three subfamilies by distinct features: GRK1 and 7 are the retinal kinases; GRKs2 and 3 contain a C-terminal pleckstrin homology domain and are recruited to the cell membrane dependent on binding to the $\beta\gamma$ subunit of a G protein; GRK5 and 6 are permanently associated with the plasma membrane [87]. Three distinct functional domains can be found in a GRK. (1) The N-terminal region contains an RH (RGS homology) domain. RGS stands for *regulator of G protein signaling*, i.e. these domains can bind to G_α subunits and deactivate them. However, this has so far only been described

for GRKs 2 and 3 [91]. (2) The central part of a GRK holds the catalytic domain for its kinase activity [83]. (3) The C terminal regions of GRKs vary. All GRKs bear some form sub-cellular targeting motif at this site, mostly via lipid binding to the cell membrane. As pointed out, GRK2 and 3 hold a C-terminal PH domain, which is responsible for the recruitment of the GRK to the receptor via interaction with the $\beta\gamma$ subunit of the already bound G protein. Yet it was shown that the pleckstrin homology domain of GRKs2 and 3 also attenuates $G_{\beta\gamma}$ signaling via sequestration of the molecule [92], much like the N-terminal RH domain does with distinct G_α subunits.

Apart from GPCR phosporylation, GRKs are known to interact with a plethora of other molecules. Studies showed many non-GPCR molecules to be substrates of certain GRKs, as well as a variety of phosphorylation-independent interactions (review: [93]).

At the μ receptor there are around 20 potential phosphorylation sites at intracellular parts of the receptor [94]. Both GRK2 and 3 were shown to contribute to receptor phosphorylation in vitro [95, 96]. The investigation of their respective contributions to phosphorylation and β-arr recruitment is complicated by the fact that only GRK3- but not GRK2-knockout mice are viable [97]. Nonetheless, studies using phosphorylation-specific antibodies continue to shed light on the matter. Ser375 turned out to be of particular importance for β-arr recruitment and consequent receptor internalization [98, 99] along with Thr376 and Ser379 [100]. Moreover, these studies also showed that low-efficacy agonists (especially morphine) are a lot less effective in inducing phosphorylation than high-efficacy agonists (e.g. DAMGO). This is compatible with findings that the function of GRK2 (and 3) relies on the $\beta\gamma$ subunits of activated G proteins. As a consequence, morphine is a very weak inducer of receptor internalization in recombinant expression systems, yet this ability can be enhanced markedly by overexpression of GRK2 [96, 101, 102]. Moreover, it was shown that phosphorylation of Thr370 and Ser375 induced by DAMGO is mediated by GRK2 whereas phosphorylation of Ser375 induced by morphine is mainly put into effect by GRK5 [103].

GPCR SIGNALING Binding of a ligand to a GPCR leads to activation of the receptor and, subsequently, the activation of a G protein within a sub-second timeframe [61]. The activated receptor will then recruit a GRK, which in turn phosphorylates one or more serine or threonine residues at the C terminus of the receptor. The catalytic activity of the GRK is activated by binding to the receptor [104]. Recent findings suggest that different GRKs phosphorylate distinct serine or threonine residues at the C terminus of a receptor and that this phosphorylation pattern influences the way β-arr promotes signaling into the cell via specific conformational changes [105]. Furthermore, the location and number of residues being phosphorylated was found to

be ligand-dependent in at the μ receptor [106]; this, of course, adds a whole new dimension to the complexity of receptor signaling. Phosphorylation of the receptor results in a high affinity for a β-arr, which will be recruited to the receptor in a next step. Binding of β-arr to the receptor terminates signaling and causes the G protein to dissociate from the receptor. By then, the G protein will have initiated two distinct downstream signals: (1) activation/inhibition of an adenylyl cyclase or activation of phospholipase C by the α subunit, depending on the G protein subtype; (2) regulation of ion channels by the βγ subunit complex.

The receptor-bound β-arr engages in G protein-independent signaling pathways as has been described above. Still, it will first and foremost facilitate the internalization of the receptor into endosomes via the formation of clathrin-coated pits. While it was long thought that internalized receptors were inactive, for two G_s coupled GPCRs, the thyrotropin receptor (TSHR) [107] and the parathyroid hormone receptor (PTHR) [108], it has been shown that they continue signaling via cAMP after internalization. As a result, the activation of a receptor causes cAMP levels in a cell to change more than once over the course of time [109, 110]. In any case the internalized receptor will traffic through various stages of endosomal compartments and eventually be recycled to the cell surface or subjected to lysosomal degradation [83].

1.3 μ-OPIOID RECEPTOR

Opioid receptors are a family of G protein-coupled receptors. There is ongoing debate in the scientific community on how many subtypes of opioid receptors exist. The International Union of Basic and Clinical Pharmacology (IUPHAR) currently recognizes the following:

- δ-opioid receptor
- κ-opioid receptor
- μ-opioid receptor (μ receptor)
- nociceptin receptor

The δ, κ, and μ receptor show ∼60% amino acid sequence identity in humans, the nociceptin receptor a little less so [111].

The activation of each opioid receptor subtype leads to a variety of physiological effects. In general, μ receptors activation causes strong analgesia together with respiratory depression, reward, and constipation as the most relevant undesired effects. All these effects are diminished in μ receptor knock-out animals [112–114]. Additionally, outcomes in μ receptor-deficient animals depend on which of the exons was deleted [115]. This finding has so far not led to consequences in

opioid-based pain therapy, yet. δ-opioid receptors convey analgesia as well, however usually at comparably high ligand concentrations. One reason for this finding might be that δ-opioid receptors have repeatedly been shown to be localized preferably inside cells rather than at the membrane, which, of course, makes them less accessible for their ligands [116, 117]. However, the δ-opioid receptor seems to play a role in morphine tolerance, a phenomenon which is diminished in mice lacking the receptor [118]. Moreover, such receptor-deficient mice show decreased levels of anxiety in behavioral studies [119]. Animals lacking of κ-opioid receptors have no altered overall nociceptive sensitivity, however they are more sensitive to chemical visceral pain and κ-selective agonists do not induce dysphoria in these animals as would be expected in wild-type conspecifics [120].

The natural (endogenous) ligands of opioid receptors are peptides. They share a common N-terminal sequence (Tyr-Gly-Gly-Phe-Leu or Tyr-Gly-Gly-Phe-Met) [121]. In addition to that, many synthetic peptide ligands are known. One such μ-sepecific peptide is DAMGO [29], see section 1.1.

The μ-opioid receptor is the one among the opioid receptors, by which the majority of the pharmaceutical drug effects are mediated. All opioids in clinical use today are μ receptor ligands, but not all are μ receptor-specific, e.g. buprenorphine (also see section 1.1). As a receptor in a contemporary sense it was first described in 1973 [122, 123] and has been subject of extensive research ever since. The receptor was eventually cloned in 1993 [124]. μ receptors are predominantly expressed in the central nervous system, with enhanced expression in the amygdala, the periaqueductal grey, the nucleus raphe magnus, and the locus coeruleus (brain), as well as the dorsal horn (spinal cord) [125]. Expression in the mesenteric plexus accounts for gastrointestinal side effects of opioids [126, 127]. Recent studies also suggest a role of peripheral μ receptors [128]. The analgesic effect is mediated by a hyperpolarization of afferent neurons by means of decreased cAMP levels and increased intracellular potassium as a consequence of inhibitory G protein activation (see section 1.2).

As with all opioid receptors, only one encoding gene is known for each receptor, OPRM1 in the case of the μ receptor. However, to this day ten splice variants have been identified [129] with uncertain physiological relevance. Interestingly, there are subtype-specific ligands (μ2 [130]); μ3 responds to alkaloid opioids but not peptides [131]. In this work the full-length human receptor as encoded by OPRM1 cDNA was used for all experiments.

An important contribution to the understanding of μ receptor function was made in 2012 when the crystal structure of an antagonist-bound receptor was solved [58]. Two findings stood out: (1) the orthosteric binding pocket is very well accessible from the extracellular space, notably more so than in many other GPCRs, where the lig-

and is often partially buried by residues of the receptor's TMs. This allows for uncommonly bulky moieties to be attached to an agonist scaffold without generally hindering proper binding. (2) The receptor crystalizes as a dimer with two different interaction interfaces. This is of interest, because oligomerization of (opioid) receptors has been suggested before [132] and is subject to ongoing debate. Very recently, the μ receptor crystal structure was solved with an agonist and a G protein mimetic nanobody bound to it [133]. Furthermore, nuclear magnetic resonance (NMR) studies confirmed the absolute need of a G protein (or a structure mimicking its function) in order to obtain the fully activated receptor state [134].

1.4 RESONANCE ENERGY TRANSFER AND ITS IMPLICATIONS IN LIFE SCIENCES

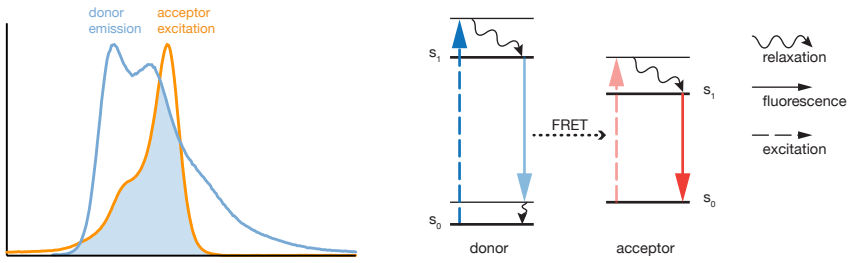

(a) Spectral overlap required for RET (b) Energy diagram of FRET

Figure 3: (a) Exemplary spectral properties of two compatible fluorophores. The donor emission and the accpetor excitation spectra behave in such a way that they overlap to some extent. This spectral overlap (light blue area) is required for RET of any kind to occur. (b) Energy diagram of FRET. The acceptor gets excited (blue dashed arrow). Instead of returning to a stable energy state by emitting a photon (semi-transparent blue arrow), energy is transferred in a radiation-free manner to the acceptor. Thus, the acceptor is in an excited state and emits a photon of distinct wavelength (red arrow). Adapted from [135]

FUNDAMENTAL PRINCIPLES OF FRET FRET is a physical concept that describes radiation-free transfer of energy between two electric dipoles over very short distances (several nanometers). The concept is based on and named after work by German scientist Theodor Förster [136]. Generally, FRET occurs between two apt molecules (the donor and the acceptor) if they fulfill the following three conditions: (1) donor and acceptor must be in close proximity, usually no more than 10 nm. (2) The optical spectra of donor and acceptor must behave in such a way that the emission spectrum of the donor overlaps the excitation spectrum of the acceptor to a certain degree (see figure 3a). (3) For optimal energy transfer efficiency, the dipoles should be oriented

in parallel to each other. In biochemical applications, compliance with this last criterion is often times left to chance.

The eventual read-out in most FRET experiments is *quantum yield*, i.e. the efficiency with which the donor transfers its energy to the acceptor. This efficiency is dependent on the aforementioned three criteria. Of particular importance is the distance between the two chromophores, as the energy transfer efficiency is inversely proportional to the sixth power of the distance. The radiation-free nature of the energy transfer is often times deemed elusive, as its quantum-mechanistic explanation involves the existence of a so called "virtual photon" which facilitates the energy transfer. However, work by Andrews [137] in 1989 pointed out that radiation-free and radiative energy transfer are merely the short-range and the long-range limit of a common dipole-dipole interaction principle. At larger separations of the two dipoles, relativistic effects will cause the transition from the 10^{-6} correlation between distance and efficiency of the radiation-free transfer to the (more commonly known) 10^{-2} correlation for radiative transfer [137, 138]. A graphic summary of the underlying proceedings during FRET is given in the energy diagram in figure 3b.

FRET APPLICATIONS First practical implementations of the Förster principle were described in the 1960s and 1970s, when it was mainly used as a spectroscopic ruler [139]. With present day microscopy technology at hand, FRET can be used to study interactions of molecules in living cells in real time. An early approach to such an implementation was described by Uster and Pagano [140] in 1986. They used fluorescence microscopy to measure FRET between fluorescent probes in membranes of living cells. Today, three FRET applications for biomedical research predominate [141]: (1) *Photobleaching FRET*, where constant excitation of the donor causes the gradual loss of fluorescence, a phenomenon called "photobleaching". The presence of a near-by acceptor decreases the amount of photobleaching per time. The comparison of photobleaching rates with and without the acceptor yields the FRET efficiency. (2) *Fluorescence lifetime* measurements make use of the fact that an excited donor will take less time in that state before emitting a photon when an acceptor is present. (3) In *sensitized emission* experiments, the FRET donor is excited by a light source and will in turn excite the acceptor, if it is in close enough proximity. When donor and acceptor change their distance from or relative orientation towards each other due to movements of the molecules they are attached to, a change in FRET efficiency can be observed. Sensitized emission is the FRET technique used in this work. Technical details are described in section 2.2.6.

FLUORESCENT DYES As in this work, often times variants of green fluorescent protein (GFP) are used as donor and acceptor, respectively.

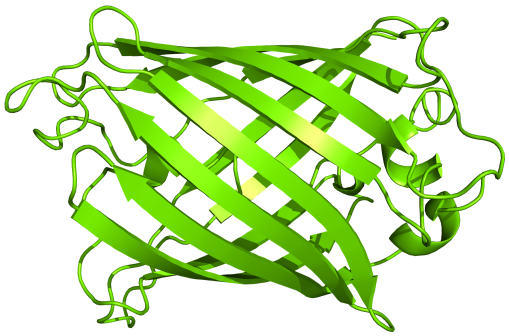

Figure 4: Cartoon rendering of a 1.9 Å crystal structure of the green fluorescent protein of Aequorea victoria [142]. The barrel-like tertiary structure is conserved in all GFP mutants. Image rendered from PDB ID 1EMA using PyMol.

Many, yet not all of these fluorescent proteins are mutants of a fluorescent protein naturally expressed in the jellyfish *Aequorea victoria* (see figure 4). It was found and described as a research tool in the 1990s by several groups nearly at the same time [142–144]. Osamu Shimomura, Martin Chalfie, and Roger Y. Tsien were awarded the Nobel Prize in Chemistry in 2008 for "the discovery and development of the green fluorescent protein, GFP".[1] Today, a wealth of GFP variants, other fluorescent proteins, and fluorescent small molecules can be used as FRET interaction partners [145]. The decision for a specific pair of fluorophores will eventually be influenced by practical biotechnical considerations besides the pure physical requirements that need to be met. For example, fluorescent proteins can be fused to the protein of interest genetically, i.e. both are expressed as one fusion protein. This can be an advantage as no labeling is required. However, the relatively large size of GFP (27 kDa) can interfere with the biological processes that were to be investigated in the first place. Small molecules can be an alternative in this case. Yet, these are of non-peptide nature, which means they need to be attached to the protein of interest in a separate process. This usually requires a specific binding site to be introduced into the protein, which then can bind the fluorophore. Depending on the technique used, such binding sites can themselves be several kDa to only six amino acids in size [146, 147].

BRET A more recent variation of FRET which has been established in biomedical research is BRET. There, instead of a donor fluorophore, a light-emitting enzyme - a so-called luciferase - is genetically fused to one of the interaction partners [148]. One major advantage is the loss of an external light source, which tends to significantly add to the noise in FRET experiments. Additionally and for several reasons not

1 "The Nobel Prize in Chemistry 2008 - Press Release". Nobelprize.org. Nobel Media AB 2014. Retrieved from the internet 17 Jan 2016. <http://www.nobelprize.org/nobel_prizes/chemistry/laureates/2008/press.html>

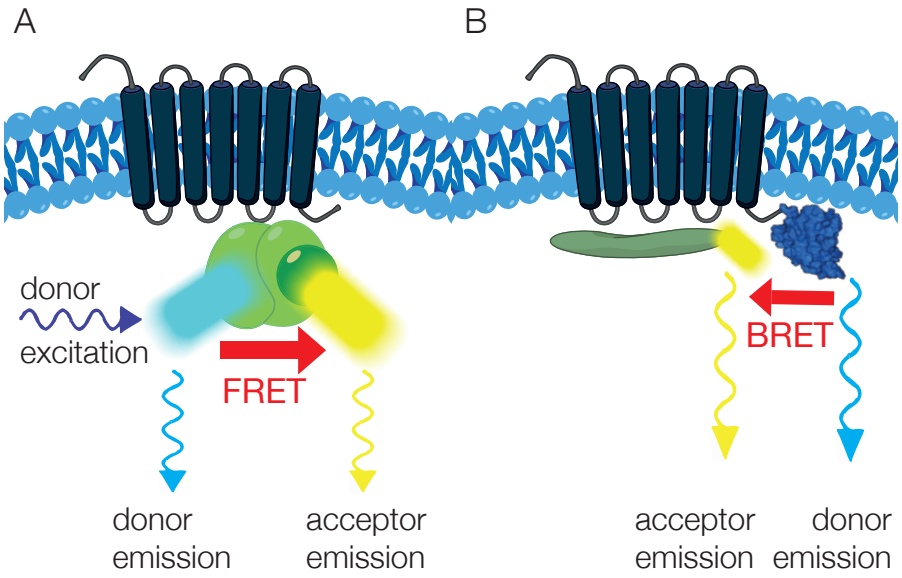

Figure 5: Principle of FRET and BRET in protein interaction sensors used in this work. Note that the FRET sensor (A) requires an external light source for the excitation of the donor fluorophore. Donor and acceptor are fused to a subunit of a trimeric G protein, respectively. Activation of the G protein by an agonist-bound receptor will lead to movement of the subunits relative to each other, thereby changing the fluorophores' distance from and/or orientation towards each other. The donor in BRET (B) is a luciferase fused to the receptor, which emits light of a distinct wavelength spectrum in the presence of its substrate. When the β-arr, which is fused to the acceptor fluorophore, binds to the activated receptor, the two fluorophores will be in close enough proximity for resonance energy transfer to occur. In both applications, donor and acceptor emissions are recorded separately and the ratio of both serves as a quantitative readout.

to be outlined in detail, BRET is superior to FRET in high-throughput screening [149]. Together, FRET- and BRET-based biosensors have proven to be valuable tools for a diversity of applications: protein-protein interactions [150], detection of intramolecular conformational changes [61], and real-time determination of cytosolic second messenger concentrations [151], just to name a few. A simplified depiction of exemplary FRET and BRET sensors used in this work is given in figure 5.

1.5 BIASED AGONISM

PRINICIPLES OF BIASED AGONISM The concept of *biased agonism* (sometimes also termed *functional selctivity*) was introduced to the scientific community at the beginning of this century. In brief, biased agonism describes the propensity of a (G protein-coupled) receptor

to transduce different downstream signaling patterns to the cytosol depending on the ligand it was activated by. To put it another way, two ligands, both agonists at the same receptor, can elicit different downstream signaling. Until recently, when a receptor was thought of as a machine which can exist in exactly two distinct states - on and off - it has been hard to conceive how this one active receptor state would be capable of modulating fine-tuned signaling patterns.

In terms of GPCR biased agonism, one straightforward example is selectivity of a ligand for either G protein activation or β-arr recruitment. While most ligands tend to engage in both signaling pathways, they do so to different extents. It was shown that at the β_2-AR, carvedilol is a β-arr-biased agonist [152]. Moreover, it induced phosphorylation of the receptor at sites which were found to be phosphorylated only by GRK6 but not GRK2 [105]. This idea of a "phosphorylation barcode" was also propagated for the μ receptor [153], where different phosphorylation patterns lead to distinct signaling outcomes [99, 154]. Apart from β-arr-related signaling, it was also shown that a biased ligand can selectively target signaling through single G protein subunits [155].

As mentioned above, receptors were imagined to appear in one on and one off-state until only several years ago. With the development of ever more sophisticated technical possibilities, this concept is facing growing challenge. For example, by means of fluorescence spectroscopy, Swaminath et al. [156] could show multiple active states of the β_2-AR. Similarly, Liu et al. [157] found conformational states for G protein and β-arr-biased ligands. Using NMR techniques, they showed that G protein-specific active states are effected through conformational changes in transmembrane helix VI and ICL3, whereas bias towards β-arr is effected through the conformation of helix VII (for orientation, see figure 1). Changing the equilibrium of conformational changes in those two regions is suggested to be the mechanistic correlate of biased agonism at the β_2-AR and could serve as a general model to explain this phenomenon at GPCRs. The latest model of GPCR activation depicts the receptor as a highly dynamic entity which spontaneously and rapidly switches between several unstable conformations. The mechanistic basis of this is a complex so-called "energy landscape" that is influenced by bound ligands and effector molecules likewise. Different constellations of receptor-ligand-effector interactions stabilize distinct energy profiles resulting in receptor conformations and thereby also explaining biased agonism [158, 159].

QUANTIFICATION OF BIASED AGONISM With these conceptual considerations in mind, the need for experimental quantification of biased agonism arises. Several approaches have been suggested to this day. One way or another, they all compare efficacies and/or poten-

cies of ligands across a given set of signaling pathways. The simplest way of comparing ligand signaling efficiencies would be to compare (1) signal amplitudes at a given ligand concentration (equimolar approach) or (2) ligand concentrations required to elicit the same signal (eqiactive approach). Both have been described in the literature [160–162]. Both approaches often make use of output parameters from standard three- or four-parameter sigmoidal fits, i.e. maximum response (E_{max}) and concentration of half-maximum response (EC_{50}). The main concern with these two approaches is that they are not very robust with respect to confounding influences. Specifically, these approaches do not take into consideration the receptor density, the coupling efficiency with signal transducers (e.g. G proteins), and amplification of downstream signals (e.g. cAMP levels). In addition, signaling properties of a ligand can differ tremendously between single-cell and in vivo experiments [163]. Thus, the detection of weak bias is difficult and one can merely describe qualitative bias. Therefore, more elaborate ways for bias quantification were developed. Such truly quantitative approaches in a way combine the aforementioned methods and expand them by using an operational model of receptor pharmacology (Black and Leff [164]). Two slightly different ways of bias calculation predominate in the scientific community to this date: Rajagopal et al. [165] and Kenakin et al. [166]. The two approaches mainly differ in the necessity of expressly gathering binding data for the ligands under investigation. While Rajagopal et al. support independent binding experiments, Kenakin et al. state that ligand affinity is dependent on the transducer bound to the receptor at any given time. Therefore, mere binding affinities might not be of great use and they claim the term K_A of the operational model represents "functional affinity" and is, as such, integrated in the pharmacological model in the first place. Either way, no clear evidence for the superiority of one of the approaches was shown and it seems like they yield rather similar results [165]. As of now, there is ongoing debate between the leading authors (Kenakin and Christopoulos [167] and Rajagopal [168]), but powerful tools for the quantification of ligand bias do exist. In this work, the approach by Kenakin et al. was chosen, not least because of their convincing points about ligand binding experiments. Technical details of the calculations are given in section 2.2.11. For a comprehensive review on the matter of biased agonism, see [169].

CLINICAL IMPLICATIONS In recent years, pharmaceutical research has started to take advantage of the insights into biased agonism. In conditions where one signaling pathway of a given receptor is known to have beneficial effects, while another might be less favorable, targeted screening for biased ligands can be a promising approach. For example, a β-arr-biased angiotensin II receptor type 1A (AT_{1A}-R) ligand was shown to have positive inotropic and lusitropic effects in

cardiac myocytes in vitro [170]. With TRV027, such a β-arr-biased AT_{1A}-R agonists has proven to have beneficial effects on acute heart failure in vivo, too [171] and is currently in phase-II clinical testing [172]. Another biased ligand, TRV130, is a μ receptor agonist biased for G_i protein activation. After experiments with β-arr2 knock-out mice showed enhanced analgesia and reduced desensitization upon morphine treatment [173], also severe side effects of morphine like respiratory depression and obstipation were found to be attenuated in such animals [174]. The thereafter identified compound TRV130 showed favorable behavior in vitro and in vivo [175] and was granted Breakthrough Therapy status by the U.S. Food and Drug Administration (FDA) in early 2016 (Oliceridine, OLINVO^{TM}) for the therapy of moderate to severe pain.

1.6 TOLL-LIKE RECEPTOR 4 AND ITS INVOLVEMENT IN OPIOID SIGNALING

Toll-like receptors are a family of mammalian *pattern recognition receptors*. They play an important role in the innate immune system, as they detect structures possibly harmful to the organism - so called pathogen-associated molecular patterns (PAMPs) - without previous sensitization. Unlike GPCRs, TLRs span the plasma membrane only once (see figure 6). Their name is derived from homology to the *toll* gene in Drosophila.

TLR4 GENERAL REMARKS The human TLR4 was the first toll-analogous structure identified in humans [176]. To this day, thirteen TLRs are known, ten of which are expressed in humans. TLR4 responds to several PAMPs. The one most looked into so far probably is lipopolysaccharide (LPS), which is part of the cell wall of gram-negative bacteria [177]. For their ground-breaking work on innate immunity and TLRs in particular, Bruce A. Beutler and Jules A. Hoffmann were awarded one half of the Nobel Prize in Medicine or Physiology in 2011.[2]

TLR4 does not confer signaling by itself, but interacts with other proteins [178, 179]. CD14 is expressed on the surface of lymphatic cells and is the genuine, high-affinity LPS binding protein. It has no signaling capacity of its own but merely binds LPS and mediates binding to TLR4. Furthermore, MD-2, a soluble protein, also binds the LPS-TLR4-CD14 complex. TLR4 signaling is abolished with no MD-2 present [178]. For intracellular signal transduction there are two major pathways. One is common to several TLRs and is effected by a protein called *MyD88*. *MyD88* is an adaptor protein which then

2 "The 2011 Nobel Prize in Physiology or Medicine - Press Release". Nobelprize.org. Nobel Media AB 2014. Web. 23 Jan 2016. <http://www.nobelprize.org/nobel_prizes/medicine/laureates/2011/press.html>

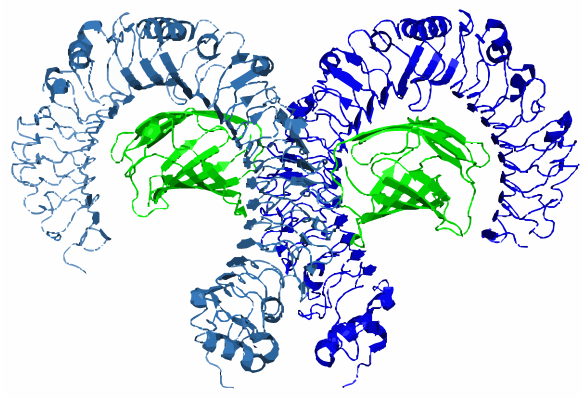

Figure 6: Cartoon rendering of a 2.4 Å crystal structure of a TLR4 dimer (blues) in complex with MD-2 (green). Rendered using PyMol from PDB ID 4G8A.

recruits a cascade of effectors, finally resulting in the release of NF-κB and inflammatory cytokines [180]. The other signaling pathway is specific to TLR4 and originates from an adaptor protein called *TIRAP* or *Mal*. *TIRAP*-dependent signaling will lead to the production of Interferon type I. Moreover and similar to the *MyD88* pathway, it will also induce a (late) NF-κB release [180, 181]. An abriged scheme of signaling processes at the TLR4 is given in figure 7. The immunologic significance of TLR4 is stressed further by the identification of single nucleotide polymorphisms in humans. Most profoundly investigated so far are the two polymorphisms D229G and T399I. They seem to be related to an increased susceptibility to gram-negative infections and septic shock [182–184].

TLR4 AND OPIODS The involvement of TLR4 in pain and opioids is not all obvious and has been postulated only in the last ten years. In 2005, Tanga et al. [185] reported a role of TLR4 as a glial activator in the central nervous system that could induce neuropathy. Based upon these findings, Hutchinson et al. [186] postulated both stereoisomers of Naltrexon to be antagonists of TLR4. As such, they would be able to alleviate neuropathic pain. Two years later, the morphine metabolite morphine-3-glucuronide was found to induce allodynia and hyperalgesia (both painful conditions) in rats. This effect was ascribed to TLR4s expressed in spinal cord microglial cells [187]. This work also suggested possible morphine binding to MD-2 in a way similar to LPS in *in silico* docking studies. This hypothesis was confirmed biochemically by Wang et al. [188], who further postulated morphine was able to induce TLR4 dimerization, which is a generally accepted part of the receptor activation cascade. A central work on opioid effects on TLR4 signaling was published in 2010. Herein, the authors found several opioid agonists to activate TLR4 signaling in the same *in vitro* assay used in this work [189]. Those were, among oth-

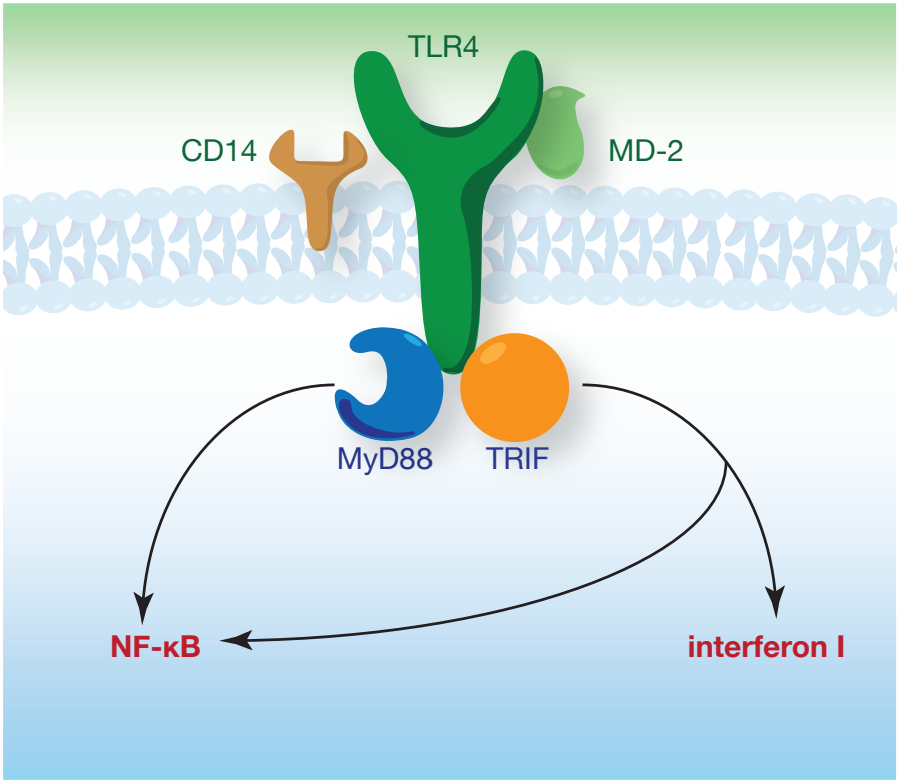

Figure 7: Basic schematic of TLR4 signaling. For reasons of simplicity, not all signaling and adaptor proteins involved are depicted.

ers, (+)- and (-)-morphine, (+)- and (-)-methadone, oxycodon, pethidine, buprenorphine, fentanyl, and morphine-3-glucuronide. Interestingly, M-6-G was no TLR4 agonist in this study. Both stereoisomers of Naloxone inhibited opioid induced TLR4 signaling in a concentration-dependent fashion. Moreover, the authors found blocking of TLR4 to support morphine induced analgesia and attenuate tolerance, hyperalgesia, and withdrawal symptoms in rats. In TLR4 knock-out animals morphine analgesia was found to be more potent than in the wild-type. In 2013, work by a different group showed results not entirely in line with the previous findings. Morphine and fentanyl were found to produce close to no signal in a comparable *in vitro* assay, whereas they acted as non-competitive antagonists when administered together with LPS [190].

In summary, the significance of opioid signaling at the TLR4 is far from clear to this day. Especially so, as parts of the work by Hutchinson in 2010 could not be reproduced by another lab a few years later [191]. However, some of the findings are intriguing and more efforts will need to be made to resolve the issue.

1.7 AIM OF THIS WORK

Probably unlike any other class of drugs, when it comes to opioids, "clinical" utilization has preceded basic research for the major part of their existence. As a result, many opioid drugs are in use today with comparatively little knowledge available about the molecular processes which are influenced by them. Yet, opioids remain the gold standard in the therapy of severe pain despite a variety of substantial undesired effects with no alternatives is the foreseeable future. With this in mind, a more detailed understanding of the signaling processes surrounding opioid therapy is urgently needed. From the existence of endogenous opioids and the observations on how they work, one must assume that much more effective and at the same time safer therapeutic opioids should be possible. To achieve this goal, several mechanisms need to be uncovered, especially the exact signaling properties on a molecular level of each opioid in use today. This also includes pathways that go beyond what is now considered to confer analgesia. Recent findings show that a lot more signaling is activated by opioid drugs than would be necessary for pain relieve alone. With the latest insights into biased agonism, a first step into designing more advanced analgesics is to identify ways to understand and make use of biased signaling in such a way that it allows for more "analgesia-specific" opioids. This work seeks to contribute to that by (1) describing signaling efficiencies for a wide range of clinically used opioids in a systematic approach. The focus lies on G protein activation and recruitment of β-arr 1 and 2. (2) Applying recent insights into biased agonism on the opioid system in order to identify possibly biased ligands among those already in use. Efforts of the pharmaceutical industry highlight the potential of such substances. Having a biased ligand approved for use in patients would allow for far reaching clinical research on the matter of biased agonism, thus connecting molecular and applied research. (3) Exploring the possibility that structures and systems beyond the classic opioid system are involved in the way these drugs exert their influence in an organism. Recent studies suggested TLR4 as a potential receptor engaged in opioid signaling. As a start, this work aims to reproduce previous experiments with opioid ligands in a TLR4 signaling assay to lay the groundwork for possible future research extending beyond this very piece of work.

2 MATERIALS AND METHODS

2.1 MATERIALS

2.1.1 *Chemicals and Reagents*

Agar	Applichem, Darmstadt, Germany
Ampicillin-Na	Sigma-Aldrich, Taufkirchen, Germany
Benzamidine-HCl 99%	Sigma-Aldrich, Taufkirchen, Germany
Bovine serum albumin (BSA)	New England Biolabs, Frankfurt/Main, Germany
Calcium chloride ($CaCl_2$)	Applichem, Darmstadt, Germany
Dimethyl sulfoxide (DMSO)	BioChemica/Applichem, Darmstadt, Germany
Ethidium bromide	Applichem, Darmstadt, Germany
Ethanol	Roth, Karlsruhe, Germany
G418 (Geneticin sulphate)	Gibco Life Technologies Eggenstein, Germany
Glucose, anhydrous	Applichem, Darmstadt, Germany
HEK-Blue ^{TM} Detection	InvivoGen, San Diego, CA, USA
HEK-Blue^{TM} Selection	InvivoGen, San Diego, CA, USA
HEPES	Applichem, Darmstadt, Germany
Immersion oil for microscopy	Applichem, Darmstadt, Germany
Isopropanol	Sigma-Aldrich, Taufkirchen, Germany
KCl	Applichem, Darmstadt, Germany
L-glutamine 200 mM	Sigma-Aldrich, Taufkirchen, Germany
Lipopolysaccharide (LPS)	InvivoGen, San Diego, CA, USA
Methanol	Sigma-Aldrich, Taufkirchen, Germany
$MgCl_2{*}6H_2O$	Applichem, Darmstadt, Germany
Milk powder	Applichem, Darmstadt, Germany
NaCl	Applichem, Darmstadt, Germany
NaOH	Applichem, Darmstadt, Germany
Nonidet P40	Sigma-Aldrich, Taufkirchen, Germany
Normocin^{TM}	InvivoGen, San Diego, CA, USA
Penicillin G 10000 U/ml, Streptomycin sulfate 10 mg/ml	Sigma-Aldrich, Taufkirchen, Germany
PMSF	ThermoFisher Scientific, Brunswick, Germany
Poly-D-Lysine hydrobromate	MP Biomedicals, Eschwege, Germany
PEG 3000	Applichem, Darmstadt, Germany
SDS Sodium dodecyl sulfate	Applichem, Darmstadt, Germany
Soybean trypsin inhibitor	Sigma-Aldrich, Taufkirchen, Germany
TEMED	Sigma-Aldrich, Taufkirchen, Germany
Tris-acetate	Applichem, Darmstadt, Germany
Tris$*$HCl	Applichem, Darmstadt, Germany

Tryptone	Applichem, Darmstadt, Germany
Tween 20	Applichem, Darmstadt, Germany
Universal agarose	Peqlab, Erlangen, Germany
Yeast-extract	Applichem, Darmstadt, Germany
Zeocin (phleomycin D1)	InvivoGen, San Diego, CA, USA

2.1.2 *Cell Culture Consumables*

DMEM+++
Dulbecco's modified Eagle's medium (DMEM) supplemented to contain 2mM L-glutamine, 0.1 U/l penicillin G, 0.1 g/l streptomycin sulfate, and 10% fetal calf serum (FCS)

DMEM+++ (STABLE CELLS)
DMEM+++ containing 40mg/l Zeocin and 800 mg/l G418, additionally

DMEM CELL FREEZING MEDIUM
Dulbecco's modified eagle medium supplemented to contain 4.5 g/l glucose containing 2 mM L-glutamine, 0.1 U/l penicillin G, 0.1 g/l streptomycin sulfate, 10 % FCS and 10 % dimethyl sulfoxide (DMSO)

DPBS
Dulbecco's phosphate buffered saline (Sigma-Aldrich, Taufkirchen, Germany)

EFFECTENE® TRANSFECTION REAGENT
for transfection of eukaryotic cells (Qiagen, Hilden, Germany)

KCM BUFFER 5X
500 mM potassium chloride (KCl), 150 mM calcium chloride ($CaCl_2$), 250 mM magnesium chloride ($MgCl_2$); for transformation of competent E. coli

LYSOGENY BROTH (LB)
16g/l peptone, 10 g/l yeast, 5 g/l sodium chloride (NaCl)

LB WITH SELECTIVE ANTIBIOTICS
80 μg/l ampicillin or 50 μg/l kanamycin, respectively

LB AGAR
LB supplemented to contain 8 g/l agar

OPTI-MEM®
Modified Eagle's minimum essential media, no phenol red (ThermoFisher Scientific, Waltham, MA, USA)

TRYPSINE-EDTA SOLUTION
(PAN-Biotech Aidenbach, Germany)

2.1.3 *Molecular Biology*

PCR DNA primers were custom-synthesized by Eurofins Genomics, Ebersberg, Germany. Thermus aquaticus (Taq) deoxyribonucleic acid (DNA) polymerase, restriction enzymes, bacteriophage T4 (T4) DNA ligase and their corresponding buffers were from New England Biolabs, Frankfurt, Germany. Purification of polymerase chain reaction (PCR) products from agarose gels (1% agarose in Tris base, acetic acid, EDTA (TAE) buffer) was done with a DNA gel extraction kit (Merck Millipore, Darmstadt, Germany). DNA preparation from E. coli lysates was performed using the NucleoBond® Xtra Midi kit (Macherey Nagel, Düren, Germany).

Cloning Vectors

PCDNA3 VECTOR
: Invitrogen, Darmstadt, Germany

PCDNA3.1 VECTOR
: Invitrogen, Darmstadt, Germany

PFC14K HALOTAG® CMV FLEXI® VECTOR
: Promega, Mannheim, Germany

PFC15K HALOTAG® CMVD1 FLEXI® VECTOR
: Promega, Mannheim, Germany

PFC16K HALOTAG® CMVD2 FLEXI® VECTOR
: Promega, Mannheim, Germany

PFC17K HALOTAG® CMVD3 FLEXI® VECTOR
: Promega, Mannheim, Germany

PFN21K HALOTAG® CMV FLEXI® VECTOR
: Promega, Mannheim, Germany

PFN22K HALOTAG® CMVD1 FLEXI® VECTOR
: Promega, Mannheim, Germany

PFN23K HALOTAG® CMVD2 FLEXI® VECTOR
: Promega, Mannheim, Germany

PFN24K HALOTAG® CMVD3 FLEXI® VECTOR
: Promega, Mannheim, Germany

PFC32K NLUC CMV-NEO FLEXI® VECTOR
: Promega, Mannheim, Germany

cDNA

OPRM1
: human μ receptor, transcript variant 1 (provided by C. Hoffmann)

ARRB2
: bovine β-arr2 (provided by C. Hoffmann)

Plasmids

μ RECEPTOR (OPRM1) IN PCDNA3
: provided by C. Hoffmann

G_β-2A-VENUS-$G_{\gamma 2}$-IRES-$G_{\alpha i1}$-MTQ2 IN PEGFP-C1
: provided by J. Goedhart

GRK2 IN PCDNA3
: provided by C. Hoffmann

PFC32K-OPRM-NLUC IN CMV-NEO FLEXI® VECTOR
: this work; U. Zabel

PFC14K-β-ARRESTIN2-HALOTAG IN CMV FLEXI® VECTOR
: this work; U. Zabel

PFC15K-β-ARRESTIN2-HALOTAG IN CMVD1 FLEXI® VECTOR
: this work; U. Zabel

PFC16K-β-ARRESTIN2-HALOTAG IN CMVD2 FLEXI® VECTOR
: this work; U. Zabel

PFC17K-β-ARRESTIN2-HALOTAG IN CMVD3 FLEXI® VECTOR
: this work; U. Zabel

PFN21K-HALOTAG-β-ARRESTIN2 IN CMV FLEXI® VECTOR
: this work; U. Zabel

PFN22K-HALOTAG-β-ARRESTIN2 IN CMVD1 FLEXI® VECTOR
: this work; U. Zabel

PFN23K-HALOTAG-β-ARRESTIN2 IN CMVD2 FLEXI® VECTOR
: this work; U. Zabel

PFN24K-HALOTAG-β-ARRESTIN2 IN CMVD3 FLEXI® VECTOR
: this work; U. Zabel

2.1.4 *Western Blot*

The following buffers and solutions were prepared:

APS 10% ammonium persulfate in water (H_2O)

LAEMMLI SAMPLE BUFFER
50 ml Tris(hydroxymethyl)aminomethane (Tris) 1M pH 6.8, 50 ml sodium dodecyl sulfate (SDS) 20%, 100 ml Glycerol 20%, 0.01 g bromophenol blue, ad 200 ml H_2O

UPPER BUFFER
2 g SDS, 250 ml Tris 1M pH 6.8, ad 500 ml H_2O

LOWER BUFFER
4 g SDS, 500 ml Tris 3M pH 8.8, ad 1000 ml H_2O

RUNNING BUFFER 10X
30.3 g Tris, 144 g Glycine, 10 g SDS, ad 1000ml H_2O

TRANSFER BUFFER
2.4 g Tris, 11.2 g Glycine, 200 ml Methanol, ad 1000 ml H_2O

PHOSPHATASE INHIBITOR
50 mM sodium pyrophosphate ($Na_4P_7O_2$), 1mM sodium orthovanadate (Na_3VO_4), 0.02% sodium azide (NaN_3), in H_2O

PROTEASE INHIBITOR
2 mg/ml soybean trypsin inhibitor, 6 mg/ml benzamidine, in 50 mM Tris

PMSF
100mM phenylmethylsulfonyl fluoride (PMSF) in ethanol

BLOCKING BUFFER
15 g milk powder, 1.75 g NaCl, 3 ml Tris 1M pH 7.6, 0.3 ml Tween 20

WASH BUFFER
50 ml Tris 1M pH 7.4, 8.8 g NaCl, 2 g bovine serum albumin (BSA), 2 ml Nonidet P-40 2 ml, ad 1000 ml H_2O

TOWBIN BUFFER
3.03 g Tris base, 14.4 g glycine, 500 ml diH_2O, 200 ml methanol, ad 1000 ml diH_2O

The following antibodies were used for protein detection:

ANTI-HALOTAG MOUSE MONOCLONAL ANTIBODY G9211
Promega, Mannheim, Germany

ANTI-GRK2 C15 RABBIT ANTIBODY SC-562
Santa Cruz Biotechnologies, Heidelberg, Germany

ANTI-β-ACTIN MOUSE ANTIBODY A5441
Sigma-Aldrich, Taufkirchen, Germany

Protein quantification was done using the Pierce™ BCA protein assay kit (ThermoFisher Scientific, Brunswick, Germany).
Antibodies were used in the concentrations and with buffers recommended by the respective manufacturer.
Electrophoresis was performed in a Mini-PROTEAN® Tetra Vertical Electrophoresis Cell (Bio-Rad Laboratories, Munich, Germany). Proteins were blotted onto Immobilon-P membranes (Merck Chemicals, Darmstadt, Germany) membranes using a Trans-Blot® Semi-Dry Transfer Cell (Bio-Rad Laboratories, Munich, Germany).
Amersham ECL Western Blotting Detection Reagent (GE Healthcare, Freiburg, Germany) was used for chemiluminescent detection on an ImageQuant LAS4000 biomolecular imager (GE Healthcare, Freiburg, Germany).

2.1.5 *Cell Lines*

All living cell experiments were performed in human embryonic kidney (HEK)-293 cells. Competent E. coli were used for plasmid transformation.

HEK-293 CELLS were provided by Prof. Hoffmann.

HEK ELUCC-OPRM1/ARRB1-ELUCN and

HEK ELUCC-OPRM1/ARRB2-ELUCN
: stably transfected cells were generously provided by Prof. Ozawa (Tokyo, Japan).

HEK-BLUE™ HTLR4 CELLS
: were purchased from InvivoGen, San Diego, CA, USA

HEK-BLUE™ NULL2 CELLS
: were purchased from InvivoGen, San Diego, CA, USA

COMPETENT E. COLI DH5α™
: were purchased from Invitrogen, Darmstadt, Germany.

2.1.6 *Opioids*

BUPRENORPHINE HYDROCHLORIDE
: Reckitt Benckiser Healthcare, Slough, UK

[D-ALA², N-ME-PHE⁴, GLY-OL]-ENKEPHALIN
: Bachem, Weil am Rhein, Germany

FENTANYL CITRATE
: Braun Melsungen, Melsungen, Germany

HYDROMORPHONE HYDROCHLORIDE
: Sigma-Aldrich, Taufkirchen, Germany

LEVOMETHADONE HYDROCHLORIDE
Sanofi-Aventis Deutschland, Frankfurt, Germany

MORPHINE HYDROHCLORIDE
Caesar & Loretz, Hilden, Germany

MORPHINE-6-GLUCURONIDE
Sigma-Aldrich, Taufkirchen, Germany

NALOXONE HYDROCHLORIDE
Braun Melsungen, Melsungen, Germany

NALTREXONE HYDROCHLORIDE
Sigma-Aldrich, Taufkirchen, Germany

OXYCODON HYDROCHLORIDE
Mundipharma, Limburg, Germany

PETHIDINE HYDROCHLORIDE
Hameln Pharmaceuticals, Hameln, Germany

PIRITRAMIDE
Janssen-Cilag, Neuss, Germany

REMIFENTANIL HYDROCHLORIDE
GlaxoSmithKline, Munich, Germany

SUFENTANIL HYDROGEN CITRATE
Janssen-Cilag, Neuss, Germany

TAPENTADOL HYDROCHLORIDE
Sigma-Aldrich, Taufkirchen, Germany

TILIDINE
Gödecke, Germany (now Pfizer)

TRAMADOL HYDROCHLORIDE
Grünenthal, Aachen, Germany

2.1.7 *Custom-made Buffers and Solutions*

FRET MEASURING BUFFER
140 mM NaCl, 5.4 mM KCl, 2 mM $CaCl_2$, 1 mM $MgCl_2$, 10 mM 4-(2-hydroxyethyl)-1-piperazineethanesulfonic acid (HEPES), pH 7.3

KCM BUFFER 5X
500 mM KCl, 150 mM $CaCl_2$, 250 mM $MgCl_2$

2.1.8 *Microscopes and Other Instruments*

AXIOVERT 200 INVERTED MICROSCOPE
Zeiss, Jena, Germany

LEICA TCS SP8 CONFOCAL MICROSCOPE
Leica, Wetzlar, Germany

ENVISION 2104 MICROTITER PLATE READER
Perkin Elmer, Waltham, MA, USA

GLOMAX DISCOVER MICROTITER PLATE READER
Promega, Mannheim, Germany

SPECTRAMAX PLUS 384 SPECTROPHOTOMETER
Molecular Devices, Sunnyvale, CA, USA

THERMOMIXER
Eppendorf, Hamburg, Germany

APPLIED BIOSYSTEMS 2720 THERMAL CYCLER
Thermo Fisher, Brunswick, Germany

NANODROP SPECTROPHOTOMETER
Thermo-Fisher, Brunswick, Germany

2.1.9 *Expendable Supplies and Materials*

CELL CULTURE DISHES AND FLASKS
Nunc Fisher Scientific, Schwerte, Germany

CELL SCRAPERS
Hartenstein Laborbedarf GmbH, Würzburg, Germany

CRYO-TUBES
Nunc Fisher Scientific, Schwerte, Germany

FALCON TUBES
BD Biosciences, Heidelberg, Germany

GLASS COVERSLIPS 24 MM
Hartenstein Laborbedarf GmbH, Würzburg, Germany

MULTI-WELL PLATES
Nunc Fisher Scientific, Schwerte, Germany
Sarstedt, Nümbrecht, Germany
Brandt, Wertheim, Germany

PIPET TIPS
Eppendorf, Hamburg, Germany

2.1.10 *Software*

ADOBE CREATIVE SUITE 6 Adobe Systems, San Jose, CA, USA

AXOSCOPE 10.3 Molecular Devices, Sunnyvale, CA, USA

CLAMPEX 10.3 Molecular Devices, Sunnyvale, CA, USA

GRAPHPAD PRISM 6 GraphPad, La Jolla, CA, USA

FIJI/IMAGEJ open-source freeware

LEICA LAS AF Leica, Wetzlar, Germany

OFFICE FOR MAC 15.15 Microsoft, Redmond, WA, USA

ORIGIN 9.1 Origin Labs, Northampton, MA, USA

SNAPGENE VIEWER 2.8 GSL Biotech, Chicago, IL, USA

2.2 METHODS

2.2.1 *Eukaryotic Cell Culture*

HEK-293 cells for transient transfection were kept in DMEM+++, stable HEK-293 cell lines were kept in the respective DMEM+++ supplemented with suitable selective antibiotics. These were Zeocin and G418 for the stable split-luciferase cell lines (HEK ElucC-OPRM1/ARRB1-ElucN and HEK ElucC-OPRM1/ARRB2-ElucN), Normocin and Zeocin for the HEK-Blue Null2 cells, and Normocin, Zeocin, and HEK-Blue Selection^{TM} for the HEK-Blue hTLR4 cells, respectively. Cells were cultured at 37 °C in a 5% carbon dioxide (CO_2) atmosphere and routinely split every two to three days at ∼60% confluency. Before splitting, HEK cells were washed gently with a few milliliters of Dulbecco's phosphate buffered saline (DPBS), which was immediately removed afterwards. The cells were then treated with 1 ml trypsin-ethylenediaminetetraacetic acid (EDTA) for 30 seconds. Supernatant trypsin was removed. The cell culture dish was tapped vigorously several times until the cells detached from the bottom of the dish. Subsequently, the cells were resuspended in 5 ml of DMEM+++, thus deactivating the remainder of the trypsin and seeded to a new culture dish (10 or 20 mm) in a sufficient volume of fresh growth medium.

For FRET experiments on G_i activation, cells were harvested at ∼40% confluency, seeded to D-polylysine-coated 24 mm round glass cover slips, and kept in 6-well plates. There they were kept in the incubator overnight in order for the cells to adhere properly to the glass. Then, the cells were transfected with 2.5 μg/plate human wild-type μ-opioid receptor (OPRM) DNA and 2.5 μg/plate G_i trimer

($G_{\alpha i}$-mTq2-$G_{\beta wt}$-G_{γ}-Venus) DNA using Effectene transfection reagent according to the manufacturer's protocol (20 μl enhancer, 50 μl Effectene). Growth medium was renewed after 24 hours and experiments were performed after a total of 48 hours.

In the μ receptor:β-arr interaction luciferase complementation experiments, HEK-293 cells were used which stably expressed the μ receptor and β-arr 1 or 2 with half an enhanced click beetle luciferase (Eluc) genetically attached to the receptor and the arrestin, respectively (HEK ELucC-OPRM1 / ARRB1-ELucN and HEK ELucC-OPRM1 / ARRB2-ELucN). The used constructs were designed by our collaborator in analogy to previously published GPCR/β-arr split luciferase pairs [192]. In preparation of the experiments, cells were harvested at 70% confluency and seeded onto 96-well microtiter plates (72,000 cells/well). The seeded cells were incubated in phenol red-free DMEM without selective antibiotics at 37 °C in a 5% CO_2 atmosphere for 24 hours.

For the μ receptor:β-arr2 BRET experiments, $1.0 \cdot 10^6$ HEK-293 cells were seeded to a regular 55 mm cell culture dish. After 3 hours in the incubator at 37 °C the cells were eventually transfected with 0.2 μg OPRM-Nluc DNA, 2 μg β-arr2-HaloTag DNA, and, when indicated, 1 μg GRK2 DNA. Growth medium was renewed after 24 hours. 48 hours after transfection the cells were counted again and 18,000 cells per well were seeded to a 96-well plate in Opti-MEM growth medium. The seeded cells were given three hours to attach to the wells' bottoms before experiments were performed. Counting of cells was done in a Neubauer counting chamber in each instance.

HEK-Blue TLR4 experiments were performed under the most aseptic conditions possible at all times. HEK-Blue hTLR4 were kept in DMEM+++ additionally supplemented with 100 μg/ml Normocin and 1x HEK-Blue Selection, which are both mixtures of (selective) antibiotics undisclosed by the manufacturer. HEK-Blue Null2 cells were cultured in DMEM+++ additionally supplemented with 100 μg/ml Normocin and 100 μg/ml zeocin. Both cell lines were seeded to 75 ml cell culture flasks, kept in a 5% CO_2 atmosphere at 37 °C in an incubator for tested mycoplasma-free cells only, and split regularly every two to three days as elaborated above.

Whenever it was necessary to freeze HEK cells for later use, they were grown on 200 mm cell culture dishes to ∼80% confluency. After gentle washing with DPBS they were detached as described before and resuspended in 5 ml DMEM+++ freezing medium. 1 - 1.25 ml of this suspension were transferred into each cryo tube and put into an iced tube rack, immediately. The tubes were put in a -20 °C freezer overnight, immediately. After that, the tubes were transferred either to a -80 °C freezer or liquid nitrogen for long-term storage.

2.2.2 *E. coli Transformation*

Competent E. coli (stored at -80 °C) were slowly thawed on ice. Afterwards, ~50 ng of the desired plasmid DNA were mixed with 100 µl of E. coli suspension and 100 µl KCM buffer stock solution and incubated for 20 minutes on ice and another ten minutes at room temperature. Next, 900 µl lysogeny broth (LB) were added and the suspension was incubated in a Thermomixer™ at 37 °C shaking at 300 rpm.

After incubating, the suspension was centrifuged at 200·g for 5 minutes. Most of the supernatant was discarded, the rest was used to resuspend the bacteria pellet. Of this suspension, 50-100 µl, depending on prior transformation efficiency, were plated onto an LB agar dish with the selective antibiotic (ampicillin or kanamycin) and kept at 37 °C overnight.

On the following day, a single colony was picked and cultured overnight in LB with selective antibiotics at 37 °C, shaking at 300 rpm.

2.2.3 *DNA Midi Preparation*

Preparation of plasmid DNA from E. coli transformed as described above was performed using the NucleoBond Xtra kit (Macherey-Nagel, Düren, Germany) according to the manufacturer's instructions. DNA concentration and purity were measured using a NanoDrop 2000 spectrophotometer. When needed, DNA was diluted in purified H_2O. Dissolved plasmid DNA was stored at -20 °C.

2.2.4 *Cloning of µ Receptor / β-Arrestin2 BRET Constructs*

The purchased NanoBRET® expression vectors come in a variety of versions. Both the NanoLuciferase (Nluc) and the HaloTag vectors exist with the target protein DNA insertion site upstream or downstream of the luciferase or HaloTag coding region, respectively. This allows to determine the position of the desired protein relative to Nluc/HaloTag (C-or N-terminal). Additionally, the HaloTag vectors come in four different versions for C- and N-terminal expression, each. Those four vector variants differ in the length of the cytomegalovirus (CMV) promotor, which is supposed to control protein expression levels in a differentiated manner. That is why there is one vector with the full CMV promotor (742 bases) and three more with gradually truncated promotors (121, 73, and 66 bases; see figure 8). Findings of this work could confirm the usefulness of truncated promotors only to a certain degree (see figure 13).

The plasmid constructs used in this work were cloned by Ulrike Zabel roughly as follows: The desired protein's cDNA sequence was

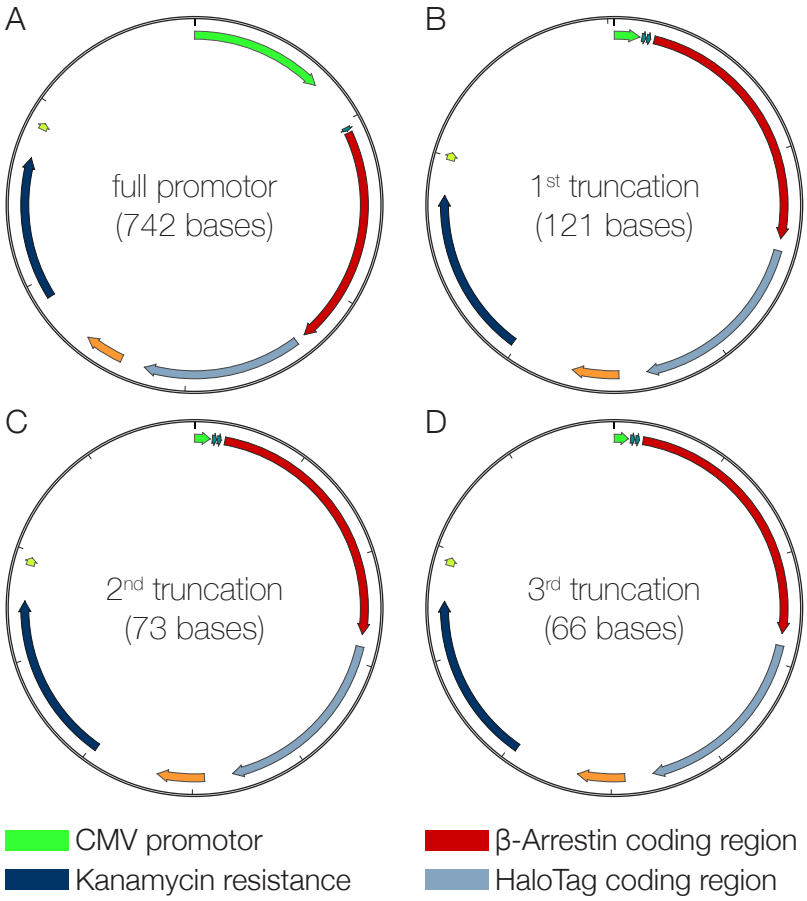

Figure 8: Plasmid maps of four cloned β-arr2-HaloTag fusion constructs. (A) Full CMV promotor length (742 bases). The promotors in (B-D) are gradually truncated (121, 73, and 66 bases)

aplified by PCR from the above-mentioned sources. Cloning primers for μ receptor and β-arr2 DNA were chosen in such a way that a 5‘ SgfI restriction site and a 3‘ PmeI restriction site were appended to the protein-coding region. The expression vector plasmids contain a lethal gene (barnase) in a locus between those very two restriction enzymes. Digesting the expression vectors with SgfI and PmeI removes the lethal gene and produces a linear DNA strand, which was separated from the barnase-coding region by electrophoresis in a 1% agarose TAE gel. An analog procedure yields the protein-coding PCR product with "sticky ends". The so treated complementary DNA fragments were mixed at a 1:3 (vector:insert) molar ratio and ligated by T4 DNA ligase. Purified ligation products were delivered into competent E. coli for replication as described. Screening of successfully transformed E. coli was effected by means of antibiotic selection (kanamycin). All cloned plasmid constructs used in this work were sequenced (Eurofins Genomics, Ebersberg, Germany).

2.2.5 *Confocal Microscopy*

Confocal microscopy was used to control transfection efficiency, expression, and cellular localization of fluorescent proteins. To this end, HEK-293 cells were harvested, suspended in growth medium and then seeded onto poly-D-lysin coated 24 mm glass coverslips in a 6-well cell culture dish to an initial confluence of $\sim$ 30%. Cells were then kept in an incubator at 37 °C in a 5% CO_2 atmosphere for three hours. Following this, cell were transfected with amounts of plasmid DNA varying from 16 - 450 ng per well. Transfections were done using Effectene transfection reagent according to the manufacturer's recommendations. Cells were kept in an incubator as described above for 48 hours, with renewal of the growth medium after 24 hours.

The glass coverslips bearing the cells to be imaged were then mounted in an Attofluor cell chamber (ThermoFisher Scientific) and onto the microscope immediately before the experiment. During that time, the cells were kept in measuring buffer. Depending on the fluorescent dyes used, the maximum imaging magnification was set in such a way that the Nyquist criterion be met at all times. Cyan fluorescent proteins (CFP and mTq2) were excited with a 442 nm diode laser, yellow fluorescent proteins (YFP and Venus) were excited with a 514 nm argon laser. Optimum use of the detectors' dynamic range was ensured before imaging.

Images were recorded and stored in a Leica proprietary file format (*.lif). All image editing was done with a Fiji distribution of ImageJ [193–195].

2.2.6 *FRET experiments*

FRET measurements were done through a Zeiss Axiovert 200 inverted microscope. It was equipped with an oil immersion 63x objective lens and a dual-emission photometric system (Till Photonics, Gräfelfing, Germany). Setups very similar to this one have been used before and described in the literature [61, 64]. Cover slips prepared as described in section 2.2.1 were mounted onto the microscope shortly before the experiment. The transfected cells were excited with light from a polychrome IV (Till Photonics). The excitation light spectrum was first capped by a dichroic long-pass beamsplitter at 460 nm and after that narrowed down to 436 $\pm$ 10 nm by a band-pass filter. Illumination during FRET measurements was set to 40 ms applied with a frequency of 10 Hz.

Light emitted from the samples was split into acceptor and donor beams by a dichroic long-pass beam splitter at 505 nm. Two band-pass filters restricted the recorded emissions wavelengths (donor 480 $\pm$ 20 nm; acceptor 535 $\pm$ 15 nm). Signals from cyan fluorescent proteins (CFP and modified Turquoise 2 fluorescent protein (mTq2)) and

yellow fluorescent proteins (YFP and Venus) were recorded simultaneously as well as the ratio of both (math = $\frac{acceptor}{donor}$). FRET ratios were offline corrected for bleed-through of cyan fluorescent protein (CFP) emission to the yellow fluorescent protein (YFP) channel and direct excitation of YFP fluorophores (correction factors 0.85 and 0.12, respectively) using Origin 9.

During FRET measurements, the cells were maintained in measuring buffer and permanently superfused with said buffer using a computer-assisted solenoid valve-controlled rapid superfusion device (ValveLink 8.2, Automate Scientific). Fluorescence signals were detected by photodiodes and digitalized using an analogue-digital converter (Digidata 1440A, Axon Instruments). All data were recorded on a PC running Clampex 10.3 software (Axon Instruments). Every array of application of various concentrations of a ligand was succeeded by the application of 10 μM DAMGO as a reference compound. In order to obtain reliable concentration-response curve fits, every ligand was measured in at least six different concentrations. Every concentration of every ligand was usually measured at least five times independently on at least three separate days. One exception were experiments with antagonists, where three repeated measurements showing no change in FRET signal were regarded sufficient.

2.2.7 *Luciferase Complementation Assay*

The μ receptor:β-arr luciferase complementation experiments were conducted by Stefanie Meyer as part of her MD thesis (not published yet).

On the day of the experiment, the cells in 96-well plates were incubated with different concentrations of ligand for 12 min at 37 °C in a 5% CO_2 atmosphere. 100 μl/well of Bright-Glo Assay ReagentTM (Promega, Mannheim, Germany) were added . The assay reagent contains the luciferase substrate and also lyses the cells. To ensure complete cell lysis and light adaptation the cells were incubated for another 2 min inside the EnVision microplate reader.

Eluc activities were measured for 1 sec per well using an emission filter detecting luminescence at 400-700 nm as a quantitative readout of receptor:β-arr interaction. On every plate, measurements were done in duplicates. As a control to subtract background luminescence FRET measuring buffer was used. 100 μM DAMGO served as a reference. All measurements were performed four times on different days.

2.2.8 *BRET Assay*

Cells for BRET experiments were prepared as described in 2.2.1. At the beginning of the experiments, each well of a white flat-bottom 96-well microtiter plate (pureGrade^{TM}, Brand GmbH, Wertheim, Ger-

many) contained 90 μl of cells resuspended in Opti-MEM. 25 μl of a 50 μM NanoGlo® substrate stock (luciferase substrate; Promega, Mannheim, Germany) were then added to each well, eventually resulting in a 10 μM final concentration. The substrate was added to the microtiter plates manually and it turned out that the time the pipetting took was sufficient for maximum luciferase emission to occur (also see figure 14). Next, 12.8 μl of 10x concentrated stocks of the desired opioid ligand concentrations were added to the wells. Readout in the GloMax Discover plate reader was started immediately thereafter, usually resulting in a latency time from ligand addition to signal readout of $\sim$120 seconds for every single well. Measurements were done in duplicates. Also, four wells of unlabeled HaloTag acceptor constructs (i.e. without acceptor fluorophor) were measured as a background control on every plate. Moreover, four wells were stimulated with a saturating concentration of DAMGO (100 μM), which then served as a reference for normalization for each respective concentration-response curve. Every ligand was measured in eleven concentration increments at least three times independently on different experimental days.

Results were exported by the plate reader's software to Microsoft Excel files. Output variables were donor emission, acceptor emission and BRET ratio, where

$$\text{ratio} = \frac{\text{acceptor emission}}{\text{donor emission}}.$$

2.2.9 *Western Blot*

Western blotting was performed according to the following scheme: Cells were seeded in such a way that they reached 70-80% confluency on the day of cell lysis. If the target protein was to be extracted from transiently transfected cells, transfection was done 48 hours in advance in a 100 mm cell culture dish.

First, cells were washed with ice-cold DPBS and 1 ml of fresh Laemmli sample buffer (see 2.1.4) was added to the cells. The plates were stored on ice and slowly shaken for 20 minutes. After this, the lysed cells were scraped off the dish and sonicated in a 1.5 ml Eppendorf tube for one second. The sonicated lysates were stored on ice or frozen at -20 °C for future use.

Quantification of protein contained in the lysates was effected by means of the Pierce BCA protein assay kit according to the manufacturer's protocol. The GloMax Discover plate reader was used for colorimetric readout.

SDS gels were prepared in a BioRad electrophoresis cell (see section 2.1.4) as follows. For the lower gel 13.5 ml H_2O, 7.9 ml lower buffer, 10.1 ml acrylamide, 15.75 μl TEMED, and 204.8 μl ammonium persulfate (APS) were mixed and transferred to the casting stand. Iso-

propanol was pipetted on top to ensure a smooth surface of the gel. As soon as the gel was set, the isopropanol was removed and the upper gel mix (8.3 ml H_2O, 3.3 ml upper buffer, 1.7 ml acrylamide, 13.2 μl TEMED, 132 μl APS) was transferred to the casting stand. A gel comb was inserted and the upper gel polymerized within 15 minutes.

The volume of lysate loaded to each well was adjusted to yield the desired amount of protein. The various amounts of protein used varied between experiments and are pointed out in detail in the respective results sections. Electrophoresis took place in fresh running buffer at 80 V in the upper part and at 150 V in the lower part of the gel. After completion of the electrophoresis, the gel was transferred to filter paper soaked in Towbin buffer. The proteins were blotted onto a Millipore Immobilon-P membrane in a BioRad semi-dry transfer cell during 60 minutes at 15 V. The mebrane was activated beforehand according to the manufacturer's recommendations with methanol and pre-soaked with Towbin buffer.

After blotting was finished, the filter was left in blocking buffer on the shaker for one hour at room temperature. Subsequently, the blocking buffer was discarded and the filter was incubated with the primary antibody at 4 °C shaking overnight.

The following day, the gel was washed in wash buffer six times for ten minutes each. Next, the gel was incubated with the secondary antibody shaking for 60 minutes at room temperature. This was followed by another washing step in analogy to the one described above.

Chemiluminescent imaging was done as indicated by the manufacturer of the detection reagent (see section 2.1.4).

2.2.10 *HEK-Blue Reporter Gene Assay*

To investigate whether and to what extent the opioids used in this study could induce TLR4 signaling, a commercial reporter gene assay (HEK-Blue, InvivoGen) was implemented. This reporter gene assay was used before for similar experiments in the literature [189]. In brief, activation of TLR4 in the cells will lead to increased production of NF-κB, which in turn promotes the synthesis of a secreted embryonic alkaline phosphatase (SEAP). SEAP will eventually cause a special detection medium to change its color from red to blue, which can be read out as a semiquantitative measure of receptor activation. A TLR4-deficient, but otherwise identical cell line (HEK-Blue Null2) served as a control.

Proper TLR4 signaling is dependent on the additional presence of MD2, a secreted adaptor protein and CD14, which functions as a co-receptor. Both proteins are stably expressed in the cell lines. The natural ligand of TLR4 is LPS, also known as endotoxin from the outer membrane of Gram-negative bacteria. LPS was used as positive control in the experiments.

For the TLR4 activation experiments, HEK-Blue hTLR4 and HEK-Blue Null2 cells were grown to 50-80% confluency under conditions described in 2.2.1. Cells were then washed cautiously with DPBS. This DPBS was removed and fresh 2-5 ml of DPBS were added to the cells. The flask was then put into the incubator at 37 °C for two minutes. After that, the flask was tapped lightly to detach the cells. They were suspended in the DPBS and counted. A suspension was prepared to contain ∼140,000 cells/ml (HEK-Blue hTLR4) or 280,000 cells/ml (HEK-Blue Null2) in HEK-Blue Detection medium. 20 μl of sample solution or LPS as a positive control or sterile water as a negative control, respectively were given into each well of a 96-well plate. Then, 180 μl of the prepared cell suspension were added to those wells, resulting in a concentration of 25,000 cells per well (50,000 cells per well in the case of HEK-Blue Null2 controls). An incubation time of 12-16 hours was needed for the SEAP to catalyze the color reaction. After that time span, the extinction at 655 nm was determined using a spectrophotometer (SpectraMax Plus 384).

2.2.11 *Data Manipulation and Analysis*

FRET experiments (section 2.2.6): All obtained signal amplitudes were normalized to the signal amplitude elicited by 10 μM DAMGO in each respective experiment. Normalized data points of corresponding ligand concentrations were pooled and fit to a four-parameter sigmoidal curve with the bottom set to zero; all other parameters were fit freely. Luciferase complementation experiments (2.2.7): Emission intensities were averaged and normalized to 100 μM DAMGO. Standard four-parameter sigmoidal curve fitting was done using GraphPad Prism 6. Bottom was set to zero, all other parameters were fit freely. For each ligand, four concentration-response curves were plotted seperately. The pharmacological parameters E_{max} and EC_{50} were averaged from the respective four independent fits.

BRET experiments (2.2.8): Unlabeled acceptor control BRET ratios were subtracted from ligand-stimulated BRET ratios to control for bleed-through from the donor into the acceptor channel. These corrected ratio duplicates were plot independently for every ligand on every plate. Four parameter sigmoidal curve fitting was performed and the output bottom value was used to define zero when normalizing the data. Also, the data were normalized to their plate's 100 μM DAMGO reference signal. Normalized data were fit again to a four-parameter sigmoidal curve with bottom fixed at zero; all other parameters were fit freely.

Calulation of ligand bias was done largely as described by Kenakin et al. [166]. In brief, the concentration-response data were fitted to

the operational model of pharmacological agonism by Black and Leff [164] according to the following equation:

$$response = \frac{E_m[A]^n\tau^n}{[A]^n\tau^n + ([A] + K_A)^n} \quad ,$$

where E_m is the maximum response of the system, $[A]$ is the agonist concentration, n is the transducer slope, K_A is the agonist equilibrium dissociation constant and τ is the ratio $[R_t]/K_E$, with $[R_t]$ being the receptor density and K_E being the intrinsic efficacy of the agonist for one specific signaling pathway. As always, curve-fitting was done with GraphPad Prism 6. Standard output parameters were τ, K_A, $\log\tau$, $\log K_A$, and their respective standard errors and confidence intervals. The software was additionally programmed to fit the desired transduction coefficient $\log(\tau/K_A)$ as a parameter of its own.

Curve-fitting was performed like this for all ligands and all signaling pathways seperately. Thereafter, $\Delta\log(\tau/K_A)$ values were calculated as the difference between $\log(\tau/K_A)_{ligand}$ and $\log(\tau/K_A)_{reference}$. The difference between $\Delta\log(\tau/K_A)_{pathway1}$ and $\Delta\log(\tau/K_A)_{pathway2}$ returns $\Delta\Delta\log(\tau/K_A)$ for any two signaling pathways and each ligand. As a slight aberration from the approach in [166] the propagation of standard errors was approximated as follows:

$$error = \sqrt{{error_A}^2 + {error_B}^2}$$

for each arithmetic operation. The final standard errors were transformed into confidence intervals for depiction in the bias plots (see section 3.7).

3 RESULTS

3.1 OPTIMIZATION OF A G_i FRET SENSOR

The activation of G_i at the μ receptor was quantitatively assesed by a FRET-based sensor as described in section 2.2.6. In order to ensure proper expression of all three G protein subunits, confocal images of HEK cells transfected with the μ receptor and the G_i sensor trimer in the same way as for the FRET experiments were taken. figure 9 shows the expression of both fluorophores (mTq2 and Venus), i.e. the protein subunits they were genetically attached to (G_α and G_γ, respectively). Both subunits are located near the cell membrane. This makes the existence of a functional trimer reasonable, thus suggesting also proper expression of the non-fluorescent β subunit. Relative abundance of Venus over mTq2 may be derived from the images, although no quantification to this end was done. This finding would be in line with the plasmid's authors claiming an approximately 3:1 expression ratio (upstream:downstream of the IRES sequence) [196].

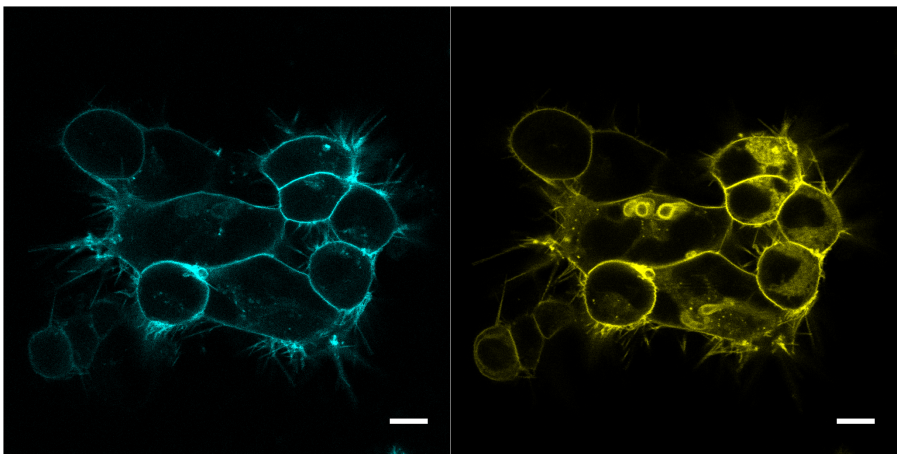

Figure 9: Confocal image of HEK-293 cells transfected with the G_i trimer plasmid; left: mTq2 channel, right: Venus channel. Scale bars represent 25 μm.

The search for optimal DNA amounts of receptor and G protein for transfection was an iterative process. When transfecting with 2.5 μg of each plasmid per 6-well plate, a loss in normalized FRET ratio of more than 20% could be achieved (figure 10, bottom red trace). Incremental addition of ligand concentrations led to ever more loss in FRET ratio. Final application of a saturating DAMGO concentration (10 μM) gave the reference signal for this very experiment. The yellow and blue traces show the corresponding signals from the Venus and

mTq2 channels. The two signals developing in an antiparallel manner was another proof of a functioning FRET system: loss in signal from one fluorophore translates into gain of the other and vice versa. As the α and the $\beta\gamma$ subunits move away from each other or even dissociate upon activation [64], incremental loss in FRET ratio during the course of the experiments was reasonable, too.

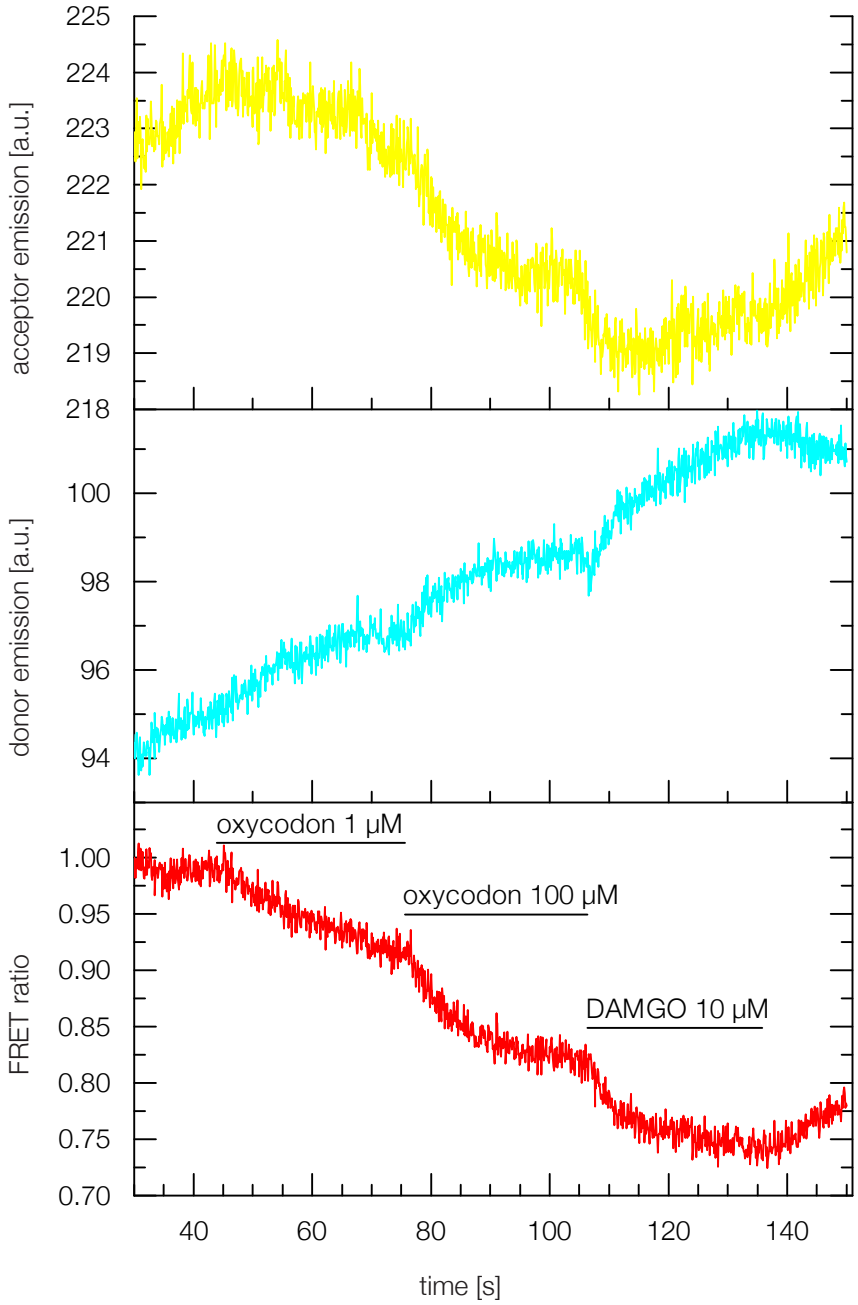

Figure 10: Exemplary traces of a single FRET measurement. All three traces were recorded simultaneously. Bars indicate the addition of ligand during that period of time. Note that the depicted donor and acceptor traces were not yet corrected for bleed-through and direct excitation, whereas the FRET ratio trace was calculated from corrected values.

3.2 LIGAND-DEPENDENT ACTIVATION OF G_i AT THE μ RECEPTOR

With the described sensor at hand, the pharmacological dynamics of G_i activation by 17 opioid ligands were examined. The data sufficed to cover the full concentration-response range for all of the opioids. Standard sigmoidal four parameter fit allowed for the following classification of the ligands into subgroups:

FULL AGONISTS
: DAMGO, buprenorphine, fentanyl, L-methadone, piritramide, remifentanil, sufentanil

PARTIAL AGONISTS
: hydromorphone, M-6-G, morphine, oxycodone, pethidine, tapentadol, tilidine, tramadol

ANTAGONISTS
: naloxone, naltrexone

Graphed concentration-response curves are given, grouped in the same manner: full agonists (figure 11) and partial agonists / antagonists (figure 12). Graphs were derived from standard four-parameter sigmoidal fits. The full agonists cover a potency range of around 2.5 log levels, with $logEC_{50}$s ranging from -8.48 (remifentanil) to -6.12 (piritramide). The reference compound DAMGO lies in between ($logEC_{50}$=-7.43).

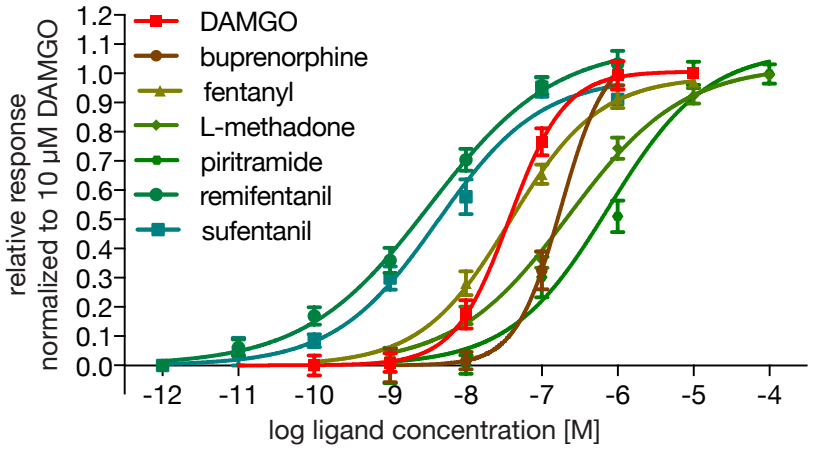

Figure 11: Concentration-response curves of full agonists for G_i activation. Error bars denote SEM, n≥3.

For four opioids a plateau signal could not be reached, which adds extra uncertainty to their respective E_{max} and EC_{50} values. Pethidine, tapentadol, and tramadol turned out to be rather low-potency agonists (EC_{50} 42500 and 138000 nM). Higher ligand concentrations than the ones used could not be prepared for the experiments. Buprenorphine has high potency (179 nM) and very high receptor binding

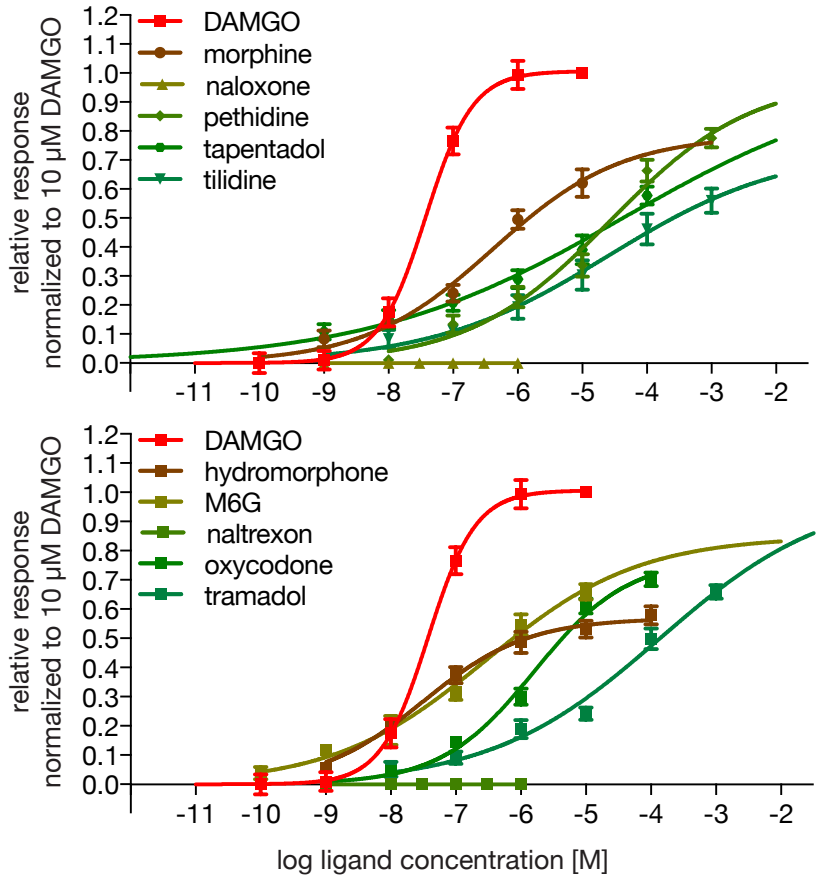

Figure 12: Concentration-response curves of DAMGO and partial agonists for G_i activation. Error bars denote SEM, n≥3.

affinity, which made it difficult to determine its maximum response relative to a reference substance (also see Discussion, section 4.1). Detailed pharmacological properties of all ligands are given in table 2.

	Emax (S.E.M.)	$EC50$ $[nM]$	logEC50 (S.E.M.)
DAMGO	1.01 (0.07)	37.5	−7.43 (0.15)
Buprenorphine*	< 1 –	179	−6.75 –
Fentanyl	0.99 (0.02)	38.1	−7.42 (0.04)
Hydromorphone	0.57 (0.03)	31.7	−7.50 (0.15)
M6G	0.85 (0.12)	290	−6.54 (0.40)
L-Methadone	1.03 (0.03)	227	−6.65 (0.09)
Morphine	0.79 (0.14)	412	−6.39 (0.46)
Naloxone	0.0 –	–	– –
Naltrexone	0.0 –	–	– –
Oxycodone	0.77 (0.06)	1610	−5.79 (0.17)
Pethidine*	0.98 (0.21)	26900	−4.57 (0.62)
Piritramide	1.08 (0.12)	758	−6.12 (0.27)
Remifentanil	1.1 (0.03)	3.32	−8.48 (0.08)
Sufentanil	0.99 (0.07)	4.22	−8.38 (0.18)
Tapentadol*	> 0.6 –	42500	−3.86 (0.98)

	Emax (S.E.M.)	$EC50$ $[nM]$	logEC50 (S.E.M.)
Tilidine	0.74 (0.11)	25700	−4.59 (0.47)
Tramadol*	> 0.7 –	138000	−3.86 (0.98)

Table 2: Pharmacological properties of 17 opioid ligands for the activation of G_i. (*) Maximum agonist response could not be obtained, corresponding EC50 values are an approximation.

3.3 Ligand-dependent recruitment of β-arrestins 1 and 2 to the μ receptor (luciferase complementation)

Data on β-arr 1 and 2 recruitment were determined by a luciferase complementation assay, which was performed by Stefanie Meyer as part of her MD thesis (unpublished work). An overview of the data is given in table 12 in section A.2 of the appendix. These data served in part as the basis for the calcuation of ligand bias performed in this work.

3.4 Implementation of a BRET-based β-arrestin 2 recruitment assay

In order to implement the NanoBRET™ assay as a tool for measuring μ receptor:β-arr2 interaction, first the coding regions of both the receptor and the arrestin were cloned into the respective vectors. This was mainly done by Ulrike Zabel. As pointed out in section 2.2.4, the empty cloning vectors came in different configurations such that one can position the Nluc or HaloTag at the N or C terminus of the respective target protein. Additionally, the HaloTag cloning vectors came with different promotor truncations for alledged control of protein expression. The μ receptor was cloned only to have the Nluc attached to the C terminus. The N terminus of the receptor lies outside the cell and is therefore too far apart from a possibly binding β-arr for BRET to occur. β-arr2 was cloned with the HaloTag attached to both termini and with all four promotor truncations, each. No constructs with the luciferase at the arrestin and the HaloTag at the receptor were created. Eventually, nine plasmid constructs were created to screen for an ideal BRET pair: one receptor-luciferase(C), four HaloTag(N)-arrestins, and four arrestin-HaloTag(C)s. Successful cloning was confirmed by plasmid sequencing (data not shown).

The effect of the truncated CMV promotors on protein expression levels was controlled by Western blotting from cell lysates of HEK

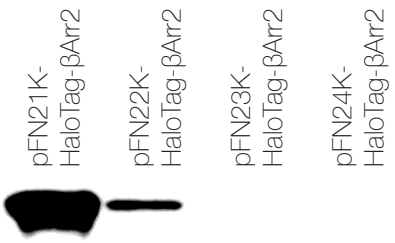

Figure 13: Western blot of the four different β-arr2 plasmid constructs with an N-terminal HaloTag. Total protein amount per well: 70 μg. Digital contrast enhancement and background subtraction was performed.

cells transfected with 2 μg plasmid DNA per 100 mm dish 48 hours prior to cell lysis. Western blots were done as explained in section 2.2.9 using an antibody against the HaloTag. The constructs with the full promotor showed strong protein expression, those with the longest truncation were found to cause expression levels still detectable in the blots. The plasmids with the two shortest promotor versions (73 and 66 bases) did not cause any traceable protein expression. These findings were confirmed in repeated blots for both C and N terminally attached HaloTags. figure 13 shows an exemplary blot from 70 μg total protein per well of the four N terminal constructs.

With these results at hand, the decision for the best HaloTag/arrestin fusion protein had to be made choosing from the four constructs that were expressed at all in the cells (pFC14K-β-arr2-HaloTag, pFC15K-β-arr2-HaloTag, pFN21K-HaloTag-β-arr2, pFN22K-HaloTag-β-arr2). To this end, BRET experiments were performed with cells transfected with 0.2 μg pFC32K-Nluc-OPRM, 2.0 μg of the arrestin / HaloTag construct in question, and 1.0 μg GRK2. The receptor kinase was co-transfected to ensure sufficient receptor phosphorylation. General assay preparations were done as described in section 2.2.8. After a first read-out in the plate reader without ligand added, DAMGO was added to a resulting concentration of 100 μM. Figure 14 shows the kinetics of the corrected BRET signal of all four plasmid pairs. It turned out that the constructs with the full promotor caused a steeper and higher increase in BRET ratio than the plasmids with the 121 bases truncated promotors. Moreover, the full signal was achieved in the first measurement after ligand addition for all four constructs. The time between manual ligand addition and first read-out varied slightly from experiment to experiment, but generally was in the range of 50 to 60 seconds. These findings were confirmed in repeated experiments (data not shown).

To eventually choose one HaloTag construct as BRET interaction partner, repeated endpoint measurements were performed with pFC14K-β-arr2-HaloTag and pFN21K-HaloTag-β-arr2. BRET ratios were corrected and normalized to the baseline signal before ligand addition.

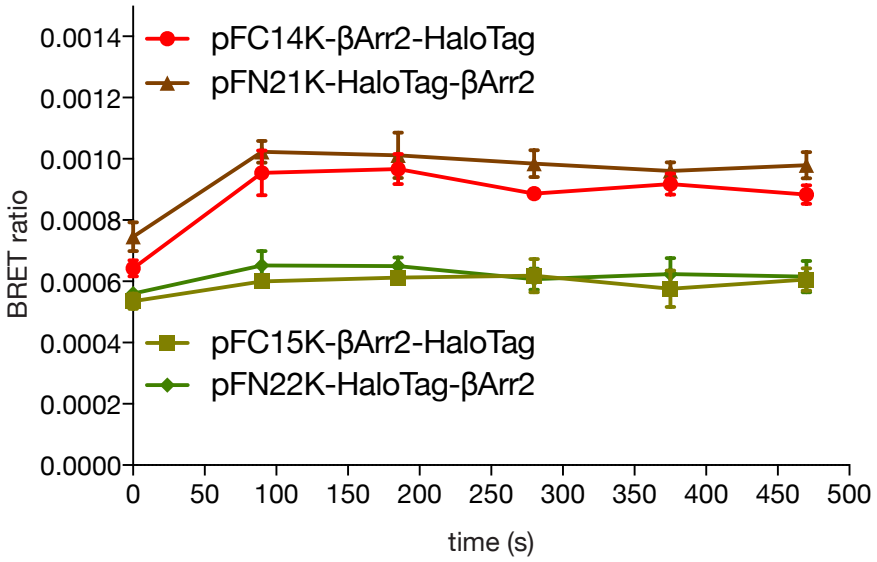

Figure 14: Time course of the BRET ratios of four different β-arr2-HaloTag plasmid constructs used for transfection. Addition of a saturating concentration of DAMGO took place after acquisition of the data point at time point zero. Error bars indicate SD, n=2.

By this approach, the BRET pair with the highest dynamic range, i.e. largest difference between lowest and highest detectable signal, could be identified. Results are shown in figure 15. Both BRET pairs show maximum responses of around 3-fold over baseline. Even if pFC14K-β-arr2-HaloTag presented with slightly more scatter than pFN21K-HaloTag-β-arr2, the former was eventually chosen as BRET acceptor due to its higher signal intensity.

As a last step of sensor optimization the ratio of used plasmid DNA was varied. The following ratios of receptor:arrestin were under investigation:

- 0.02 : 2.0
- 0.1 : 2.0
- 0.2 : 2.0
- 1.0 : 2.0 and
- 1.0 : 1.0

The highest signal could be achieved with 0.1 and 0.2 μg arrestin with no major differences between the two. When approaching a 1:1 ratio, signal intensities decreased markedly. However, decreasing the amount of receptor DNA to only 0.02 μg did not further enhance signal quality (detailed data not shown). Eventually, the transfection ratio with 0.2 μg receptor and 2.0 μg arrestin was maintained as it produced robust signals throughout the optimization process and no substantial improvements seemed possible.

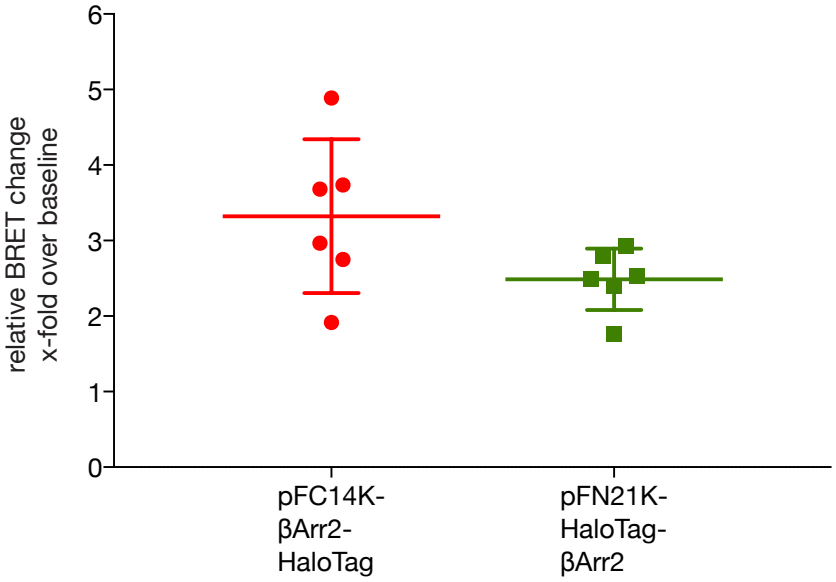

Figure 15: Scatter plot of maximum BRET responses to a saturating DAMGO concentration of 100 μM. Error bars indicate SD, n=6.

3.5 LIGAND-DEPENDENT RECRUITMENT OF β-ARRESTIN 2 TO THE μ RECEPTOR (BRET)

With the optimized BRET assay at hand, ligand and concentration-dependent recruitment of β-arr 2 to the μ receptor was investigated in detail. Since there were supply shortages for tilidine, full datasets are available for 16 opioids. By their capability to bring the arrestin to the receptor, the opioids can be categorized as follows:

FULL AGONISTS AND SUPERAGONISTS
: DAMGO, fentanyl, L-methadone, pethidine, remifentanil, sufentanil, tapentadol.

PARTIAL AGONISTS
: hydromorphone, M-6-G, morphine, oxycodone, piritramide, tramadol.

ANTAGONISTS
: buprenorphine, naloxone, naltrexone.

With efficacies higher than the full-agonist reference DAMGO, L-methadone (E_{max}=1.13), remifentanil (E_{max} = 1.20), and tapentadol (E_{max} = 1.20) qualified as super-agonists. However, remifentanil was the only one among those three with markedly higher potency than DAMGO ($logEC_{50}$ -7.53 vs. -6.98). The full agonists covered a wide range of potencies from from pethidine ($logEC_{50}$ = -3.94) to sufentanil ($logEC_{50}$ = -8.17) with DAMGO in between ($logEC_{50}$ = -6.98). All the partial agonists presented with rather high efficacies with oxycodone being the weakest (E_{max}=0.68). Solely tramadol fell out of line

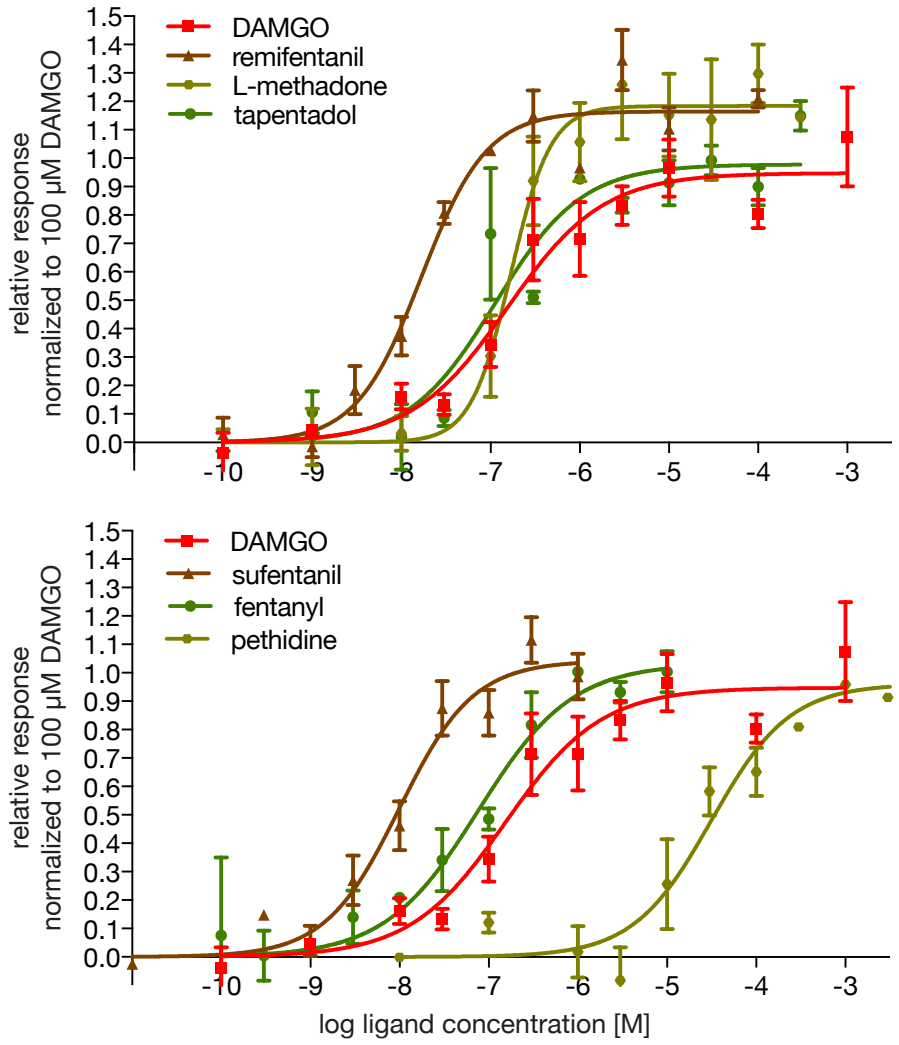

Figure 16: Concentration-response curves of full agonists and superagonists for β-arr2 recruitment to the μ receptor. Data are derived from BRET experiments, GRK2 was overexpressed in the cells. Error bars denote SEM, n=2.

(E_{max}=0.34). Antagonists were naloxone and naltrexone, as expected, and buprenorphine.

Signal plateaus could be obtained for all agonists, yet again standard errors increase with decreasing potency and efficacy. Full concentration-response curves can be found in figure 16 for full agonists and superagonists and in figure 17 for partial agonists and antagonists. As opposed to the G_i data in section 3.2, β-arr BRET data were not pooled. The graphed data therefore represent only one of usually three independent experiments. Curves are derived from standard four parameter sigmoidal fits.

A complete overview of the pharmacological properties of the 16 opioids can be found in table 3. Note that the values given there

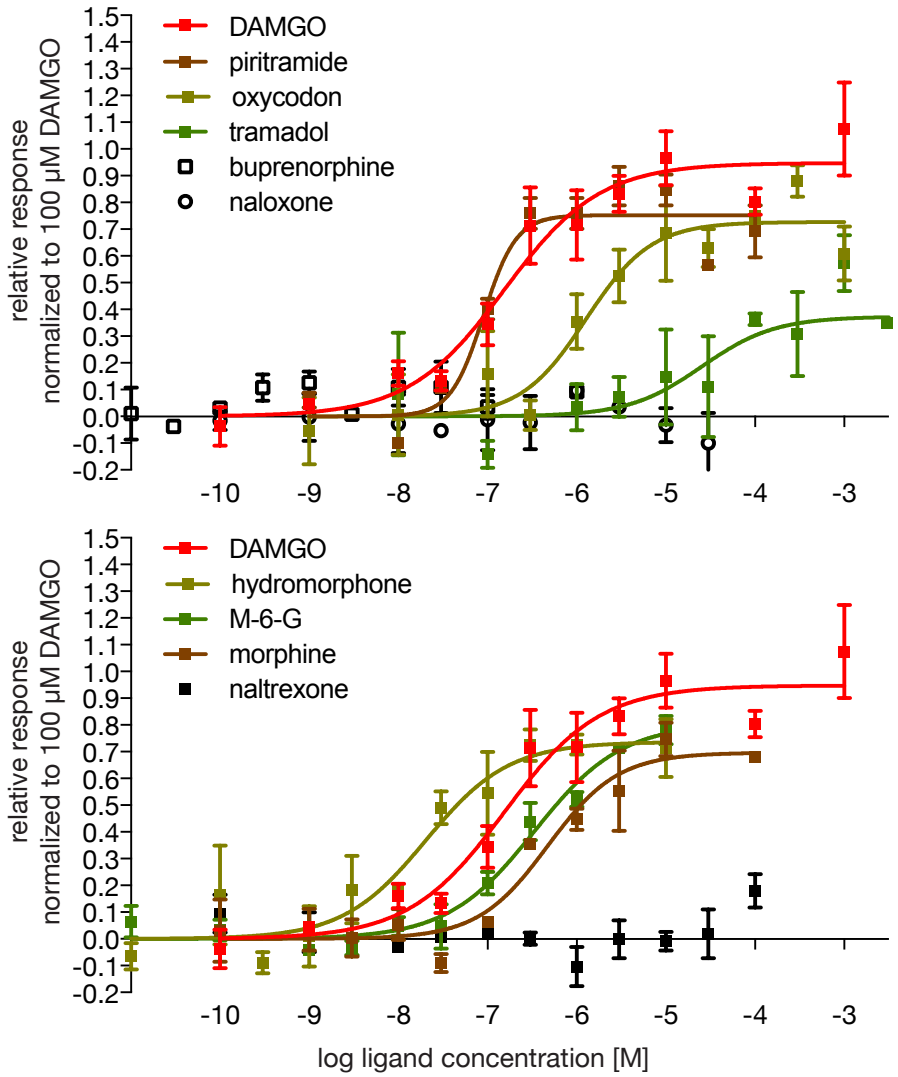

Figure 17: Concentration-response curves of partial agonists and antagonists for β-arr2 recruitment to the μ receptor. Data are derived from BRET experiments, GRK2 was overexpressed in the cells. DAMGO is shown for orientation purposes. Error bars denote SEM, n=2.

are means from all individual experiments for each ligand and might therefore not entirely match the shown concentration-response curves.

	Emax (S.E.M.)	$EC50$ $[nM]$	logEC50 (S.E.M.)
DAMGO	0.98 (0.10)	106	−6.98 (0.27)
Buprenorphine	0.0 –	–	– –
Fentanyl	1.05 (0.14)	42.0	−7.38 (0.30)
Hydromorphone	0.72 (0.12)	32.8	−7.48 (0.30)
M6G	0.91 (0.32)	313	−6.51 (0.54)
L-Methadone	1.13 (0.09)	233	−6.63 (0.19)
Morphine	0.83 (0.09)	390	−6.41 (0.20)
Naloxone	0.0 –	–	– –
Naltrexone	0.0 –	–	– –
Oxycodone	0.68 (0.10)	1090	−5.96 (0.38)
Pethidine	1.14 (0.66)	116000	−3.94 (1.72)
Piritramide	0.88 (0.09)	117	−6.93 (0.26)
Remifentanil	1.20 (0.09)	29.2	−7.53 (0.16)
Sufentanil	0.97 (0.11)	6.75	−8.17 (0.21)
Tapentadol	1.20 (0.20)	265	−6.58 (0.47)

	Emax (S.E.M.)	$EC50$ $[nM]$	logEC50 (S.E.M.)
Tilidine		#	
Tramadol	0.34 (0.16)	78800	−4.10 (1.35)

Table 3: Pharmacological properties of 16 opioid ligands for β-arr2 recruitment. GRK2 was overexpressed in the cells. Error bars indicate SEM, n=3. # no data acquired due to ligand supply shortages.

Initially, these experiments were thought as a reproduction of the data already obtained by Stefanie Meyer with the luciferase complementation approach (table 12). The intention was to already have a reliable dataset for comparison when implementing the BRET assay. However, marked differences between the two datasets could be found: Almost throughout, efficacies were increased (higher E_{max}) as were potencies (lower $logEC_{50}$). Also, no superagonists were found in the luciferase complementation data. Probably most strinkingly, in the luciferase complementation data, there were four antagonists next to naloxone and naltrexone (buprenorphine, tapentadol, tilidine, and tramadol). In the BRET assay, of these four only Buprenorphine remained, with tapentadol even acting as a superagonist. There were no data for tilidine in this assay, as was pointed out earlier.

To further elucidate these findings and to make the results more comparable, all BRET experiments were performed again without cotransfection of GRK2. The cell lines provided to us for the luciferase complementation experiments did not overexpress the kinase. GRK2 expression was not different compared to the HEK cells used in the BRET experiments. This was confirmed by repeated western blots, as shown in figure 18.

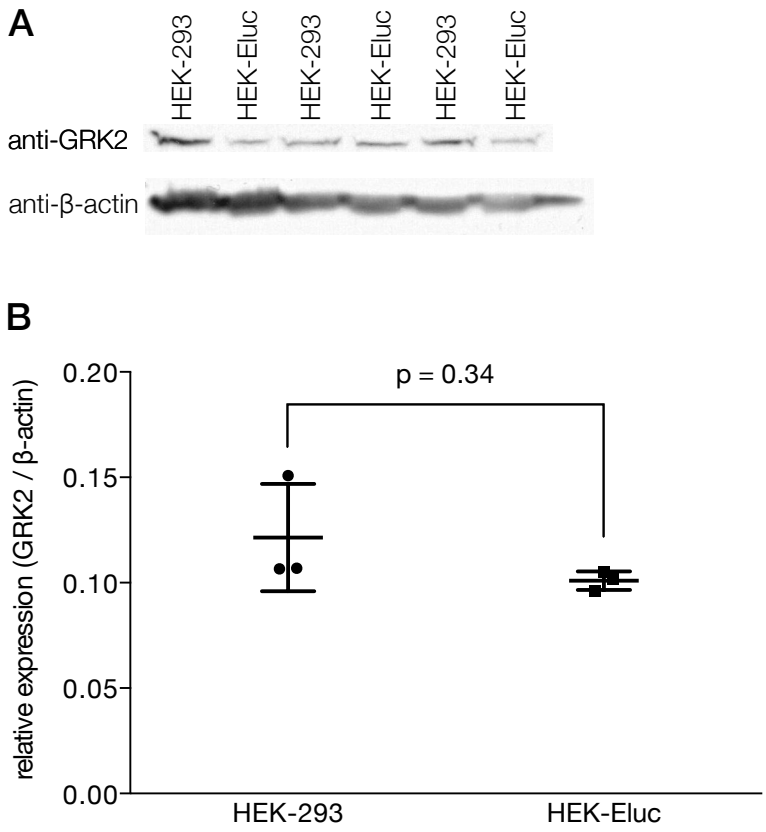

Figure 18: (A) Western blots of GRK2 expression in native HEK-293 and HEK-Eluc-OPRM1-β-arr2 cells. Lysates of three separate experiments with both cell lines were blotted side by side. β-actin was used as housekeeping protein for comparison. Total protein load was adjusted to 50 µg in both wells. Digital contrast enhancement and background correction was performed for better visibility in print after quantification. (B) Quantifiction of (A); intensities of GRK2 relative to β-actin for each corresponding pair of values are shown. Bars denote mean ± SD. Paired, two-sided t test, n=6, p=0.3433

3.6 INFLUENCE OF GRK2 OVEREXPRESSION ON THE RECRUITMENT OF β-ARRESTIN 2

The following experiments were performed entirely in analogy to those in section 3.5 except for the here omitted over-expression of GRK2. From the results, the opioids could be categorized as follows:

FULL AGONISTS
: DAMGO.

STRONG PARTIAL AGONISTS
: fentanyl, L-methadone, remifentanil, sufentanil.

WEAK PARTIAL AGONISTS
: hydromorphone, morphine, oxycodone, pethidine, piritramide, tapentadol.

ANTAGONISTS
: buprenorphine, naloxone, naltrexone, tramadol.

DAMGO as the reference compound was the only full agonist (by definition). Classified as strong partial agonists were ligands with an E_{max} > 0.5. All which met this criterion were full agonists or super-agonsists in the experiments where GRK2 was overexpressed. The remainder of substances fell within the group of weak partial agonists; tramadol turned into an antagonist. Sufentanil again had the highest potency of all ligands ($logEC_{50}$=- 7.81). The other strong partial agonists were close to DAMGO in this respect ($logEC_{50}$=-6.13), the weak partial agonists all had lower potencies (morphine: $logEC_{50}$=-6.20 to pethidine: $logEC_{50}$=-3.41).

Due to prolonged supply problems, no data were obtained for M-6-G and tilidine. The corresponding concentration-response curves are shown in figure 19 (strong partial agonists), figure 20 (weak partial agonists), and figure 21 (antagonists). Again, individual experiments for each ligand were repeated at least three times, while the graphs only depict duplicate values from single experiments.

Overall, these data corresponded very well with those from the luciferase complementation assay (see table 12 in the appendix), which presumably took place in a comparable cellular proteomic environment. One noteworthy difference was tapentadol, which acted as a partial agonist (E_{max}=0.74) in the BRET assay while manifesting itself as an antagonist in earlier experiments. Detailed pharmacological properties of all tested ligands are given in table 4.

To make the influence of GRK2 overexpression vs. endogenous expression more plastic, E_{max} and EC_{50} values from the presented BRET experiments with and without GRK2 overexpression were summarized in figure 22. As for the maximum responses, all opioids presented with higher E_{max} values with GRK2 overexpression than without (figure 22A). Exceptions are, of course, DAMGO, which, as the

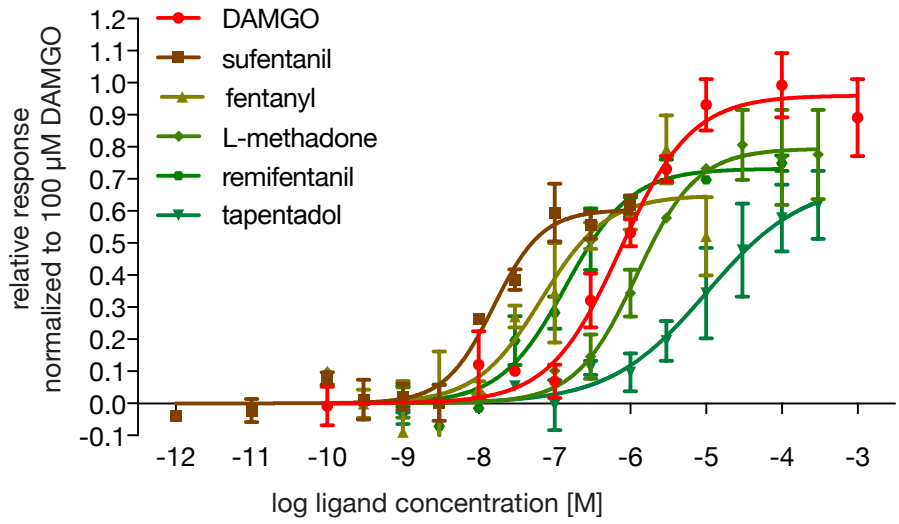

Figure 19: Concentration-response curves of DAMGO and strong partial agonists for recruitment of β-arr2. Data stem from BRET experiments, GRK2 was not overexpressed in the cells. Error bars denote SEM, $n \geq 3$

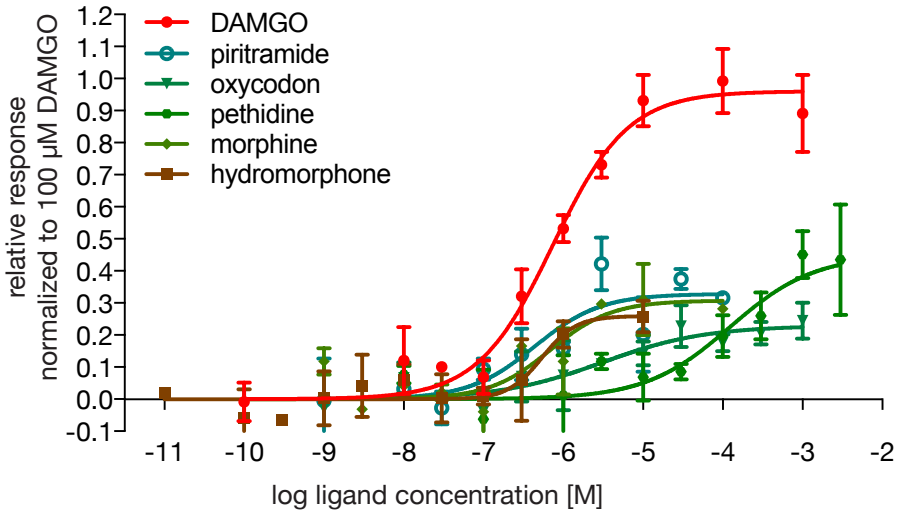

Figure 20: Concentration-response curves of DAMGO and weak partial agonists for recruitment of β-arr2. Data stem from BRET experiments, GRK2 was not overexpressed in the cells. Error bars denote SEM, $n \geq 3$

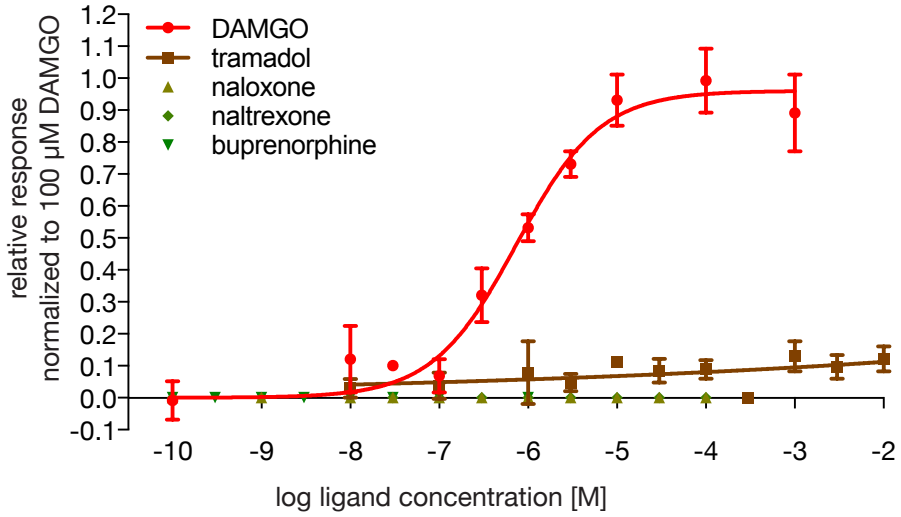

Figure 21: Concentration-response curves of DAMGO and antagonists for recruitment of β-arr2. Data stem from BRET experiments, GRK2 was not overexpressed in the cells. Error bars denote SEM, n≥3

reference compound has an E_{max} of 1 in all experiments by definition and the antagonists buprenorphine, naloxone, and naltrexone (all zero). Tramadol was turned from an antagonist under endogenous GRK2 expression into a partial agonist where the kinase was overexpressed (E_{max}=0.34). Tapentadol even went from partial agonist to superagonist (E_{max}=0.74 vs. E_{max}=1.20). The situation was comparable when looking at efficacies (figure 22B). It was only pethidine where GRK2 overexpression did not cause a left-shift of efficacy as compared to endogenous kinase expression levels. The left-shift is between one and 1.5 log units throughout the datasets. In summary, changing the expression levels of GRK2 in the cells was sufficient to significantly change the behavior regarding β-arr2 recruitment of all investigated opioids.

	Emax (S.E.M.)	$EC50$ $[nM]$	logEC50 (S.E.M.)
DAMGO	0.97 (0.09)	749	−6.13 (0.21)
Buprenorphine	0.0 –	–	– –
Fentanyl	0.73 (0.11)	96.4	−7.02 (0.30)
Hydromorphone (n=6)	0.08 (0.07)	208	−6.68 (0.34)

	Emax (S.E.M.)	$EC50$ $[nM]$	logEC50 (S.E.M.)
M6G		#	
L-Methadone	0.80 (0.08)	886	−6.05 (0.21)
Morphine	0.28 (0.10)	632	−6.20 (0.64)
Naloxone	0.0 –	–	– –
Naltrexone	0.0 –	–	– –
Oxycodone (n=5)	0.05 (0.04)	3090	−5.51 (0.38)
Pethidine (n=5), no plateau	0.21 (0.16)	393000	−3.41 (0.72)
Piritramide (n=6)	0.08 (0.12)	338	−6.47 (0.77)
Remifentanil	0.74 (0.07)	191	−6.72 (0.16)
Sufentanil	0.56 (0.11)	15.4	−7.81 (0.27)
Tapentadol	0.74 (0.15)	8000	−5.10 (0.39)
Tilidine		#	
Tramadol	0.0 –	–	– –

Table 4: Pharmacological properties of 15 opioid ligands for β-arr2 recruitment. Data originate from BRET experiments, GRK2 was not overexpressed in the cells. Error bars indicate SEM, n=3 unless denoted otherwise. # no data acquired due to ligand supply shortages.

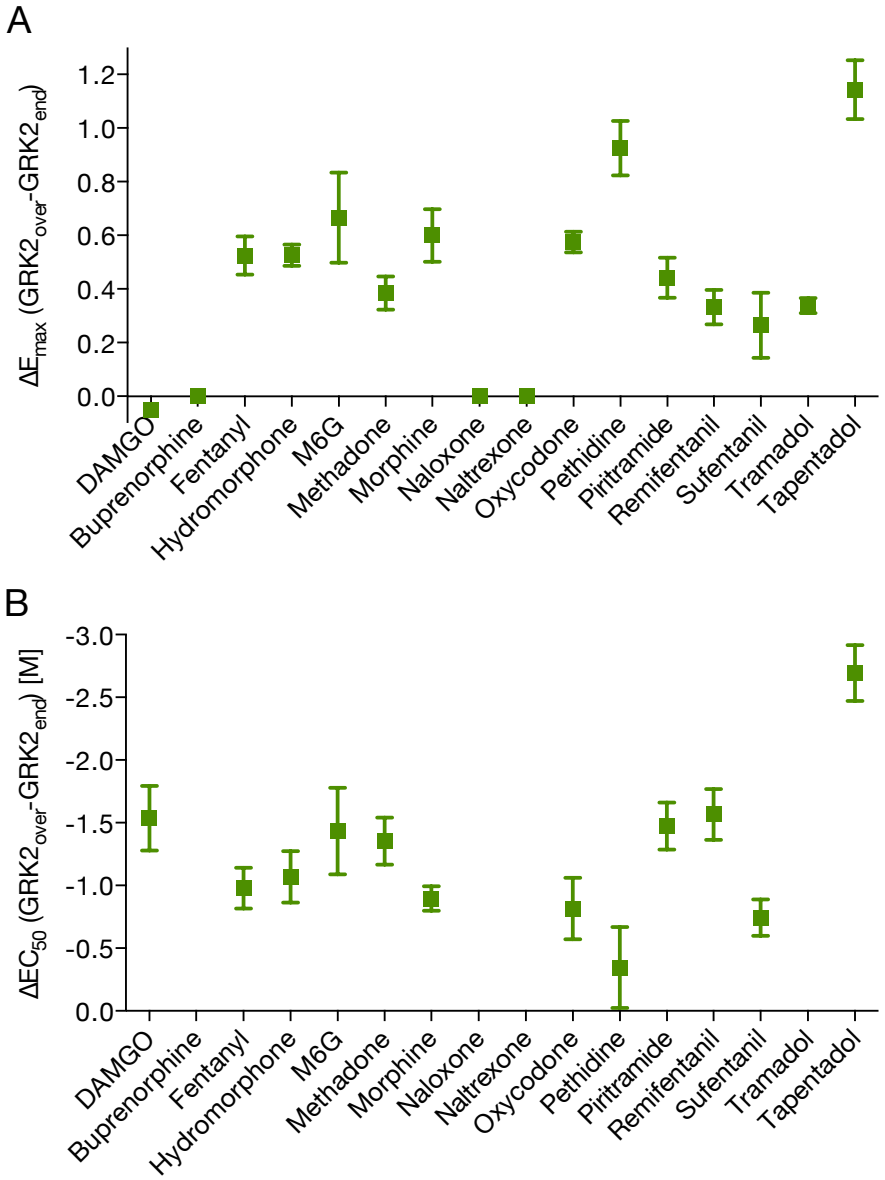

Figure 22: Changes in E_{max} (A) and EC_{50} (B) values from BRET experiments with and without GRK2 overexpression. Bars indicate mean and SEM of the calculated differences between the respective values with and without GRK2 overexpression, n=3. $GRK2_{over}$: values from cells overexpressing GRK2; $GRK2_{end}$: values from cells with endogenous GRK2 expression

3.7 CALCULATION OF BIASED AGONISM BETWEEN G_i, β-ARRESTIN 1, AND β-ARRESTIN 2

The abundance of pharmacological data collected to this point allowed for further analysis of signaling properties of the μ receptor. As introduced earlier, agonism bias is a concept which is capable of providing valuable insights in the entirety of signaling starting from a certain receptor. For the approach favored here [166] it was necessary to fit concentration-response data to the operational model of pharmacological agonism. Details were explained in section 2.2.11. Output fit values were, among others τ and K_A, which, as a compound parameter $\log \frac{\tau}{K_A}$ served as the basis for further calculations. $\log \frac{\tau}{K_A}$ values were first compared between ligand and reference compound within each pathway (resulting in $\Delta \log \frac{\tau}{K_A}$, data not shown) and then pairwise between pathways ($\Delta\Delta \log \frac{\tau}{K_A}$). $\Delta\Delta \log \frac{\tau}{K_A}$ is a numerical measure on a log scale for a ligand's tendency to prefer the activation of one pathway over another. Positive numbers indicate bias towards the first signaling pathway and vice versa, thus making the signs of the numbers subject to convention. These calculations were performed on the basis of the FRET G_i data and the β-arr 1 and 2 recruitment data from the luciferase complementation experiments. An overview on $\Delta\Delta log \frac{\tau}{K_A}$ values for all the opioids is given in table 5.

	$G_i - \beta$-arr1	$G_i - \beta$-arr2	β-arr1 $- \beta$-arr2
DAMGO	0 (−)	0 (−)	0 (−)
Buprenorphine*	1 (−)	1 (−)	−
Fentanyl	−1.27 (1.61)	−0.37 (0.76)	0.91 (1.67)
Hydromorphone	0.19 (4.66)	0.42 (1.70)	0.23 (4.70)
M6G	#	0.40 (3.00)	#
L-Methadone	−0.67 (0.70)	0.32 (0.60)	0.34 (0.83)
Morphine	0.93 (3.09)	0.42 (1.44)	−0.51 (3.20)
Naloxone	−	−	−
Naltrexone	−	−	−
Oxycodone	1.00 (4.32)	0.37 (1.51)	−0.62 (4.34)
Pethidine	0.63 (2.35)	0.52 (1.47)	−0.11 (2.61)
Piritramide	−0.06 (0.92)	−0.62 (0.82)	−0.56 (1.13)
Remifentanil	1.35 (1.21)	0.88 (0.56)	−0.47 (1.22)
Sufentanil	−0.55 (0.75)	−0.76 (0.66)	−0.21 (0.87)
Tapentadol*	1 (−)	1 (−)	−

	$G_i - \beta$-arr1	$G_i - \beta$-arr2	β-arr1 $-$ β-arr2
Tilidine*	1 (−)	1 (−)	−
Tramadol*	1 (−)	1 (−)	−

Table 5: $\Delta\Delta \log \frac{\tau}{K_A}$ values of 17 opioid ligands between G_i signaling and β-arr1 and β-arr2 recruitment. GRK2 was not overexpressed in the cells. Numbers in brackets indicate 95% CI. *$\Delta\Delta \log \frac{\tau}{K_A}$ values for bias between G_i and either β-arr were arbitrarily set to 1 (see text). #No data for β-arr1 recruitment due to shortages in ligand supply.

Significant ligand bias was assumed only if $\Delta\Delta \log \frac{\tau}{K_A}$ and its complete 95% CI lied above or below zero. CIs were derived from approximations of propagated standard errors. Visualizations of $\Delta\Delta \log \frac{\tau}{K_A}$ plus CI (bias plots) help to identify significant ligand bias more easily. figure 23 shows a bias plot for a selection of opioids with significant ligand bias.

From our data, only sufentanil appeared to show bias towards the recruitment of β-arr2 ($\Delta\Delta \log \frac{\tau}{K_A}$ = -0.76 $\pm$ 0.66). Bias between G_i and β-arr1 pointed in the same direction but was not significant ($\Delta\Delta \log \frac{\tau}{K_A}$ = -0.55 $\pm$ 0.75). Remifentanil was biased towards G_i activation compared to both β-arrs 1 and 2 ($\Delta\Delta \log \frac{\tau}{K_A}$ = 1.35 $\pm$ 1.21 and $\Delta\Delta \log \frac{\tau}{K_A}$ = 0.88 $\pm$ 0.56, respectively). Four opioids in the experimental set at hand eluded the exact calculation of ligand bias: buprenorphine, tapentadol, tilidine, and tramadol. These four did not recruit any arrestins, thus leaving them with zero potency and missing efficacy values. This rendered calculation of a bias factor impossible. They were arbitrarily assigned $\Delta\Delta \log \frac{\tau}{K_A}$ values of 1, expressing their obvious bias towards G_i. After all, $\Delta\Delta \log \frac{\tau}{K_A}$ values lie on a log scale, i.e. a value of 1 translates into tenfold stronger activation of one pathway on a linear scale. DAMGO as the reference substance has $\Delta\Delta \log \frac{\tau}{K_A}$s of zero by definition in all signaling pathway comparisons. Generally, there was no bias between the two arrestins within a single ligand. A complete bias plot including all non-significant values is given in figure 37 of the Appendix.

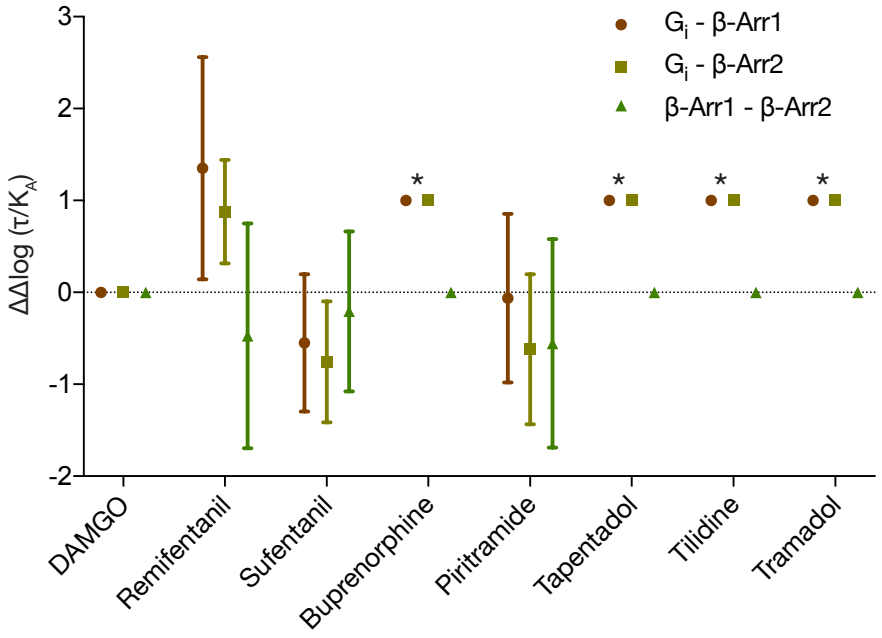

Figure 23: Bias plot of selected opioid agonists. Bias was calculated based on FRET G_i data and β-arr recruitment data from luciferase complementation. GRK2 was not overexpressed in the cells. Positive $\Delta\Delta \log \frac{\tau}{K_A}$ values indicate bias towards the signalling pathway named first in the respective legend, and vice versa. Error bars denote 95% CI. Values marked with an asterisk (*) are arbitrarily assigned to 1. Here, bias could not be calculated due to missing activity in both β-arr pathways (see text for details).

3.8 INFLUENCE OF GRK2 OVEREXPRESSION ON AGONISM BIAS

Results described in detail in section 3.6 suggested a key influence of GRK2 expression levels on the pharmacodynamics of β-arr recruitment. One would expect this to also change agonism bias fundamentally. Ligand bias in section 3.7 was calculated from data derived from cells expressing endogenous levels of GRK2. However, the pharmacodynamics of β-arr2 (not β-arr1) recruitment under GRK2 overexpression have already been described in section 3.5. Thus, it stood to reason to calculate agonism bias for this set of data as well. Operational model fitting and calculation of ligand bias was done as described above. As there were no data on β-arr1 recruitment under GRK2 overexpression to begin with, only one pairwise comparison per ligand was calculated. figure 24 shows the corresponding bias plot.

	$\Delta\Delta \log \frac{\tau}{K_A}$	95% CI
DAMGO	0	–
Buprenorphine*	1	–
Fentanyl	−0.52	1.18
Hydromorphone	−0.09	1.48
M-6-G	−0.11	1.56
L-Methadone	−0.71	1.17
Morphine	0.04	1.31
Naloxone	–	
Naltrexone	–	
Oxycodone	−0.10	1.56
Pethidine	−0.14	1.25
Piritramide	−1.22	1.35
Remifentanil	0.22	1.01
Sufentanil	−0.30	1.22
Tapentadol	−1.18	1.25
Tilidine	#	
Tramadol	1.50	2.78

Table 6: $\Delta\Delta \log \frac{\tau}{K_A}$ values of 16 opioid ligands between G_i signaling and β-arr2 recruitment. *$\Delta\Delta \log \tau/K_A$ values were arbitrarily set to 1 (see text). #No data due to shortages in ligand supply.

Most of the significant bias was abolished by the overexpression of GRK2. $\Delta\Delta \log \frac{\tau}{K_A}$ of Sufentanil is still slightly negative, but far from

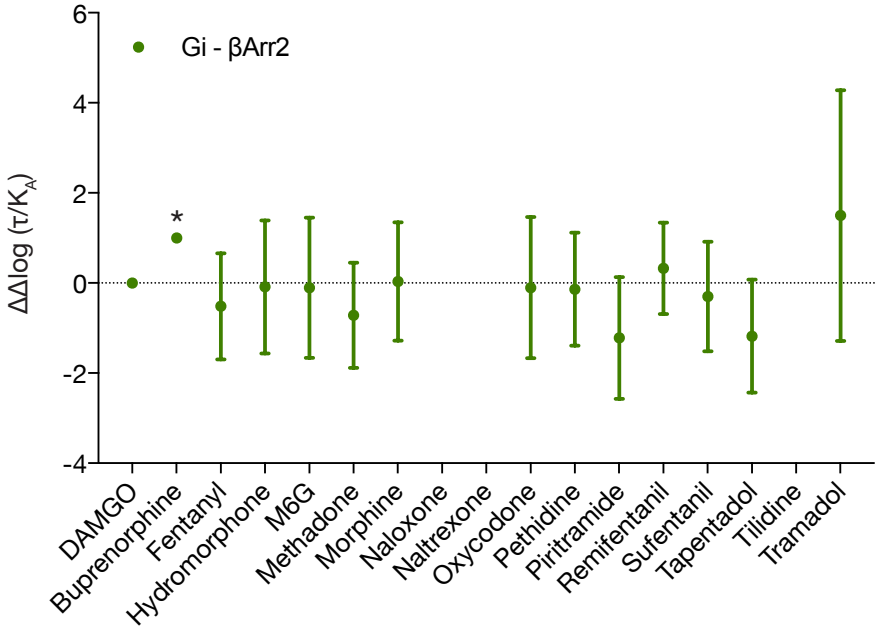

Figure 24: Bias plot of selected opioid agonists in cells overexpressing GRK2. Bias was calculated based on FRET G_i data and β-arr2 recruitment data from BRET experiments. Positive $\Delta\Delta \log \tau/K_A$ values indicate bias towards the signalling pathway named first in the respective legend, and vice versa. Error bars denote 95% CI. Values marked with an asterisk (*) are arbitrarily assigned to 1 (for details, see text).

significance (-0.30 $\pm$ 1.22). The same was true, under inverse signs for Remifentanil ($\Delta\Delta \log \frac{\tau}{K_A}$ = 0.22 $\pm$ 1.01). Tapentadol ($\Delta\Delta \log \frac{\tau}{K_A}$ = -1.18 $\pm$ 1.25) and Tramadol ($\Delta\Delta \log \frac{\tau}{K_A}$ = 1.50 $\pm$ 2.78) appeared non-biased (i.e. balanced) with the overexpression of the kinase; for Tilidine there were no β-arr2 recruitment data. Solely Buprenorphine did not elicit any β-arr2 recruitment and was therefore again considered to be biased towards G_i with an assigned $\Delta\Delta \log \frac{\tau}{K_A}$ of 1.

3.9 IMPLEMENTATION OF A REPORTER GENE ASSAY FOR TLR4 SIGNALING

An involvement of TLR4 in undesired effects caused by opioids has been discussed in recent literature as pointed out in figure 1.6. To investigate whether and to what extent the opioids used in this study could induce TLR4 signaling, a commercial reporter gene assay (HEK-Blue, InvivoGen) was implemented. In short, activation of TLR4 in the cells will lead to increased production of NF-κB, which in turn promotes the synthesis of a SEAP. SEAP will eventually cause a special detection medium to change its color from red to blue, which can be read out as a semiquantitative measure of receptor activation. A TLR4-deficient, but otherwise identical cell line (HEK-Blue Null2)

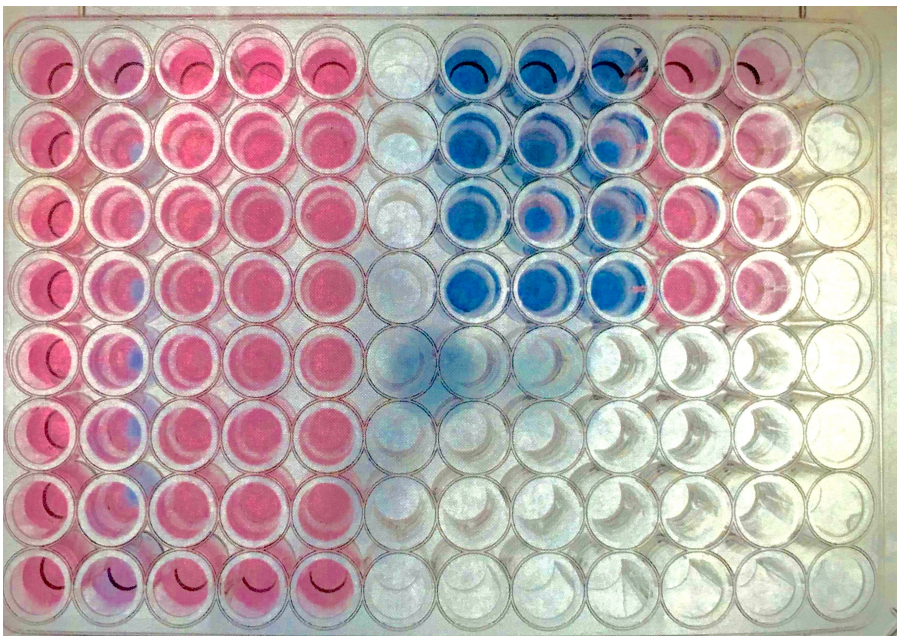

Figure 25: Photograph of an exemplary HEK-Blue assay microtiter plate. Some wells were treated with the positive control LPS, which causes the medium to turn blue.

served as a control. The implementation of the assay was successful after a few attempts; figure 25 Shows an experiment in a 96-well microtiter plate. Wells that were exposed to 10 ng/ml LPS changed their color to blue after an incubation period of 12 hours (A7-D9). Wells containing Null-cells did not turn blue, neither without (E1-H5 on the plate) nor with (A10-D11) addition of LPS.

To begin with, a subset of opioids were then tested with this assay: DAMGO, fentanyl, sufentanil, tramadol, piritramide, and morphine. Water and LPS served as negtive and positive control, respectively. As can be seen from figure 26, DAMGO elicited some signal (around $\frac{1}{4}$ of the LPS signal). The other tested opioids did not cause any detectable response, neither did water.

In parallel to these first experiments the technical processes surrounding the conduct of the assay were further refined. Special focus was laid on the adherence to strict endotoxin-free procedures. This was eventually ensured by the use of an limulus amebocyte lysate (LAL) gel clot test (Lonza, Basel, Switzerland), which was sensitive up to a concentration of 0.06 EU/ml. By this method, contamination with endotoxin could effectively be ruled out for all media, buffers, and ligand solutions used.

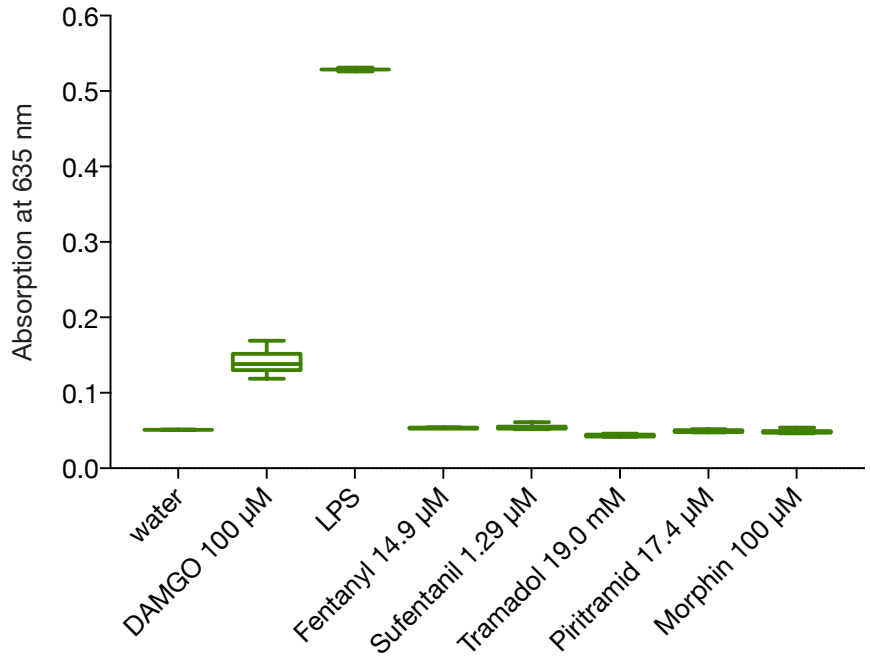

Figure 26: Box plot of optical absorption values for several opioid ligands in an early HEK-Blue assay. Boxes and whiskers denote interquartile range and complete range, respectively; n=8.

3.10 ACTIVATION OF TLR4 BY OPIOID LIGANDS

With the assay set up as described in section 3.9, structured testing of all used opioid ligands was initiated. To this end, opioids were used in concentrations which would be considered saturating in the context of the μ receptor. Again, 10 ng/ml LPS and water were used as controls. Data were normalized to the maximum LPS signal from each plate in order to make the results comparable between experiments. However, it turned out that in repeated independent measurements no more signal could be evoked apart from the LPS reference. Thawing of new cell batches and preparation of fresh ligand stock solutions did not change this finding. figure 27 shows an example of such an experiment. In conclusion it must be assumed that without external endotoxin contamination, opioids do not elicit TLR4 response detectable with this assay.

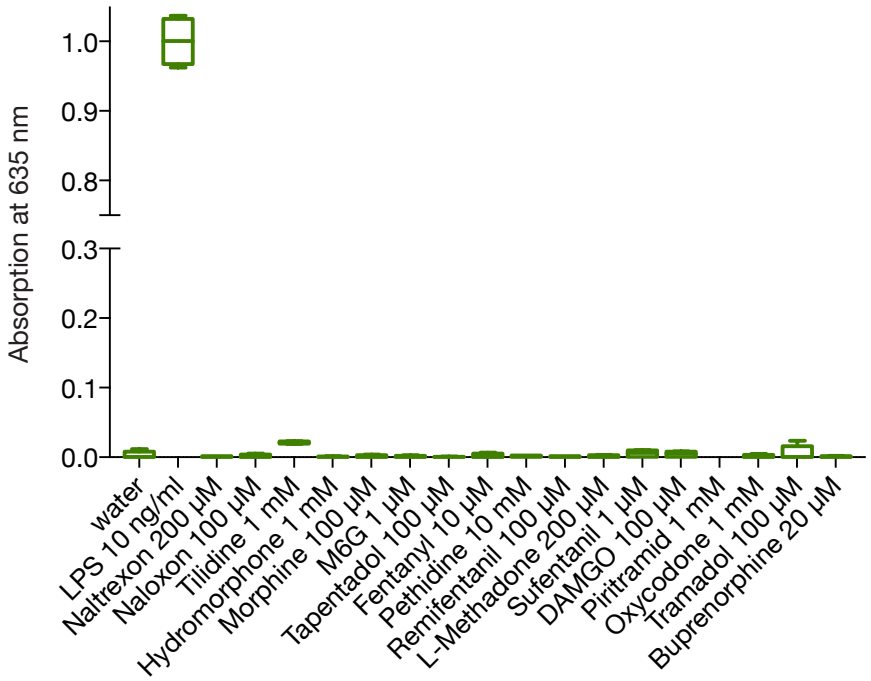

Figure 27: Box plot of optical absorption values for several opioid ligands in a HEK-Blue assay performed under endotoxin-free conditions. Values are normalized to the mean LPS response. Boxes and whiskers denote interquartile range and complete range, respectively; n=8.

4 DISCUSSION

In the work at hand, a total of 17 opioid ligands were thoroughly investigated with regard to signaling processes on a molecular level occurring directly at the μ receptor. Three distinct pathways were studied, namely the activation of the inhibitory G protein G_i and the recruitment of both β-arrestins. In addition to that, expression levels of the central mediating protein for β-arr recrutiment, GRK2, were varied to determine their influence on the recruitment. The set of opioids reflected upon here mainly consisted of opioid agonists which are used in clinical routine. In order to have a full spectrum of ligands, two μ receptor antagonists, naloxone and naltrexone, were included as well. Furthermore, the main active metabolite of morphine in humans, M-6-G, served to link this work to a study performed previously in the same institute [197]. Finally, the synthetic peptide agonist DAMGO was used as a reference compound. This is very common in literature connected to the current subject, not least because it acts as a full agonists in all three signaling pathways.

FRET-based techniques were used to study the signaling pathways seperately in real time and in living cells. For the analysis of biased agonism, data from work by Stefanie Mayer from the same lab were used. Those data were acquired using a luciferase complementation assay and compared very well to collected BRET data from this work.

Several aspects of opioid signaling as examined in this study shall be elaborated on a little more in the following chapter. Results will be interpreted and brought in line with relevant literature on the matter. Also, methodological and conceptual limitations of this work will be discussed.

The part of this work concerning the involvement of TLR4 in opioid signaling fell rather short due to the unforeseeable dynamics inherent to any scientific work. A few concluding remarks on the subject shall be made nevertheless.

4.1 ACTIVATION OF G_i BY OPIOID LIGANDS

The dataset at hand comprises concentration-response data for G_i activation of 17 μ receptor ligands. Using various techniques, several authors have reported such data over the years. Earlier studies often relied on indirect measures of G_i activation like G protein-gated potassium currents through G protein-coupled inwardly-rectifying potassium (GIRK) channels [95, 198] or inhibition of cAMP accumulation [199]. Although measurements of this kind correlate well with G pro-

	McPherson	Molinari	Frölich	this work
DAMGO	1.04	0.91		1.01
Buprenorphine	0.55	0.65		$< 1^*$
Fentanyl	1.14	0.98		0.99
M-6-G	0.87		~ 1	0.85
Methadone	1.18			1.03
Morphine	0.98	0.73	~ 1	0.79
Oxycodone	0.95			0.77
Pethidine	*	0.86		0.98^*

Table 7: Efficacies of G_i recruitment compared to values from recent literature. *Curve-fitting yielded no plateau, value is extrapolated. External data are cited from:
McPherson et al. [201], Molinari et al. [202], Frölich et al. [197].

tein activity in general, a certain degree of signal amplification will occur between the actual G protein activation and the measured effect. So, if one wants to know about bias between pathways, experimental read-outs as close to the signaling biomolecule as possible are advantageous. Later approaches relied on [^{35}S]GTPγS binding assays as a more direct measure of G protein activation [199, 200]. In brief, these assays make use of a non-hydrolyzable form of GTP, [^{35}S]guanosine-5'-O-(3-thio)triphosphate ([^{35}S]GTPγS). [^{35}S]GTPγS is bound by an activated G_i in exchange for GDP (also see section 1.2), after which the turnover cycle of the G protein is halted. The amount of bound [^{35}S]GTPγS can be determined as a measure of G protein activation. The downside of this experimental approach is that it needs to be done in membrane preparations of cell lysates. Therefore, the read-out takes place outside the intact cell, which can easily lead to distortions of the actual signaling properties.

Nevertheless, [^{35}S]GTPγS binding data by McPherson et al. [201] and Molinari et al. [202] represent the most recent and most comparable data available in the literature on the matter of G protein activation. One exception is a piece of work by Frölich et al. [197], who used a FRET sensor similar to the one in this work. The largest overlap between the sets of opioids can be found with the work by McPherson et al.. With the mentioned methodological differences and constraints in mind, it is even more convincing to see how well in line the values actually are. Slight differences are found for morphine and oxycodone, which McPherson et al. classify as full agonists (E_{max} 0.98 and 0.95, respectively) whereas this work sees them as strong partial agonists (E_{max} 0.79 and 0.77). Similarily in line are findings by Molinari et al.. Frölich et al. do not provide numerical values for the effi-

	McPherson	Molinari	Frölich	this work	
	EC_{50}	$logEC_{50}$	EC_{50}	EC_{50}	$logEC_{50}$
DAMGO	11.2	−7.5	46	37.5	−7.43
Buprenorphine	14.5	−8.8		179	−6.75
Fentanyl	56.8	−8.0		38.1	−7.42
M-6-G	81.0		37	290	−6.54
Methadone	87.2			227	−6.65
Morphine	97.5	−7.8	15	412	−6.39
Oxycodone	564			1,610	−5.79
Pethidine	> 10,000	−5.6		26,900	−4.57

Table 8: Potencies of G_i recruitment compared to values from recent literature. Ligand concentrations are given in nM. External data are cited from McPherson et al. [201], Molinari et al. [202], Frölich et al. [197].

cacies, but they are derived from depicted curve fits. For an overview, see table 7.

In terms of potencies, the situation is similar. McPherson et al. generally find slightly higher potencies, but in no case (except buprenorphine) by more than half a log level. This may be explained by the comparably smaller receptor reserve of the $[^{35}S]GTP\gamma S$ assay compared to overexpressed functional G proteins. For buprenorphine, values diverge by a factor of 10 (EC_{50} 14.5 nM vs. 179). In this special case, the method used in this work might indeed be inferior. Buprenorphine is known to have a very high binding affinity for the μ receptor in the sub-nanomolar range (0.08 nM, [203]). In an assay like the one used here, where after each array of measurements addition of DAMGO as a reference is necessary, this high binding affinity might impair proper binding of DAMGO. As was pointed out in section 3.2, the G_i activation data of Buprenorphine were not easily fitted. The values from Molinari et al. are a little more off, yet constantly so, by 1-1.5 log levels, buprenorphine set aside. Again, the decreased receptor reserve might serve as an explanation. As to what extent the assays of Molinari et al. and McPherson et al. differ in technical details to account for the differences in their respective datasets, is beyond the author's knowledge. Compared to the findings of Frölich et al., again, in this work potencies tend to be lower (i.e. higher EC_{50}). While results for DAMGO match just fine (46 nM and 37.5 nM), M-6-G and Morphine differ by a factor of 10-20. Apart from a slightly different sensor construct, there is no obvious explanation for this.

Beyond buprenorphine, a few more ligands could not be concentrated high enough in order to obtain a maximum plateau signal: pethidine, tapentadol, and tramadol. These are, by far the least potent opioids used in this set of ligands and, with the exception of

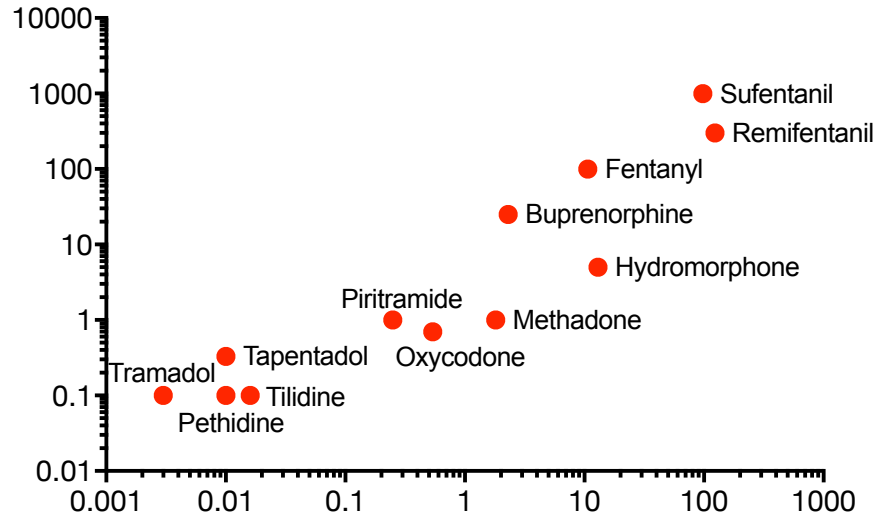

Figure 28: Scatter plot of experimentally determined potencies for G_i activation and clinical potencies from the literature (see table 1) of several opioids. Values were normalized to morphine for better comparability. Spearman's $\rho = 0.93$, $p < 0.0001$. For details, see text.

pethidine they are partial agonists in terms of G_i activation. However, it should be mentioned that the categorization as a partial agonist is not entirely accurate if one cannot determine the maximum signal with certainty. It is theoretically possible that those ligands are in fact full agonists, be it in a system/tissue with higher signal amplification, or at even higher concentrations. In the context of this study, labeling them partial agonists is legitimate insofar, as there are "real" full agonists in the same assay system. Practically, this is all of little importance, as the following example might illustrate. Tramadol, for example, is not supposed to be dosed higher than 400 mg per day in a patient. With its molecular weight of 263,38 g/mol this translates into 1.52 mmol tramadol per day. At an assumed blood volume of 5 l in an adult, hematocrit of around 0.5, and even with 100% bioavailability and a very low volume of distribution (both of which are not the case), the highest plasma concentration possible would be approximately 0.4 mM. This is a concentration that was still within the the tested range in this study. After all, tramadol might in theory be a full agonist, for a pharmacology based on humans however this is of subordinate importance. Similar considerations are true for the other "weak" partial agonists.

Another question to be raised in the face of the data at hand might be, to what extent the potencies with regard to activation of a G protein are correlated with those found in clinical application. As was pointed out in the introduction, opioids are assessed by their capability to ease pain compared to morphine. Thus, if analgesic effects were truly mediated by G protein activation first and foremost, there

	EC_{50} G_i activation [nM]	K_i [nM]
Buprenorphine	179	0.21
Fentanyl	38.1	1.3
Hydromorphone	31.7	0.37
Methadone	227	3.4
Morphine	412	1.2
Oxycodone	1,620	25.9
Pethidine	26,900	450
Sufentanil	4.22	0.14
Tramadol	138,000	12.5

Table 9: Potencies of G_i activation from this work put next to binding affinities as determined by Volpe et al. [204], where available.

should be a correlation. And indeed, as figure 28 shows, when plotting experimental G_i potencies and observed clinical potencies, there is nearly perfect rank order correlation between the two. Taking into account that the molecular event of activating a G protein and the subjectively conceived clinical outcome of analgesia certainly are influenced by a plethora of confounders, the unambiguity of the correlation is surprising. This merely serves to demonstrate that the experimental data obtained in this work are of some practical value. It has never been the intention of this work to find such correlations, nor have data on clinical potencies of opioids been collected.

One last aspect worth discussing in the light of G_i activation is its association with ligand-receptor binding. Data of this kind were not collected in this study, yet a rather strong correlation is to be expected. It is out of the question that an activated (i.e. agonist-bound) receptor is needed to activate a G protein. Also, no activators of G proteins other than active-state GPCRs are known. So, if the ligands of interest are sufficiently selective for the μ receptor, receptor binding and G protein activation should be closely correlated. As there is no possibly amplifying instance in between receptor and G protein, it is only the turnover rate of the active receptor (i.e. how many G proteins one receptor can activate before it is silenced by an arrestin), which determines the difference between binding affinity and G_i activation potency. This is a phenomenon referred to as receptor reserve. The crux with binding data is that they tend to differ a lot between experiments in different laboratories. A recent study found affinity ranges of as much as four log levels for a single opioid ligand in the literature [204]. However, the authors also provided affinity values from their own experiments for many of the opioids used in the work at hand, so those are at least internally consistent. When comparing the experimental G_i potencies of this study with those binding affinities,

they appear to match rather well (see table 9). Higher affinity leads to higher potency and vice versa. The binding affinity of each ligand is higher than its respective G_i activation potency, which is reasonable. Aside from buprenorphine and tramadol, where potencies were not exactly determinable, the log distance between binding affinity and potency of every ligand varies in a narrow range between ~ 1.5 (fentanyl) and ~ 2 (hydromorphone) for those ligands where binding data are available from Volpe et al. [204]. All taken together, the data on G_i activation appear conclusive both in itself and in comparison with previously published data.

4.2 RECRUITMENT OF β-ARRESTINS TO THE RECEPTOR

Recruitment of β-arr2 to the μ receptor was thoroughly looked into in this work as a second important interaction occuring at and with the activated receptor apart from G_i activation. Data for β-arr1 recruitment were not collected in this work; however, for ensuing calculation of ligand bias, unpublished data by Stefanie Mayer were used (also see section 3.3). In-depth analysis will be left up to her. Only two brief statements concerning these data shall be made: (1) For β-arr2 recruitment, results from luciferase complementation experiments and from the NanoBRET assay match well under comparable assay conditions. EC_{50} values for any ligand were never more than one log level apart between the two assays. One marked exception is tapentadol. In the luciferase complementation assay it seems to be an antagonist, whereas with NanoBRET it is a partial agonist with micromolar potency. From the data available, there is no obvious explanation for this that would go beyond speculation. For detailed results of the luciferase complementation experiments, see table 12 in the appendix. (2) Potencies for β-arr1 recruitment were equal or lower than those for β-arr2 throughout the set of ligands. This is in line with generally accepted previous findings, suggesting that class A GPCRs have higher afinity for β-arr2 than 1 [86]. After all, this validates the NanoBRET assay in comparison with a previously established assay and proves general consistency of the findings with earlier results from the literature.

Data on β-arr2 recruitment to the μ receptor in the literature are mainly found in those publications which already served for comparison of the G_i data. It is noteworthy to say that both McPherson et al. [201] and Molinari et al. [202] performed their experiments - enzyme complementation (PathHunter®) and BRET, respectively - without overexpression of GRKs, whereas Frölich et al. [197] used a FRET assay with overexpressed GRK2. In table 10, efficacies for β-arr2 recruitment from the literature are put next to respective findings from this work. The findings are in excellent accordance to those by Molinari et al. [202]. Generally, the same is true for McPherson et al. [201],

	McPherson	Molinari	Frölich	this work
DAMGO	1.24	0.89	1	0.97
Buprenorphine	0	0.02		0.0
Fentanyl	0.89	0.77		0.73
Methadone	1.14			0.80
Morphine	0.19	0.24	approx. 0.7	0.28
Oxycodone	0.18			0.05
Pethidine	0	0.41*		0.21*

Table 10: Efficacies of β-arr2 recruitment compared to values from recent literature. *Curve-fitting yielded no plateau, value is extrapolated. External data are cited from:
McPherson et al. [201], Molinari et al. [202], Frölich et al. [197].

although it needs to be mentioned that they used alfentanil instead of DAMGO as a reference compound (unlike for their G_i data). This makes DAMGO a superagonist with an E_{max} of 1.24, suggesting that, when normalizing to DAMGO instead, the indicated values would possibly be a bit lower and then match this work's finding very well, too. The two values from Frölich et al. [197] are not explicitly indicated in their work, but can be estimated from graphs. Therefore, detailed comparisons are out of the question.

When looking into potencies, the situation is rather similar. Compared to Molinari et al. [202], EC_{50} values are never off by more than half a log level. The same is essentially true for data by McPherson et al. [201]. When comparing the data to Frölich et al. [197], one has to bear in mind that they co-transfected GRK2 for their β-arr FRET experiments. Instead of the values indicated in table 11, it would be more appropriate to compare their data to those from this work obtained with GRK2 overexpression as well (DAMGO: 106 nM, morphine: 390 nM). When doing so, again the data correspond just fine. Additionally, there are data on DAMGO and morphine by Nickolls et al. [205], also acquired using the PathHunter® system. Again, $logEC_{50}$ values are in close-to-perfect accordance (DAMGO: -6.11, morphine: -6.33).

Another aspect worth looking into is how β-arr recruitment behaves compared to G_i activation. The following attracts attention: (1) The efficacy of any opioid is generally lower for β-arr2 recruitment than for G_i activation. Most straightforward, this can be seen from the fact that there are no full agonists in terms of β-arr2 recruitment in this set of ligands, whereas there are several with regard to G_i activation (fentanyl, L-methadone, pethidine, piritramide, remifentanil, sufentanil). Most of the G_i partial agonists are weaker β-arr partial agonists, some others turn into antagonists altogether, like tramadol

	McPherson	Molinari	Frölich	this work	
	EC_{50}	$logEC_{50}$	EC_{50}	EC_{50}	$logEC_{50}$
DAMGO	414	−6.7	60	749	−6.13
Buprenorphine	n/a	−7.2		n/a	n/a
Fentanyl	210	−6.6		96.4	−7.02
Methadone	2110			886	−6.05
Morphine	322	−6.4	457	632	−6.20
Oxycodone	1460			3,090	−5.51
Pethidine	n/a	−3.2		393,000	−3.41

Table 11: Potencies of β-arr2 recruitment compared to values from recent literature. Ligand concentrations are given in nM. External data are cited from:
McPherson et al. [201], Molinari et al. [202], Frölich et al. [197].

and buprenorphine (depending on the efficacy one regards as the minimum a ligand needs to have not to be an agonist in the first place, this could also be the case for hydromorphone, oxycodone, and piritramide). For potencies, things look similar. Overall, G_i activation is left-shifted compared to β-arr recruitment, from as little as 1.5 times (morphine) to around 60 times (remifentanil). The exception to prove the rule is piritramide with a right-shift by a factor of 2. The general finding of left-shifted G_i potencies does probably not have any direct implications on how GPCRs signal. In a classical receptor activation model with G_i as the active signal and β-arr as the limiting factor, it certainly makes sense to not have the signal terminated before it begins (as would be the case with a marked right-shift). However, taking into account that β-arrs are signaling proteins in their own right, such a situation is possible. After all, this leads to considerations on biased agonism and shall be discussed there (section 4.3).

4.3 BIASED AGONISM AND THE ROLE OF GRK2

While the concept of *biased agonism* or *functional selectivity* has only emerged during the last couple of years, findings which - in retrospect - hint towards such a phenomenon were reported earlier. In vivo studies in guinea pigs' ilea showed functional activation of the μ receptor but no endocytosis of the receptor by morphine [206]. Keith et al. [207] found similar results in HEK-293 cells. From such rather descriptive findings the evidence grew slightly more mechanistic over the years. In 1998, Zhang et al. [96] showed that morphine as opposed to other opioids does not phosphorylate the μ receptor, neither does it recruit β-arr to the receptor in confocal imaging. The missing β-arr recruitment by morphine was also described by Whistler

and von Zastrow [101] in the same year. Even more sophisticated were results by Bohn et al. [208] in 2004. They showed that, while morphine and heroin recruit β-arr to the μ receptor only to a minor extent, fentanyl and methadone are very successful in doing so in confocal imaging. Moreover, they could show in animal studies that morphine and heroin induced prolonged analgesia in β-arr2 knock-out mice, whereas fentanyl, methadone, and etorphine do not present with an altered phenotype. They hypothesized the missing ability of morphine and heroin to also recruit β-arr1 to the receptor diminishes receptor desensitization and therefore extends the analgesic effect. The more efficacious agonists were also able to recruit β-arr1 as proven by confocal microscopy and therefore induce normal receptor internalization even in β-arr1 knock-out mice.

When it comes to looking into actual ligand bias, there are mainly three studies in the literature which are comparable to this work in terms of methodology. Two of them - McPherson et al. [201] and Molinari et al. [202] - have been extensively cited in previous sections of this dicussion. The most recent (and most alike) work is one by Thompson et al. [209], which compared several signaling pathways at the μ receptor with regard to endogenous opioid peptides. Whereas this last work is even compatible with the one at hand in terms of the method for bias quantification, the first two are not. Molinari et al. [202] do not engage in any systematic bias quantification, at all. The focus of their work was mainly on a comparison between opioid activities at the μ and δ opioid receptor subtypes. In general, they state that there are ligands with G_i activity and no β-arr recruitment but not the other way around. This supports the findings of this present work, where the same stands true. However, this should not be too surprinsing, as it is hardly imaginable how a putative μ receptor agonist without intrinsic activity for G_i activation would induce analgesia. When they go into details about the G_i-β-arr signaling dichotomy, they do so by comparison of intrinsic activities. The one compound they find noteworthy which also appears in this work's set of ligands is buprenorphine. They do not find any β-arr2 recruitment but partial agonism for G_i activation. In such an extreme case, where on pathway is completely neglected by a ligand, it is probably fair to call that ligand biased - this work does so, too. However, it should be noted that merely comparing intrinsic activities can only provide qualitative statements on ligand bias. For example, a ligand acting as a partial agonist in two pathways cannot be assesed properly with this method, as neither receptor density in the tissue nor signal amplification are accounted for in such a model. Still, small as the overlap between their work and this one may be in this case, the findings on buprenorphine coincide.

The work by McPherson et al. [201] goes one step further. Besides G_i activation determined by [^{35}S]GTPγS binding and β-arr recruti-

ment (BRET) they also investigated receptor internalization as a distinct signaling pathway. This work refrained from doing likewise, as the aforementioned unpublished work by Stefanie Mayer will elaborate on that. As for G_i and β-arr signaling, the authors simply correlate efficacies. However, they do so using the operational efficacy parameter τ rather than EC_{50}. This rids the data from confounders like receptor density, even more so as dedicated binding experiments were performed. From their correlations they find endomorphins 1 and 2 to be slightly biased towards β-arr; neither of the compounds were used in this work. From the substances this work identified as biased, only buprenorphine is also in the set of ligands in the study of McPherson et al. [201]. They do not report it as biased explicitely, but mainly so because the lack of β-arr response - just like in this work - renders determination of an operational efficacy impossible. In principle, their finding is congruent with the one in the study at hand.

All which goes beyond the indicated overlap with data from the literature constitutes entirely new knowledge in the field of molecular μ receptor pharmacology. For the first time, a broad range of opioid ligands in everyday clinical use were subject to a structured analysis and quantification of possible ligand bias. It showed some refined bias towards β-arr2 (sufentanil) and towards G_i (remifentanil), both of which could only be detected with the use of operational model relative intrinsic efficacy comparison. More unambiguous results were found for buprenorphine, tapentadol, tilidine, and tramadol. None of these ligands recruited any β-arr to the receptor, yet all were G_i agonists to some extent.

Yet, probably the most striking findings arose when, additionally, expression levels of GRK2 were changed. G protein-coupled receptor kinases phosphorylate GPCRs in an agonist-dependent manner, in the case of the μ receptor, GRK2 is of particular importance (see section 1.2). In this work, plenty of detailed concentration-response data are available that allow for analysis of the influence GRK2 expression has on β-arr recruitment. The β-arr experiments discussed so far were all performed in HEK-293 cells with their "natural" GRK2 background. When GRK2 was overexpressed in addition to the μ receptor and β-arr, recruitment of the latter was drastically enhanced throughout all ligands. Certainly, this was to be expected when considering reports in the literature. As pointed out, overexpression of GRK2 was previously found to boost β-arr recruitment elicited by morphine [96, 101, 102]. More recently, these findings were further refined. It appears as if phosphorylation of the C-terminal tail of the μ receptor was a sequential and hierarchical process, i.e. Ser375 is the first and most important site to be phosphorylated. Subsequently, more residues will be phosphorylated in an agonist-dependent manner. At the μ receptor, this was shown to affect receptor desensitization

[154] as well as internalization [210]. This adds an entirely new dimension to the concept of bias, because now, between G_i activation and β-arr recruitment, there is another signaling process which has distinct influence on the overall signaling pattern. At the β_2-AR, this "phosphorylation barcode" was shown to even induce different β-arr2 conformations with different signaling outcomes [105]. Thus, it is reasonable to believe that similar mechanisms exist at the μ receptor as well.

Nonetheless, receptor phosphorylation and GRK expression have so far not been thoroughly investigated with regard to biased agonism. McPherson et al. [201] did assess receptor phosphorylation, but only at Ser375 and only with endogenous GRK expression. Only very recently, a study driven by the pharmaceutical industry tried a first systematic approach at the matter by using a baculovirus system for GRK2 transfection/infection and gradually adapting the multiplicity of infection [211]. The authors disclosed detailed results only for DAMGO and morphine, but so far, their findings speak the same language as this work does. For DAMGO, they report an E_{max} of 0.95 and EC_{50} of 160 nM (this work: 0.97 and 749 nM) with endogenous GRK2 expression. When inducing maximum GRK2 overexpression (multiplicity of infection = 50), the pharmacology changes as follows: E_{max}=1.10, EC_{50}=6.8 nM (this work: 0.98, 106 nM). There is a similar situation for morphine. Without GRK2 overexpression: E_{max}=0.27, EC_{50}=240 nM (this work: 0.28, 632 nM); with GRK2 overexpression: E_{max}=0.96, EC_{50}=17 nM (this work: 0.83, 390 nM). Moreover, they could not detect a β-arr signal induced by buprenorphine without the contransfection of GRK2. When overexpressing the kinase, however, they see a signal and can calculate a $\Delta\Delta\log(\tau/K_A)$ value of around 1.25 (this work: no buprenorphine signal with GRK2 overexpression, bias estimated at $\Delta\Delta\log(\tau/K_A) \sim 1$). Taking into account basic experimental differences (U2OS cells instead of HEK-293, virus infection instead of lipid transfection), differences between the findings are minimal.

Returning to this work's findings on GRK2 overexpression, the changes in β-arr recruitment were profound (see section 3.6). On top of this, all significant ligand bias was diminished except for buprenorphine (see section 3.8). These findings are of particular importance, as most of the research on biased ligands at the μ receptor these days aims towards identifying G_i biased ligands, i.e. agonists that do not recruit β-arrs. This is based on findings in knock-out mice, where morphine analgesia was improved [173]. Furthermore, the use of β-arr small interfering RNA enhanced analgesia and reduced tolerance to morphine in mice and rats [212, 213]. Also, respiratory depression and constipation were attenuated in β-arr knock-out mice [45, 174]. Subsequently, a first G_i biased μ receptor ligand, herkinorin, was reported in 2007 [214], which did not recruit β-arr and therefore

did not induce receptor internalization. Further research led to the discovery of TRV130, a novel μ receptor G_i biased agonist with analgetic potency comparable to morphine but attenuated gastrointestinal and respiratory side-effects in animals [175] and humans [215]. So far, however, the respective expression of GRK2 was left to chance in the experiments assessing biased μ receptor ligand. With the data at hand, it seems like the influence of GRK2 on the important β-arr recruitment outcome is too substantial for further studies not to control its expression. As a consequence, when screening for G_i-biased ligands like in the study put forward by Winpenny et al., general overexpression of GRK2 may be advisable in order to specifically identify structures of the likes of buprenorphine rather than, say, tramadol. There is no reason to believe that GRK2 levels in any physiological target tissue are somehow foreseeable, so a potential new drug has to be able to remain biased under all circumstances; even more so, as evidence exists for morphine-induced GRK2 up-regulation in rat brains in vivo [216]. The fact that Winpenny et al. did actually find a buprenorphine response when overexpressing the kinase might just as well be due to the design of the pharmaceutical industry's high-throughput screening assays. Usually, these assays aim at very high sensitivity at the cost of specificity, and understandably so, as missing a potential hit would be way more expensive than erroneously selecting a few false-positives. In the experience of the lab this present work was carried out in, the PathHunter® assay used in the study by Winpenny et al. tends to behave in this very manner, especially with weak partial agonists (experimental data to prove this valuation are not given).

The successful development of TVR130 as an intentionally designed biased agonist spurred further research in the field. One recent work made an effort to elucidate the value of G_i bias in even greater detail. Schmid et al. [217] could conclusively show that the degree of ligand bias has a quantitative effect on the presumed safety of an opioid drug. In their work, the researchers developed an array of μ receptor agonists with distinct degrees of G_i bias by changing the substituents at a piperidine core structure. Over a series of *in vitro* and *in vivo* experiments in mice, these newly designed compounds were found to cause less and less respiratory depression when G_i bias was enhanced while maintaining reliable analgesic potency. Thus, optimizing compounds for the greatest possible ligand bias might become a key goal in future pharmaceutical research.

4.4 TLR4 AND OPIOIDS

When basic concepts of the research work at hand were thought up in 2012, the report by Hutchinson et al. [189] claiming activity of opioid ligands at the TLR4 (also see figure 1.6) was rather new. It was reason-

able to try to investigate action profiles of opioids at the μ receptor and TLR4 simultaneously. To start with, one tried to replicate basic findings for said study in the same reporter gene cell line (HEK-Blue hTLR4).

As the presented results in this work (section 3.10) indicate, it was not possible to reconstruct these prior findings. None of the opioids used in this work elicited substantial TLR4 response in HEK-Blue hTLR4 experiments. This discrepancy can probably be ascribed to two factors: (1) As opposed to Hutchinson et al. [189], great care was taken to diminish any contamination of tested opioids with endotoxins in this work. There is no mention of such measures in the referenced study. Thus, it is possible that, in part, their signals stem from endotoxin contamination. As was pointed out, endotoxin (or LPS) is part of of the cell wall of gram-negative bacteria, of which many genera are found physiologically on and in all humans (e.g. Neisseria). (2) In the experiments presented in this work, opioid-induced TLR4 responses were normalized to a maximum LPS signal and merely corrected for the baseline signal elicited by sterile water. However, Hutchinson et al. [189] used this baseline signal as a reference and normalized all responses to it. This procedure is suited to inflate the measured responses. Still, if statistical evaluation was done properly (which has to be assumed), the corresponding errors would be inflated in a similar manner. Thus, if the authors report statistically significant responses of opioids over a baseline signal - which they do - this has to be appreciated.

Moreover, there are still remarkable findings *in vivo* that remain unaffected by possible methodological shortcomings of the HEK-Blue assay. Apart from the mentioned effects of TLR4 as a functional "antagonist" of opioid signaling [189] and - the other way around - reports that presumed inactive morphine metabolites enhance pain via TLR4 [187], the receptor was also found to play a role in opioid dependence. Interestingly, the opioid antagonists naloxone and naltrexone were found to counteract opioid-induced conditioned place preference, a behavioral test for dependence, and reduced self-administration of remifentanil in rats [218]. This is even more compelling, as the antagonists exerted their effects non-stereoselectively, which would allow for the (+)-isomers to be used as TLR4 modulators without affecting the (-)-selective opioid receptors. This situation, where results in animal studies can not readily be transferred to simplified cell-based assays calls for more sophisticated mechanistic explanations. And indeed, *in silico* docking studies and *in vitro* biochemical experiments seem to show that naloxone, naltrexone, and remifentanil can bind to the TLR4-MD2 complex [218, 219]. The involvement of the co-receptor, MD2, might be one reason for the complexity of the interrelationship of opioids and TLR4 signaling. Another one is that both (+)-naloxone and (+)-naltrexone selectively blocked the TRIF-dependent interferon

I signaling pathway of TLR4, but not MyD88-dependent NF-κB signaling [219] (also see figure 7), much in the sense of biased agonism.

In conclusion, the matter can be summed up as follows: Early findings of opioids activating TLR4 could not be reproduced, neither in this work, nor by another laboratory [191]. The authors of the initial study acknowledge this fact in a way [220] and consider the used assay not entirely suited for the purpose but, quite rightly so, refer to *in vivo* effects as well as *in silico* and *in vitro* hints towards direct binding of opioids to TLR4. At this point, TLR4 antagonism by (+)-isomers of naloxone or naltrexone as lead structures seems to be the most compelling possible application. Future research will need to elucidate the actual molecular mechanisms at the receptor by means of high resolution live-cell assays and resolving of opioid-bound TLR4 structures, even though driving forces in the field appear to be more interested in possible clinical applications.

4.5 LIMITATIONS AND OUTLOOK

In the research work at hand, great care was taken to choose appropriate assays for the respective purposes. However, when weighing up the pros and cons in each situation, there often is no single best assay to choose. In what follows, some limitations of the methods deployed in this work shall be discussed.

4.5.1 *FRET experiments for G_i activation*

The process of G_i activation has its "morphological" correlate in the movement of protein subunits relative to each other in the range of only several nanometers. It is obvious that such movements cannot be detected by means of classic light microscopy due to diffraction limitations. If, additionally, one wants to portray the process in a dynamic fashion, tools like electron or atomic force microscopy are out of the question as they require fixed samples. FRET constitutes a reasonable choice because it meets all the criteria. It can be done in living cells and also yields kinetic information at a millisecond resolution. Some arising limitations are more due to the specifics of the research subject than to the method as such. In this special case where the G protein consists of three separately encoded subunits in addition to the required receptor, one has to deal with four plasmids for transient transfections. This was done in the literature before [197], but when trying to replicate the experimental setup in this work, signal quality was found to be rather poor. Stable transfections would not critically improve the situation, as quadruple-stable cell lines are viable but not easily maintained. The most promising approach seemed to be the implementation of a single-plasmid G_i version with fixed stoichiometric ratios of the subunits [221]. This led to drastically improved signal-

to-noise ratios and greatly enhanced the experimenter's chances to investigate a cell containing all the required components in this single-cell approach. Further improvements could have been stable transfection of the remaining two plasmids (receptor and G_i trimer) or also tagging the receptor with a fluorescent dye for monitoring transfection success. This could be put into effect using a viral 2A peptide, which would be cleaved after translation. By this means, the fluorophore would not permanently stay attached to the receptor and possibly interfere with the measurement, yet its mere existence in the cytosol would prove successful expression of the receptor.

Generally, if one does not make use of the high temporal resolution, a more high throughput-compatible approach would be desirable. So far, ratiometric FRET experiments in microtiter plate readers have been implemented with only very limited success. This is most likely accounted for by the relatively high background signal in FRET experiments due to the need of an external light source and the often rather low quantum yield of the fluorophore pairs in combination with limited sensitivity and specificity of the photomultipliers. A valid alternative could be BRET, which, to the author's knowledge, has so far not been used in the context of G protein activation. Another problem with flourescence-based methods could arise from the unarguably large space the fluorophores take up. One way out would be the use of small-molecule fluorophores such as FlAsH, possibly at the cost of reduced quantum yield. In the present work however, this did not seem to be a problem as the results corresponded to findings from the literature very well (see section 4.1). After all, determining G protein activation by FRET is probably as good as it gets with regard to accuracy and temporal resolution.

4.5.2 *BRET experiments for β-arrestin recruitment*

The recruitment of β-arr2 to the μ receptor was investigated using a BRET approach in this work. Many general considerations are similar to what was said about FRET in section 4.5.1. It was chosen because it allows for dynamic studies of the interaction process in living cells. Moreover and in contrast to single-cell FRET, it is easily implemented in a microtiter format and thus data acquisition is more efficient. One reason which stood against the use of BRET for G_i activation experiments was the fast kinetics of the process under investigation. With β-arr recruitment, this is no major concern as it takes more than a minute for the interaction to occur. Such kinetics can be covered without any problems on usual microtiter plate-readers.

As a possible pitfall, again, the need for fusing a fluorophore to the proteins in question comes into consideration. However, fusion proteins with a GPCR or a β-arr at either terminus are rather standard constructs in the field. Again, the data collected in this work are very

well in line with previously published findings (see section 4.2). Even though in this work, the β-arr was actually fused to a HaloTag rather than the actual fluorophore, this does not argue much in favor of the technique in terms of this very issue as the tag and most fluorophores are comparable in size. Lastly, BRET depends on the presence of a substrate as opposed to FRET. From our results and the comparison with earlier data, there was no reason to believe that the presence of the luciferase substrate interfered with the protein interaction in any way.

4.5.3 *Analysis of agonism bias*

Experiments in this work were carefully designed in order to allow for in-depth analysis with respect to possible ligand bias using the operational model of agonist activity. Detailed characteristics of the applied approach are described in section 1.5. While the approach chosen in this work can be considered the agreed-upon best standard for agonism bias analysis, it has its limitations with very low potency agonists or antagonists. When a ligand's potency in one signalling pathway approaches zero, further calculations are rendered impossible. Recently, modifications to the operational model were proposed. Herein, the pharmacodynamics of partial agonists are evaluated more precisely in a competition assay against a reference full agonist [222]. This *competitive model* would have required additional experiments but might have helped to actually calculate bias values for ligands like buprenorphine rather than simply make estimations based on the apparently missing efficacy in the β-arr assays.

4.5.4 *Reporter gene assay for TLR4 activation*

General and fundamental problems with the HEK-Blue assay as a tool for determining TLR4 activation other than through LPS have been laid out in section 4.4. In brief, the most important concerns are: (1) NF-κB, which is the pivotal point in the assay as it controls the promotor for the synthesis of SEAP, is only one of several signaling endpoints downstream of TLR4. Even though both major pathways (MyD88 and TRIF, see figure 7) lead to the production of NF-κB, there are constellations where it is mostly unaffected [219]. (2) Very much unlike in the oversimplified schematic that is figure 7, a myriad of signaling and adaptor proteins is necessary between receptor activation and NF-κB. Many of those intermediste steps also represent intersection points with other, TLR4-unrelated pathways. This means one uses a very far downstream read-out for the detection of a membrane-bound receptor's activation. In conclusion, the experiments performed in this work were reasonable at the time, but in hindsight merely reproduced the now generally accepted finding in

the field that the used assay is not too well suited for experiments on TLR4 activation by opioids. Direct measures of ligand-receptor interaction or at least activation and recruitment of very early adaptor proteins are needed in future studies to clarify the actual opioid-related processes at toll-like receptors.

4.5.5 *Outlook*

This work provides information about the properties of a wide range of clinically deployed opioids in unprecedented detail with regard to G_i activation and β-arr recruitment to the μ receptor. These very fundamental findings will serve as a basis and reference for future studies on the subject. Future research will have to focus on the translation of these findings into even more physiological experimental systems, i.e. animal models and humans, as pain is a rather complex and subjective phenomenon which cannot be fully appreciated in isolated cell lines. This is even more true for the role of TLR4 in the development of pain and opioid-related side effects. Additionally, more attention will need to be paid to the involvement of GRKs. Maybe some of the features that are today attributed to β-arr are in reality GRK effects with β-arr being the first downstream signal of GRK. For such questions and many more, the present work poses a solid foundation.

5

SUMMARY

5.1 ENGLISH

To this day, opioids represent the most effective class of drugs for the treatment of severe pain. On a molecular level, all opioids in use today are agonists at the μ-opioid receptor (μ receptor). The μ receptor is a class A G protein-coupled receptor (GPCR). GPCRs are among the biological structures most frequently targeted by pharmaceuticals. They are membrane bound receptors, which confer their signals into the cell primarily by activating a variety of GTPases called G proteins. In the course of the signaling process, the μ receptor will be phosphorylated by GRKs, increasing its affinity for another entity of signaling proteins called β-arrestins (β-arrs). The binding of a β-arr to the activated μ receptor will end the G protein signal and cause the receptor to be internalized into the cell. Past research showed that the μ receptor's G protein signal puts into effect the desired pain relieving properties of opioid drugs, whereas β-arr recruitment is more often linked to adverse effects like obstipation, tolerance, and respiratory depression. Recent work in academic and industrial research picked up on these findings and looked into the possibility of enhancing G protein signaling while suppressing β-arr recruitment. The conceptual groundwork of such approaches is the phenomenon of biased agonism. It appreciates the fact that different ligands can change the relative contribution of any given pathway to the overall downstream signaling, thus enabling not only receptor-specific but even pathway-specific signaling.

This work examined the ability of a variety of common opioid drugs to specifically activate the different signaling pathways and quantify it by means of resonance energy transfer and protein complementation experiments in living cells. Phosphorylation of the activated receptor is a central step in the canonical GPCR signaling process. Therefore, in a second step, expression levels of the phosphorylating GRKs were enhanced in search for possible effects on receptor signaling and ligand bias.

In short, detailed pharmacological profiles of 17 opioid ligands were recorded. Comparison with known clinical properties of the compounds showed robust correlation of G protein activation efficacy and analgesic potency. Ligand bias (i.e. significant preference of any pathway over another by a given agonist) was found for a number of opioids in native HEK293 cells overexpressing μ receptor and β-arrs. Furthermore, overexpression of GRK2 was shown to fundamentally

change β-arr pharmacodynamics of nearly all opioids. As a consequence, any ligand bias as detected earlier was abolished with GRK2 overexpression, with the exception of buprenorhin. In summary, the following key findings stand out: (1) Common opioid drugs exert biased agonism at the μ receptor to a small extent. (2) Ligand bias is influenced by expression levels of GRK2, which may vary between individuals, target tissues or even over time. (3) One of the opioids, buprenorhin, did not change its signaling properties with the overexpression of GRK2. This might serve as a starting point for the development of new opioids which could lack the ability of β-arr recruitment altogether and thus might help reduce adverse side effects in the treatment of severe pain.

5.2 DEUTSCH

Nach wie vor stellen Opioide die wirkstärkste Gruppe von Medikamenten zu Behandlung starker Schmerzen dar. Auf molekularer Ebene sind alle heute gebräuchlichen Opioide Agonisten am μ-Opioidrezeptor. Der μ-Opioidrezeptor ist ein G-Protein-gekoppelter Rezeptor (GPCR) der Klasse A. GPCR zählen zu den häufigsten Zielstrukturen von Pharmaka. Sie sind membranständige Rezeptoren, die ihr Signal in erster Linie durch die Aktivierung von G-Proteine genannten GTPasen in die Zelle weiterleiten. Im Laufe des Signalprozesses wird der GPCR von GRK phosphoryliert, wodurch seine Affinität zu einer weiteren Gruppe von Signalproteinen, den sog. β-Arrestinen erhöht wird. Bindet ein β-Arrestin an den Rezeptor, beendet dies das G-Proteinsignal und veranlasst die Internalisierung des Rezeptors ins Zellinnere. Bisherige Forschung zeigte, dass das G-Proteinsignal des μ-Opioidrezeptors die erwünschte Schmerzlinderung vermittelt, wohingegen die Rekrutierung von β-Arrestin oftmals mit unerwünschten Wirkungen wie Obstipation, Toleranzentwicklung und Atemdepression in Verbindung gebracht wird. Neuere akademische und industrielle Forschung griff diese Erkenntnisse auf und erkundete die Möglichkeit, das G-Proteinsignal zu verstärken und zur gleichen Zeit die β-Arrestinrekrutierung zu inhibieren. Die theoretische Grundlage solcher Ansätze liegt im Konzept des *biased agonism*. Dieses berücksichtigt die Tatsache, dass verschiedene Liganden den Anteil eines bestimmten Signalweges am gesamten vom Rezeptor ausgehenden Signals beeinflussen kann und damit nicht nur rezeptor-, sondern sogar signalwegspezifische Signale möglich sein sollten.
Die vorliegende Arbeit untersuchte eine Reihe von gängigen Opioiden auf ihre Fähigkeit hin, die einzelnen Signalwege spezifisch zu aktivieren und quantifizierte dies mit Methoden des Resonanzenergietransfers sowie der Proteinkomplementierung in lebenden Zellen. Die Phosphorylierung des Rezeptors ist ein zentrales Ereignis in der anerkannten Abfolge der Signalprozesse an GPCR. Daher wurde in

einem weiteren Schritt die Expression der phosphorylierenden GRK erhöht und nach möglichen Auswirkungen auf die Selektivität der Signalwegaktivierung gesucht. Hierbei wurde detaillierte pharmakologische Profile von 17 Opioiden erstellt. Der Abgleich mit bekannten klinischen Wirkeigenschaften der Substanzen zeigte einen robusten Zusammenhang zwischen der Fähigkeit, G-Proteine zu aktivieren und der analgetischen Wirkstärke. *Ligand bias*, d.h. die signifikante Bevorzugung eines Signalweges gegenüber einem anderen durch einen Liganden, konnte für eine Reihe von Opioiden in lebenden HEK293-Zellen gezeigt werden, die den μ-Opioidrezeptor sowie β-Arrestine überexprimierten. Darüber hinaus konnte gezeigt werden, dass die zusätzliche Überexpression von GRK2 die pharmakodynamischen Eigenschaften nahezu aller Opioide grundlegend veränderte. In der Folge war jeder zuvor gezeigte *ligand bias* mit Ausnahme von Buprenorphin aufgehoben.

Zusammenfassend stehen die folgenden drei Erkenntnisse im Vordergrund: (1) Gängige Opioide zeigen in einem gewissen Maß Selektivität zwischen den Signalwegen. (2) *Ligand bias* wird beeinflusst von GRK2-Expressionsleveln, welche zwischen Individuen, verschiedenen Gewebetypen oder auch im zeitlichen Verlauf variieren können. (3) Als einziges der untersuchten Opioide änderte Buprenorphin seine Signaleigenschaften durch die Überexpression von GRK2 nicht. Dies könnte als Anknüpfungspunkt in der Entwicklung neuer Opioide dienen, die keinerlei β-Arrestinrekrutierung bewirken und dadurch helfen könnten, unerwünschte Wirkungen in der Behandlung starker Schmerzen zu verhindern.

A

APPENDIX

A.1 CHEMICAL STRUCTURES OF OPIOID LIGANDS

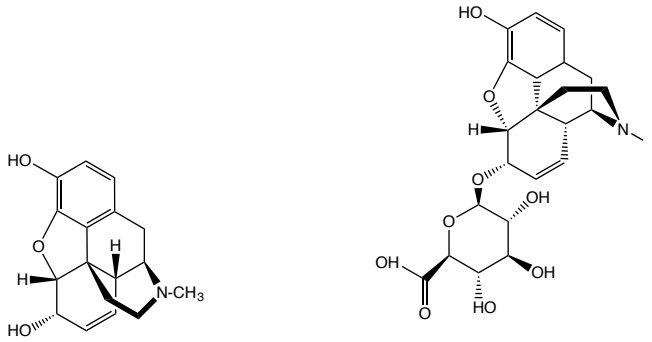

(a) Morphine (b) M-6-G

Figure 29: Structural formulae of opium alkaloids used in this work

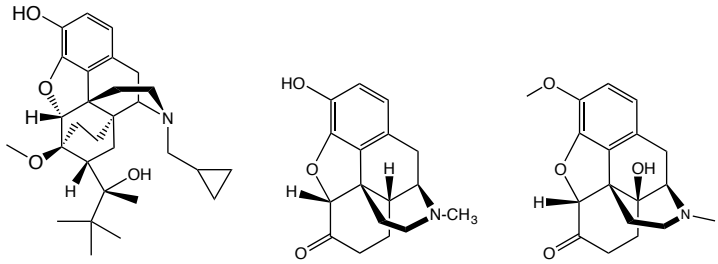

(a) Buprenorphine (b) Hydromorphone (c) Oxycodone

Figure 30: Structural formulae of semi-synthetic alkaloid derivatives used in this work

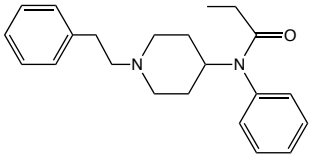

(a) Fentanyl

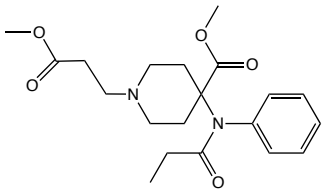

(b) Remifentanil

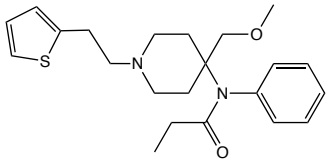

(c) Sufentanil

Figure 31: Structural formulae of synthetic opioids used in this work: Anilidopiperidines

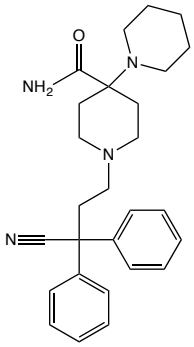

(a) Piritramide

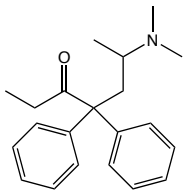

(b) Methadone

Figure 32: Structural formulae of synthetic opioids used in this work: Diphenylpropylamine derivatives

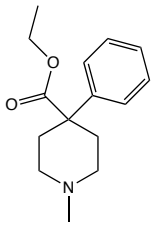

(a) Pethidine

Figure 33: Structural formula of synthetic opioids used in this work: Phenylpiperidines

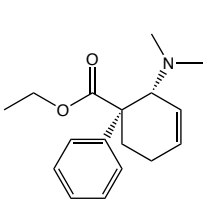

(a) Tilidine

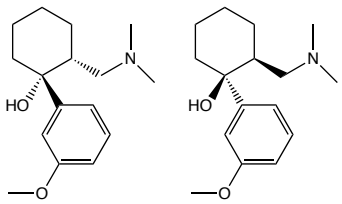

(b) (1R,2R)- and (1S,2S)-Tramadol

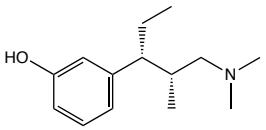

(c) Tapentadol

Figure 34: Structural formulae of synthetic opioids used in this work: Others

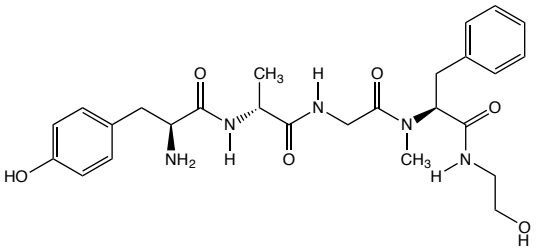

(a) DAMGO

Figure 35: Structural formula of synthetic peptide opioids used in this work: DAMGO

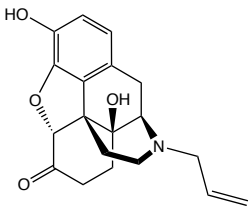

(a) Naloxone

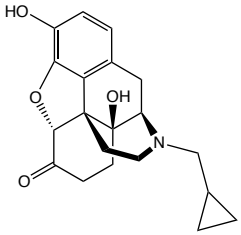

(b) Naltrexone

Figure 36: Structural formulae of synthetic opioids used in this work: Antagonists

A.2 β-ARRESTIN 1 AND 2 RECRUITMENT TO THE μ RECEPTOR (LUCIFERASE COMPLEMENTATION)

As pointed out previously, the data on β-arr 1 and 2 recruitment as determined by luciferase complementation are part of a separate, still unpublished work by Stefanie Meyer. The following table 12 shall hereby explicitly be declared a citation of the aforementioned unpublished work.

	β-arrestin1 recruitment			β-arrestin2 recruitment		
	Emax (S.E.M.)	$EC50$ $[nM]$	logEC50 (S.E.M.)	Emax (S.E.M.)	$EC50$ $[nM]$	logEC50 (S.E.M.)
DAMGO	0.99 (0.16)	9,150	−5.04 (0.36)	1.01 (0.08)	3,630	−5.44 (0.18)
Buprenorphine	0.0 (−)	–	– –	0.0 –	–	– –
Fentanyl	0.53 (0.06)	856	−6.07 (0.13)	0.53 (0.06)	400	−6.40 (0.19)
Hydromorphone	0.05 (0.01)	70.0	−7.16 (0.21)	0.19 (0.02)	384	−6.42 (0.14)
M6G		#		0.26 (0.64)	8,480	−5.07 (1.89)
Methadone	0.65 (0.07)	5,030	−5.30 (0.15)	0.75 (0.07)	5,240	−5.28 (0.16)
Morphine	0.12 (0.07)	9,830	−5.01 (0.54)	0.23 (0.02)	3,080	−5.51 (0.12)

	β-arrestin1 recruitment			β-arrestin2 recruitment		
	Emax (S.E.M.)	$EC50$ $[nM]$	logEC50 (S.E.M.)	Emax (S.E.M.)	$EC50$ $[nM]$	logEC50 (S.E.M.)
Naloxone	0.0 –	–	– –	0.0 –	–	– –
Naltrexone	0.0 –	–	– –	0.0 –	–	– –
Oxycodone	0.06 (0.01)	24,800	−4.61 (0.18)	0.20 (0.02)	19,200	−4.72 (0.14)
Pethidine	0.10 (0.01)	251,000	−3.60 (0.19)	0.22 (0.02)	257,000	−3.59 (0.14)
Piritramide	0.34 (0.05)	18,800	−4.37 (0.28)	0.43 (0.04)	3,470	−5.46 (0.15)
Remifentanil	0.74 (0.17)	1,020	−5.99 (0.44)	0.87 (0.10)	1,080	−5.97 (0.21)
Sufentanil	0.55 (0.14)	89.1	−7.05 (0.25)	0.70 (0.10)	37.4	−7.43 (0.18)

	β-arrestin1 recruitment			β-arrestin2 recruitment		
	Emax (S.E.M.)	*EC*50 $[nM]$	logEC50 (S.E.M.)	Emax (S.E.M.)	*EC*50 $[nM]$	logEC50 (S.E.M.)
Tapentadol	0.0	–	–	0.0	–	–
	–		–	–		–
Tilidine	0.0	–	–	0.0	–	–
	–		–	–		–
Tramadol	0.0	–	–	0.0	–	–
	–		–	–		–

Table 12: Pharmacological properties of 17 opioid ligands for β-arrestin 1 and 2 recruitment. Data stem from luciferase complementation experiments, GRK2 was not overexpressed in the cells. # no data acquired due to ligand supply shortages.

A.3 BIAS PLOTS

A.3.1 *Luciferase Complementation*

The following figure 37 shows all $\Delta\Delta \log(\tau/K_A)$ values from the calculations of biased agonism with FRET G_i and luciferase complementation β-arr data. This figure is in part shown in section 3.7 (figure 23)

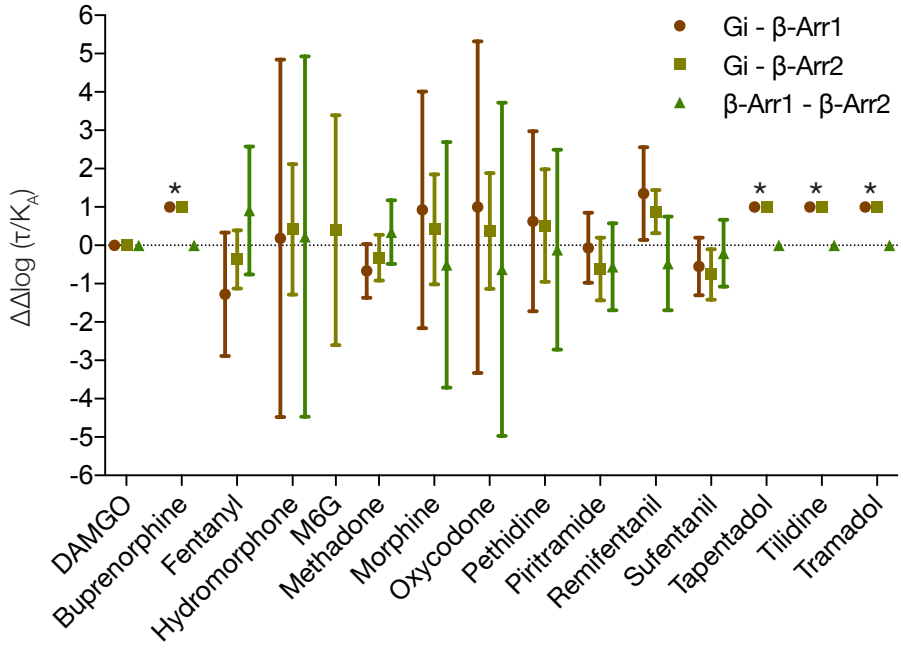

Figure 37: Bias plot of all opioid agonists. Bias was calculated based on FRET G_i data and β-arr recruitment data from luciferase complementation. Positive $\Delta\Delta \log(\tau/K_A)$ values indicate bias towards the signalling pathway named first in the respective legend, and vice versa. Error bars denote 95% CI. Values marked with an asterisk (*) are arbitrarily assigned to 1. Here, bias could not be calculated due to missing activity in both β-arr pathways.

BIBLIOGRAPHY

[1] Thomas Sydenham. *Thomae Sydenham, M.D., Opera Omnia*. The Sydenham Society, London, 1844.

[2] Michael J Brownstein. A brief history of opiates, opioid peptides, and opioid receptors. *Proc Natl Acad Sci U S A*, 90(12): 5391–5393, June 1993.

[3] Susanne Frick, Robert Kramell, Jürgen Schmidt, Anthony J Fist, and Toni M Kutchan. Comparative qualitative and quantitative determination of alkaloids in narcotic and condiment Papaver somniferum cultivars. *Journal of natural products*, 68(5):666–673, May 2005.

[4] Klaus Aktories and Wolfgang Forth. *Pharmakologie und Toxikologie*. Elsevier, Urban&Fischer Verlag, 2009.

[5] Marshall Gates and Gilg Tschudi. The synthesis of morphine. *J Am Chem Soc*, 1956.

[6] R C Heel, R N Brogden, T M Speight, and G S Avery. Buprenorphine: a review of its pharmacological properties and therapeutic efficacy. *Drugs*, 17(2):81–110, February 1979.

[7] Kabirullah Lutfy Cowan and Alan. Buprenorphine: A Unique Drug with Complex Pharmacology. *Current Neuropharmacology*, 2(4):395–402.

[8] Barbara A Coda, Anita C Rudy, Sanford M Archer, and Daniel P Wermeling. Pharmacokinetics and Bioavailability of Single-Dose Intranasal Hydromorphone Hydrochloride in Healthy Volunteers. *Anesthesia & Analgesia*, pages 117–123, July 2003.

[9] E Falk. Eukodal, ein neues Narkotikum. *Munchener Medizinische Wochenschrift*, 20:381–384, 1917.

[10] Karine Thibault, Bernard Calvino, Isabelle Rivals, Fabien Marchand, Sophie Dubacq, Stephen B McMahon, and Sophie Pezet. Molecular Mechanisms Underlying the Enhanced Analgesic Effect of Oxycodone Compared to Morphine in Chemotherapy-Induced Neuropathic Pain. *PLoS One*, 9(3):e91297–13, March 2014.

[11] Eija Kalso. How different is oxycodone from morphine? *Pain*, 132(3):227–228, December 2007.

[12] R Hess, G Stiebler, and A Herz. Pharmacokinetics of fentanyl in man and the rabbit. *European journal of clinical pharmacology*, 4(3):137–141, 1972.

[13] Theodore H Stanley. The history and development of the fentanyl series. *Journal of pain and symptom management*, 7(3 Suppl): S3–7, April 1992.

[14] Hartmut Burkle, Stuart Dunbar, and Hugo Van Aken. Remifentanil: A Novel, Short-Acting, mu-Opioid. *Anesthesia & Analgesia*, 83(3):646, September 1996.

[15] CJE Niemegeers, KHL Schellekens, WFM van Bever, and PAJ Janssen. Sufentanil, a Very Potent and Extremely Safe Intravenous Morphine-Like Compound in Mice, Rats and Dogs. *Arzneimittel-forschung*, 26(8):1551–1556, 1976.

[16] Paul AJ Janssen. Pirinitramide (R 3365), a potent analgesic with unusual chemical structure. *Journal of Pharmacy and Pharmacology*, 13(1):513–530, 1961.

[17] R Brown, C Kraus, M Fleming, and S Reddy. Methadone: applied pharmacology and use as adjunctive treatment in chronic pain. *Postgraduate medical journal*, 80(949):654–659, November 2004.

[18] Martin Michaelis, Bernward Schölkens, and Karl Rudolphi. *An anthology from Naunyn-Schmiedeberg's archives of pharmacology.*, volume 375. Science and Medical Affairs, Sanofi-Aventis Deutschland GmbH, Industriepark Höchst, Bldg. H821, 65926, Frankurt am Main, Germany. Martin.Michaelis@sanofi-aventis.com, April 2007.

[19] Kenneth S Latta, Brian Ginsberg, and Robert L Barkin. Meperidine: a critical review. *American journal of therapeutics*, 9(1):53–68, January 2002.

[20] M Herrmann, W Steinbrecher, and W Heldt. *Zur Pharmakologie eines neuen stark wirksamen Analgeticums*. Arzneimittel-Forsch, 1970.

[21] R Schulz, J Bläsig, M Wüster, and A Herz. The opiate-like action of tilidine is mediated by metabolites. *Naunyn-Schmiedeberg's Archives of Pharmacology*, 304(2):89–93, September 1978.

[22] G Osterloh, E Friderichs, F Felgenhauer, W A Gunzler, Z Henmi, T Kitano, M Nakamura, H Hayashi, and I Ishii. General pharmacological studies on tramadol, a potent analgetic agent (author's translation). *Arzneimittel-forschung*, 28(1a):135–151, 1978.

[23] B Driessen and W Reimann. Interaction of the central analgesic, tramadol, with the uptake and release of 5-hydroxytryptamine in the rat brain in vitro. *Br J Pharmacol*, 105(1):147–151, January 1992.

[24] W Reimann and F Schneider. Induction of 5-hydroxytryptamine release by tramadol, fenfluramine and reserpine. *European journal of pharmacology*, 349(2-3):199–203, 1998.

[25] M C Frink, H H Hennies, W Englberger, M Haurand, and B Wilffert. Influence of tramadol on neurotransmitter systems of the rat brain. *Arzneimittel-forschung*, 46(11):1029–1036, November 1996.

[26] Koji Hara, Kouichiro Minami, and Takeyoshi Sata. The effects of tramadol and its metabolite on glycine, gamma-aminobutyric acidA, and N-methyl-D-aspartate receptors expressed in Xenopus oocytes. *Anesthesia & Analgesia*, 100(5):1400–5– table of contents, May 2005.

[27] Stefan Grond, T Meuser, D Zech, U Hennig, and Klaus A Lehmann. Analgesic efficacy and safety of tramadol enantiomers in comparison with the racemate: a randomised, double-blind study with gynaecological patients using intravenous patient-controlled analgesia. *Pain*, 62(3):313–320, September 1995.

[28] Thomas M Tzschentke, Thomas Christoph, Babette Kögel, Klaus Schiene, Hagen-Heinrich Hennies, Werner Englberger, Michael Haurand, Ulrich Jahnel, Thomas I F H Cremers, Elmar Friderichs, and Jean De Vry. (–)-(1R,2R)-3-(3-Dimethylamino-1-ethyl-2-methyl-propyl)-phenol Hydrochloride (Tapentadol HCl): a Novel μ-Opioid Receptor Agonist/Norepinephrine Reuptake Inhibitor with Broad-Spectrum Analgesic Properties. *The Journal of pharmacology and experimental therapeutics*, 323(1): 265–276, October 2007.

[29] Balraj K Handa, Anthony C Lane, John AH Lord, Barry A Morgan, Michael J Rance, and Colin FC Smith. Analogs of Beta-Lph61-64 Possessing Selective Agonist Activity at Mu-Opiate Receptors. *European journal of pharmacology*, 70(4):531–540, 1981.

[30] Craig Hartrick, Ilse Van Hove, Jens-Ulrich Stegmann, Charles Oh, and David Upmalis. Efficacy and tolerability of tapentadol immediate release and oxycodone HCl immediate release in patients awaiting primary joint replacement surgery for end-stage joint disease: a 10-day, phase III, randomized, double-blind, active- and placebo-controlled study. *Clinical therapeutics*, 31(2):260–271, February 2009.

[31] Karl-Heinz Graefe, Werner Lutz, and Heinz Bönisch. *Pharmakologie und Toxikologie*. Duale Reihe. Georg Thieme Verlag, Stuttgart, 2011.

[32] World Health Organization. *Cancer Pain Relief*. With a Guide to Opioid Availability. World Health Organization, Geneva, second edition edition, January 1996.

[33] Detlev FJ Zech, Stefan Grond, John Lynch, Dagmar Hertel, and Klaus A Lehmann. Validation of World-Health-Organization Guidelines for Cancer Pain Relief - a 10-Year Prospective-Study. *Pain*, 63(1):65–76, October 1995.

[34] World Health Organization. WHO Model List of Essential Medicines for Adults. August 2015.

[35] Margo McCaffery. *Pain*. Clinical Manual. Mosby Incorporated, 1999.

[36] Andrea D Furlan, Juan A Sandoval, Angela Mailis-Gagnon, and Eldon Tunks. Opioids for chronic noncancer pain: a meta-analysis of effectiveness and side effects. *CMAJ : Canadian Medical Association journal = journal de l'Association medicale canadienne*, 174(11):1589–1594, May 2006.

[37] Igor Kissin. Long-term opioid treatment of chronic nonmalignant pain: unproven efficacy and neglected safety? *Journal of pain research*, 6:513–529, 2013.

[38] Roger Chou, Jane C Ballantyne, Gilbert J Fanciullo, Perry G Fine, and Christine Miaskowski. Research gaps on use of opioids for chronic noncancer pain: findings from a review of the evidence for an American Pain Society and American Academy of Pain Medicine clinical practice guideline. *The journal of pain : official journal of the American Pain Society*, 10(2):147–159, February 2009.

[39] M Noble, J R Treadwell, and S J Tregear. Long-term opioid management for chronic noncancer pain. *... Database Syst Rev*, 2010.

[40] J P Schneider and K L Kirsh. Defining clinical issues around tolerance, hyperalgesia, and addiction: a quantitative and qualitative outcome study of long-term opioid dosing in a chronic pain .... *J Opioid Manag*, 2010.

[41] Ramsin Benyamin, Andrea M Trescot, Sukdeb Datta, Ricardo Buenaventura, Rajive Adlaka, Nalini Sehgal, Scott E Glaser, and Ricardo Vallejo. Opioid complications and side effects. *Pain Physician*, 11(2 Suppl):S105–20, March 2008.

[42] A Dahan. Respiratory depression with opioids. *Journal of Pain and Palliative Care . . .*, 2007.

[43] Susan Okie. A flood of opioids, a rising tide of deaths. *N Engl J Med*, 363(21):1981–1985, November 2010.

[44] Kathryn P Anastassopoulos, Wing Chow, Stacey J Ackerman, Crisanta Tapia, Carmela Benson, and Myoung S Kim. Oxycodone-related side effects: impact on degree of bother, adherence, pain relief, satisfaction, and quality of life. *J Opioid Manag*, 7(3):203–215, 2011.

[45] Laura M Bohn and Kirsten M Raehal. Opioid receptor signaling: relevance for gastrointestinal therapy. *Current opinion in pharmacology*, 6(6):559–563, December 2006.

[46] United Nations Office on Drugs and Crime. *World Drug Report 2015*. United Nations, 2015.

[47] Laxmaiah Manchikanti, Standiford II Helm, Bert Fellows, Jeffrey W Janata, Vidyasagar Pampati, Jay S Grider, and Mark V Boswell. Opioid Epidemic in the United States. *Pain Physician*, 15(3):ES9–ES38, July 2012.

[48] Robert Fredriksson, Malin C Lagerström, Lars-Gustav Lundin, and Helgi B Schiöth. The G-protein-coupled receptors in the human genome form five main families. Phylogenetic analysis, paralogon groups, and fingerprints. *Mol Pharmacol*, 63(6):1256–1272, June 2003.

[49] Thóra K Bjarnadóttir, David E Gloriam, Sofia H Hellstrand, Helena Kristiansson, Robert Fredriksson, and Helgi B Schiöth. Comprehensive repertoire and phylogenetic analysis of the G protein-coupled receptors in human and mouse. *Genomics*, 88 (3):263–273, September 2006.

[50] Angélique Levoye, Julie Dam, Mohammed A Ayoub, Jean-Luc Guillaume, and Ralf Jockers. Do orphan G-protein-coupled receptors have ligand-independent functions? New insights from receptor heterodimers. *EMBO Rep*, 7(11):1094–1098, November 2006.

[51] Mathias Rask-Andersen, Markus Sallman Almen, and Helgi B Schiöth. Trends in the exploitation of novel drug targets. *Nature reviews. Drug discovery*, 10(8):579–590, August 2011.

[52] Kristen L Pierce, Richard T Premont, and Robert J Lefkowitz. Seven-transmembrane receptors. *Nature reviews. Molecular cell biology*, 3(9):639–650, September 2002.

[53] J N Langley. On the reaction of cells and of nerve-endings to certain poisons, chiefly as regards the reaction of striated muscle to nicotine and to curari. *The Journal of Physiology*, 33(4-5): 374–413, December 1905.

[54] Lewis T Williams, Debra Mullikin, and Robert J Lefkowitz. Identification of alpha-adrenergic receptors in uterine smooth muscle membranes by [3H]dihydroergocryptine binding. *J Biol Chem*, 251(22):6915–6923, November 1976.

[55] L T Williams, R Snyderman, and R J Lefkowitz. Identification of beta-adrenergic receptors in human lymphocytes by (-) (3H) alprenolol binding. *The Journal of Clinical Investigation*, 57(1): 149–155, January 1976.

[56] Erik Huss. The Nobel Prize in Chemistry 2012. The Royal Swedish Academy of Sciences, October 2012.

[57] T K Attwood and J B Findlay. Fingerprinting G-protein-coupled receptors. *Protein engineering*, 7(2):195–203, February 1994.

[58] Aashish Manglik, Andrew C Kruse, Tong Sun Kobilka, Foon Sun Thian, Jesper M Mathiesen, Roger K Sunahara, Leonardo Pardo, William I Weis, Brian K Kobilka, and Sébastien Granier. Crystal structure of the μ-opioid receptor bound to a morphinan antagonist. *Nature*, 485(7398):321–326, May 2012.

[59] A J Venkatakrishnan, Xavier Deupi, Guillaume Lebon, Christopher G Tate, Gebhard F Schertler, and M Madan Babu. Molecular signatures of G-protein-coupled receptors. *Nature*, 494(7436): 185–194, 02 2013.

[60] Aashish Manglik, Tae Hun Kim, Matthieu Masureel, Christian Altenbach, Zhongyu Yang, Daniel Hilger, Michael T Lerch, Tong Sun Kobilka, Foon Sun Thian, Wayne L Hubbell, R Scott Prosser, and Brian K Kobilka. Structural Insights into the Dynamic Process of β2-Adrenergic Receptor Signaling. *Cell*, 161 (5):1101–1111, May 2015.

[61] Jean-Pierre Vilardaga, Moritz Bünemann, Cornelius Krasel, Mariàn Castro, and Martin J Lohse. Measurement of the millisecond activation switch of G protein-coupled receptors in living cells. *Nature biotechnology*, 21(7):807–812, July 2003.

[62] E H Hurowitz, J M Melnyk, Y J Chen, H Kouros-Mehr, M I Simon, and H Shizuya. Genomic characterization of the human heterotrimeric G protein alpha, beta, and gamma subunit genes. *DNA research : an international journal for rapid publication of reports on genes and genomes*, 7(2):111–120, April 2000.

[63] Nina Wettschureck and Stefan Offermanns. Mammalian G proteins and their cell type specific functions. *Physiological Reviews*, 85(4):1159–1204, October 2005.

[64] Moritz Bünemann, Monika Frank, and Martin J Lohse. Gi protein activation in intact cells involves subunit rearrangement rather than dissociation. *Proc Natl Acad Sci U S A*, 100(26):16077–16082, December 2003.

[65] Gregory J Digby, Robert M Lober, Pooja R Sethi, and Nevin A Lambert. Some G protein heterotrimers physically dissociate in living cells. *Proc Natl Acad Sci U S A*, 103(47):17789–17794, 2006.

[66] Connie L Lerea, David E Somers, James B Hurley, Ingrid B Klock, and Ann H Bunt-Milam. Identification of specific transducin alpha subunits in retinal rod and cone photoreceptors. *Science*, 1986.

[67] R K Sunahara, C W Dessauer, and Alfred G Gilman. Complexity and diversity of mammalian adenylyl cyclases. *Annual Review of Pharmacology and Toxicology*, 36(1):461–480, 1996.

[68] J H Exton. Regulation of phosphoinositide phospholipases by hormones, neurotransmitters, and other agonists linked to G proteins. *Annual Review of Pharmacology and Toxicology*, 36(1): 481–509, 1996.

[69] Anne M Buhl, Nancy Lassignal Johnson, N Dhanasekaran, and G L JOHNSON. G-Alpha(12) and G-Alpha(13) Stimulate Rho-Dependent Stress Fiber Formation and Focal Adhesion Assembly. *J Biol Chem*, 270(42):24631–24634, 1995.

[70] Scott K Gibson and Alfred G Gilman. Gialpha and Gbeta subunits both define selectivity of G protein activation by alpha2-adrenergic receptors. *Proc Natl Acad Sci U S A*, 103(1):212–217, January 2006.

[71] Yuan Lin and Alan V Smrcka. Understanding molecular recognition by G protein $\beta\gamma$ subunits on the path to pharmacological targeting. *Mol Pharmacol*, 80(4):551–557, October 2011.

[72] D R Brandt and E M Ross. GTPase activity of the stimulatory GTP-binding regulatory protein of adenylate cyclase, Gs. Accumulation and turnover of enzyme-nucleotide intermediates. *J Biol Chem*, 260(1):266–272, January 1985.

[73] D E Logothetis, Y Kurachi, J Galper, E J Neer, and D E Clapham. The beta gamma subunits of GTP-binding proteins activate the muscarinic K+ channel in heart. *Nature*, 325(6102):321–326, January 1987.

[74] S R Ikeda. Voltage-dependent modulation of N-type calcium channels by G-protein beta gamma subunits. *Nature*, 380(6571): 255–258, 1996.

[75] W J TANG and Alfred G Gilman. Type-Specific Regulation of Adenylyl Cyclase by G-Protein Beta-Gamma-Subunits. *Science*, 254(5037):1500–1503, 1991.

[76] Peter Hein, Monika Frank, Carsten Hoffmann, Martin J Lohse, and Moritz Bünemann. Dynamics of receptor/G protein coupling in living cells. *EMBO J*, 24(23):4106–4114, December 2005.

[77] Soren G F Rasmussen, Brian T DeVree, Yaozhong Zou, Andrew C Kruse, Ka Young Chung, Tong Sun Kobilka, Foon Sun Thian, Pil Seok Chae, Els Pardon, Diane Calinski, Jesper M Mathiesen, Syed T A Shah, Joseph A Lyons, Martin Caffrey, Samuel H Gellman, Jan Steyaert, Georgios Skiniotis, William I Weis, Roger K Sunahara, and Brian K Kobilka. Crystal structure of the β2 adrenergic receptor-Gs protein complex. *Nature*, 477 (7366):549–555, September 2011.

[78] U Wilden, S W Hall, and H Kühn. Phosphodiesterase activation by photoexcited rhodopsin is quenched when rhodopsin is phosphorylated and binds the intrinsic 48-kDa protein of rod outer segments. *Proc Natl Acad Sci U S A*, 83(5):1174–1178, March 1986.

[79] M J Lohse, J L Benovic, J Codina, M G Caron, and Robert J Lefkowitz. beta-Arrestin: a protein that regulates beta-adrenergic receptor function. *Science*, 248(4962):1547–1550, June 1990.

[80] S S Ferguson, W E 3rd Downey, A M Colapietro, L S Barak, L Menard, and M G Caron. Role of beta-arrestin in mediating agonist-promoted G protein-coupled receptor internalization. *Science*, 271(5247):363–366, January 1996.

[81] O B Goodman, J G Krupnick, F Santini, V V Gurevich, R B Penn, A W Gagnon, J H Keen, and J L Benovic. beta-arrestin acts as a clathrin adaptor in endocytosis of the beta(2)-adrenergic receptor. *Nature*, 383(6599):447–450, 1996.

[82] S A Laporte, R H Oakley, J Zhang, J A Holt, SSG Ferguson, M G Caron, and L S Barak. The beta(2)-adrenergic receptor/-beta arrestin complex recruits the clathrin adaptor AP-2 during endocytosis. *Proc Natl Acad Sci U S A*, 96(7):3712–3717, 1999.

[83] S K Shenoy and Robert J Lefkowitz. Multifaceted roles of beta-arrestins in the regulation of seven-membrane-spanning receptor trafficking and signalling. *Biochemical Journal*, 375(Pt 3):503–515, 2003.

[84] Robert J Lefkowitz and S K Shenoy. Transduction of receptor signals by beta-arrestins. *Science*, 308(5721):512–517, April 2005.

[85] K A DeFea, J Zalevsky, M S Thoma, O Dery, R D Mullins, and N W Bunnett. beta-Arrestin-dependent endocytosis of proteinase-activated receptor 2 is required for intracellular targeting of activated ERK1/2. *J Cell Biol*, 148(6):1267–1281, 2000.

[86] R H Oakley, S A Laporte, J A Holt, M G Caron, and L S Barak. Differential affinities of visual arrestin, beta arrestin1, and beta arrestin2 for G protein-coupled receptors delineate two major classes of receptors. *J Biol Chem*, 275(22):17201–17210, June 2000.

[87] Eric Reiter and Robert J Lefkowitz. GRKs and beta-arrestins: roles in receptor silencing, trafficking and signaling. *Trends in endocrinology and metabolism: TEM*, 17(4):159–165, May 2006.

[88] J A Pitcher, N J Freedman, and Robert J Lefkowitz. G protein-coupled receptor kinases. *Annu Rev Biochem*, 67:653–692, 1998.

[89] C K Chen, K Zhang, J Church-Kopish, W Huang, H Zhang, Y J Chen, J M Frederick, and W Baehr. Characterization of human GRK7 as a potential cone opsin kinase. *Molecular vision*, 7:305–313, December 2001.

[90] C Ambrose, M James, G Barnes, C Lin, G Bates, M Altherr, M Duyao, N Groot, D Church, and J J Wasmuth. A novel G protein-coupled receptor kinase gene cloned from 4p16.3. *Human molecular genetics*, 1(9):697–703, December 1992.

[91] C V Carman, J L Parent, P W Day, A N Pronin, P M Sternweis, P B Wedegaertner, Alfred G Gilman, J L Benovic, and T Kozasa. Selective regulation of G alpha(q/11) by an RGS domain in the G protein-coupled receptor kinase, GRK2. *J Biol Chem*, 274(48): 34483–34492, 1999.

[92] Adi Raveh, Ayelet Cooper, Liora Guy-David, and Eitan Reuveny. Nonenzymatic rapid control of GIRK channel function by a G protein-coupled receptor kinase. *Cell*, 143(5):750–760, November 2010.

[93] Eugenia V Gurevich, John J G Tesmer, Arcady Mushegian, and Vsevolod V Gurevich. G protein-coupled receptor kinases: More than just kinases and not only for GPCRs. *Pharmacology & Therapeutics*, 133(1):40–69, January 2012.

[94] John T Williams, Susan L Ingram, Graeme Henderson, Charles Chavkin, Mark von Zastrow, Stefan Schulz, Thomas Koch, Christopher J Evans, and MacDonald J Christie. Regulation

of μ-opioid receptors: desensitization, phosphorylation, internalization, and tolerance. *Pharmacol Rev*, 65(1):223–254, January 2013.

[95] A Kovoor, J P Celver, A Wu, and C Chavkin. Agonist induced homologous desensitization of mu-opioid receptors mediated by G protein-coupled receptor kinases is dependent on agonist efficacy. *Mol Pharmacol*, 54(4):704–711, October 1998.

[96] Jie Zhang, Stephen S G Ferguson, Larry S Barak, Sobha R Bodduluri, Stéphane A Laporte, Ping-Yee Law, and Marc G Caron. Role for G protein-coupled receptor kinase in agonist-specific regulation of μ-opioid receptor responsiveness. *Proc Natl Acad Sci U S A*, 95(12):7157–7162, June 1998.

[97] K Peppel, I Boekhoff, P McDonald, H Breer, M G Caron, and Robert J Lefkowitz. G protein-coupled receptor kinase 3 (GRK3) gene disruption leads to loss of odorant receptor desensitization. *J Biol Chem*, 272(41):25425–25428, 1997.

[98] R El Kouhen, A L Burd, L J Erickson-Herbrandson, C Y Chang, P Y Law, and H H Loh. Phosphorylation of Ser363, Thr370, and Ser375 residues within the carboxyl tail differentially regulates mu-opioid receptor internalization. *J Biol Chem*, 276(16):12774–12780, April 2001.

[99] S Schulz, D Mayer, M Pfeiffer, R Stumm, T Koch, and V Hollt. Morphine induces terminal mu-opioid receptor desensitization by sustained phosphorylation of serine-375. *EMBO J*, 23(16): 3282–3289, 2004.

[100] Elaine K Lau, Michelle Trester-Zedlitz, Jonathan C Trinidad, Sarah J Kotowski, Andrew N Krutchinsky, Alma L Burlingame, and Mark von Zastrow. Quantitative encoding of the effect of a partial agonist on individual opioid receptors by multisite phosphorylation and threshold detection. *Science signaling*, 4 (185):ra52, August 2011.

[101] J L Whistler and M von Zastrow. Morphine-activated opioid receptors elude desensitization by beta-arrestin. *Proc Natl Acad Sci U S A*, 95(17):9914–9919, August 1998.

[102] Laura M Bohn, Raul R Gainetdinov, and Marc G Caron. G protein-coupled receptor kinase/β-arrestin systems and drugs of abuse. *NeuroMolecular Medicine*, 5(1):41–50, February 2004.

[103] Christian Doll, Florian Pöll, Kenneth Peuker, Anastasia Loktev, Laura Glück, and Stefan Schulz. Deciphering μ-opioid receptor phosphorylation and dephosphorylation in HEK293 cells. *Br J Pharmacol*, 167(6):1259–1270, October 2012.

[104] C Y Chen, S B Dion, C M Kim, and J L Benovic. Beta-adrenergic receptor kinase. Agonist-dependent receptor binding promotes kinase activation. *J Biol Chem*, 268(11):7825–7831, April 1993.

[105] Kelly N Nobles, Kunhong Xiao, Seungkirl Ahn, Arun K Shukla, Christopher M Lam, Sudarshan Rajagopal, Ryan T Strachan, Teng-Yi Huang, Erin A Bressler, Makoto R Hara, Sudha K Shenoy, Steven P Gygi, and Robert J Lefkowitz. Distinct phosphorylation sites on the β(2)-adrenergic receptor establish a barcode that encodes differential functions of β-arrestin. *Science signaling*, 4(185):ra51–ra51, August 2011.

[106] G Grecksch, S Just, C Pierstorff, A K Imhof, L Gluck, C Doll, A Lupp, A Becker, T Koch, R Stumm, V Hollt, and S Schulz. Analgesic Tolerance to High-Efficacy Agonists But Not to Morphine Is Diminished in Phosphorylation-Deficient S375A - Opioid Receptor Knock-In Mice. *J Neurosci*, 31(39):13890–13896, September 2011.

[107] Davide Calebiro, Viacheslav O Nikolaev, Maria Cristina Gagliani, Tiziana de Filippis, Christian Dees, Carlo Tacchetti, Luca Persani, and Martin J Lohse. Persistent cAMP-signals triggered by internalized G-protein-coupled receptors. *PLOS Biology*, 7(8):e1000172, August 2009.

[108] Sébastien Ferrandon, Timothy N Feinstein, Mariàn Castro, Bin Wang, Richard Bouley, John T Potts, Thomas J Gardella, and Jean-Pierre Vilardaga. Sustained cyclic AMP production by parathyroid hormone receptor endocytosis. *Nat Chem Biol*, 5 (10):734–742, October 2009.

[109] M J Lohse and D Calebiro. Cell biology: Receptor signals come in waves. *Nature*, March 2013.

[110] Roshanak Irannejad, Jin C Tomshine, Jon R Tomshine, Michael Chevalier, Jacob P Mahoney, Jan Steyaert, Soren G F Rasmussen, Roger K Sunahara, Hana El-Samad, Bo Huang, and Mark von Zastrow. Conformational biosensors reveal GPCR signalling from endosomes. *Nature*, 495(7442):534–538, March 2013.

[111] C W Stevens. The evolution of vertebrate opioid receptors. *Frontiers in bioscience: a journal and virtual library*, 2009.

[112] Horace H Loh, Hsien-Ching Liu, Antonella Cavalli, Wanling Yang, Yuh-Fung Chen, and Li-Na Wei. μ Opioid receptor knockout in mice: effects on ligand-induced analgesia and morphine lethality. *Molecular Brain Research*, 54(2):321–326, March 1998.

[113] I Sora, M Funada, and G R Uhl. The mu-opioid receptor is necessary for [D-Pen2,D-Pen5]enkephalin-induced analgesia. *European journal of pharmacology*, 324(2-3):R1–2, April 1997.

[114] P N Fuchs, C Roza, I Sora, G Uhl, and S N Raja. Characterization of mechanical withdrawal responses and effects of μ-, δ-and κ-opioid agonists in normal and μ-opioid receptor knockout mice. *Brain research*, 821(2):480–486, 1999.

[115] Maria Waldhoer, Selena E Bartlett, and Jennifer L Whistler. Opioid receptors. *Annu Rev Biochem*, 73:953–990, 2004.

[116] P Y Cheng, A L Svingos, and H Wang. Ultrastructural immunolabeling shows prominent presynaptic vesicular localization of delta-opioid receptor within both enkephalin-and nonenkephalin-containing .... *The Journal of ...*, 1995.

[117] C Qiu, I Sora, K Ren, G Uhl, and R Dubner. Enhanced δ-opioid receptor-mediated antinociception in μ-opioid receptor-deficient mice. *European journal of pharmacology*, 387(2):163–169, 2000.

[118] Y Zhu, M A King, A G Schuller, J F Nitsche, M Reidl, R P Elde, E Unterwald, G W Pasternak, and J E Pintar. Retention of supraspinal delta-like analgesia and loss of morphine tolerance in delta opioid receptor knockout mice. *Neuron*, 24(1):243–252, September 1999.

[119] D Filliol, S Ghozland, J Chluba, and M Martin. Mice deficient for δ-and μ-opioid receptors exhibit opposing alterations of emotional responses. *Nature*, 25(2):195–200, 2000.

[120] Frédéric Simonin, Olga Valverde, Claire Smadja, Susan Slowe, Ian Kitchen, Andrée Dierich, Marianne Le Meur, Bernard P Roques, Rafael Maldonado, and Brigitte L Kieffer. Disruption of the κ-opioid receptor gene in mice enhances sensitivity to chemical visceral pain, impairs pharmacological actions of the selective κ-agonist U-50,488H and attenuates morphine withdrawal. *EMBO J*, 17(4):886–897, February 1998.

[121] Gavril W Pasternak and Ying-Xian Pan. Mu opioids and their receptors: evolution of a concept. *Pharmacol Rev*, 65(4):1257–1317, 2013.

[122] Candace B Pert, G Pasternak, and Solomon H Snyder. Opiate agonists and antagonists discriminated by receptor binding in brain. *Science*, 1973.

[123] Lars Terenius. Stereospecific Interaction Between Narcotic Analgesics and a Synaptic Plasma Membrane Fraction of Rat Cerebral Cortex. *Acta pharmacologica et toxicologica*, 32(3-4):317–320, March 1973.

[124] Y Chen, A Mestek, J Liu, J A Hurley, and L Yu. Molecular cloning and functional expression of a mu-opioid receptor from rat brain. *Mol Pharmacol*, 44(1):8–12, July 1993.

[125] Michael J Kuhar, Candace B Pert, and Solomon H Snyder. Regional distribution of opiate receptor binding in monkey and human brain. *Nature*, 245(5426):447–450, October 1973.

[126] L Manara, G Bianchi, P Ferretti, and A Tavani. Inhibition of gastrointestinal transit by morphine in rats results primarily from direct drug action on gut opioid sites. *Journal of Pharmacology and . . .*, 1986.

[127] Wency Chen, Hsien-Hui Chung, and Juei-Tang Cheng. Opiate-induced constipation related to activation of small intestine opioid μ2-receptors. *World journal of gastroenterology*, 18(12):1391–1396, March 2012.

[128] Christoph Stein, Michael Schäfer, and Halina Machelska. Attacking pain at its source: new perspectives on opioids. *Nat Med*, 9(8):1003–1008, August 2003.

[129] L Pan, J Xu, R Yu, M M Xu, Y X Pan, and G W Pasternak. Identification and characterization of six new alternatively spliced variants of the human mu opioid receptor gene, Oprm. *Neuroscience*, 133(1):209–220, 2005.

[130] R M Eisenberg. TRIMU-5, a mu 2-opioid receptor agonist, stimulates the hypothalamo-pituitary-adrenal axis. *Pharmacology Biochemistry and Behavior*, 47(4):943–946, April 1994.

[131] Patrick Cadet, Kirk J Mantione, and George B Stefano. Molecular identification and functional expression of mu 3, a novel alternatively spliced variant of the human mu opiate receptor gene. *J Immunol*, 170(10):5118–5123, May 2003.

[132] B A Jordan and L A Devi. G-protein-coupled receptor heterodimerization modulates receptor function. *Nature*, 399(6737): 697–700, June 1999.

[133] Weijiao Huang, Aashish Manglik, A J Venkatakrishnan, Toon Laeremans, Evan N Feinberg, Adrian L Sanborn, Hideaki E Kato, Kathryn E Livingston, Thor S Thorsen, Ralf C Kling, Sébastien Granier, Peter Gmeiner, Stephen M Husbands, John R Traynor, William I Weis, Jan Steyaert, Ron O Dror, and Brian K Kobilka. Structural insights into mu-opioid receptor activation. *Nature*, 524(7565):315–+, 2015.

[134] Rémy Sounier, Camille Mas, Jan Steyaert, Toon Laeremans, Aashish Manglik, Weijiao Huang, Brian K Kobilka, Héléne

Déméné, and Sébastien Granier. Propagation of conformational changes during mu-opioid receptor activation. *Nature*, 524 (7565):375–+, 2015.

[135] S A Hussain, D Dey, S Chakraborty, and J Saha. Fluorescence Resonance Energy Transfer (FRET) sensor. *arXiv.org*, 2014.

[136] Theodor Förster. Zwischenmolekulare Energiewanderung Und Fluoreszenz. *Annalen Der Physik*, 2(1-2):55–75, 1948.

[137] D L Andrews. A unified theory of radiative and radiationless molecular energy transfer. *Chemical Physics*, 135(2):195–201, 1989.

[138] D L Andrews and D S Bradshaw. Virtual photons, dipole fields and energy transfer: a quantum electrodynamical approach. *European journal of physics*, 2004.

[139] L STRYER. Fluorescence Energy-Transfer as a Spectroscopic Ruler. *Annu Rev Biochem*, 47(1):819–846, 1978.

[140] Paul S Uster and Richard E Pagano. Resonance Energy-Transfer Microscopy - Observations of Membrane-Bound Fluorescent-Probes in Model Membranes and in Living Cells. *J Cell Biol*, 103(4):1221–1234, October 1986.

[141] Robert M Clegg. Chapter 1 Förster resonance energy transfer—FRET what is it, why do it, and how it's done A2 -. In *Fret and Flim Techniques*, pages 1–57. Elsevier, 2009.

[142] M Ormö, A B Cubitt, K Kallio, L A Gross, R Y Tsien, and S J Remington. Crystal structure of the Aequorea victoria green fluorescent protein. *Science*, 273(5280):1392–1395, September 1996.

[143] D C Prasher, V K Eckenrode, W W Ward, F G Prendergast, and M J Cormier. Primary structure of the Aequorea victoria green-fluorescent protein. *Gene*, 111(2):229–233, February 1992.

[144] M Chalfie, Y Tu, G Euskirchen, W W Ward, and D C Prasher. Green fluorescent protein as a marker for gene expression. *Science*, 263(5148):802–805, February 1994.

[145] J van Unen, J Woolard, A Rinken, C Hoffmann, S J Hill, J Goedhart, M R Bruchas, M Bouvier, and M J W Adjobo-Hermans. A Perspective on Studying G-Protein-Coupled Receptor Signaling with Resonance Energy Transfer Biosensors in Living Organisms. *Mol Pharmacol*, 88(3):589–595, July 2015.

[146] Marta Fernández-Suárez and Alice Y Ting. Fluorescent probes for super-resolution imaging in living cells. *Nature reviews. Molecular cell biology*, 9(12):929–943, December 2008.

[147] Carsten Hoffmann, Guido Gaietta, Moritz Bünemann, Stephen R Adams, Silke Oberdorff-Maass, Björn Behr, Jean-Pierre Vilardaga, Roger Y Tsien, Mark H Ellisman, and Martin J Lohse. A FlAsH-based FRET approach to determine G protein-coupled receptor activation in living cells. *Nat Methods*, 2(3): 171–176, March 2005.

[148] Kevin D G Pfleger and Karin A Eidne. Illuminating insights into protein-protein interactions using bioluminescence resonance energy transfer (BRET). *Nat Methods*, 3(3):165–174, March 2006.

[149] Nicolas Boute, Ralf Jockers, and Tarik Issad. The use of resonance energy transfer in high-throughput screening: BRET versus FRET. *Trends Pharmacol Sci*, 23(8):351–354, August 2002.

[150] S Angers, A Salahpour, E Joly, S Hilairet, D Chelsky, M Dennis, and M Bouvier. Detection of beta 2-adrenergic receptor dimerization in living cells using bioluminescence resonance energy transfer (BRET). *Proc Natl Acad Sci U S A*, 97(7):3684–3689, March 2000.

[151] Viacheslav O Nikolaev, Moritz Bünemann, Lutz Hein, Annette Hannawacker, and Martin J Lohse. Novel single chain cAMP sensors for receptor-induced signal propagation. *J Biol Chem*, 279(36):37215–37218, September 2004.

[152] James W Wisler, Scott M DeWire, Erin J Whalen, Jonathan D Violin, Matthew T Drake, Seungkirl Ahn, Sudha K Shenoy, and Robert J Lefkowitz. A unique mechanism of beta-blocker action: Carvedilol stimulates beta-arrestin signaling. *Proc Natl Acad Sci U S A*, 104(42):16657–16662, 2007.

[153] Christian Doll, Jens Konietzko, Florian Pöll, Thomas Koch, Volker Höllt, and Stefan Schulz. Agonist-selective patterns of μ-opioid receptor phosphorylation revealed by phosphosite-specific antibodies. *Br J Pharmacol*, 164(2):298–307, August 2011.

[154] Arsalan Yousuf, Elke Miess, Setareh Sianati, Yan-Ping Du, Stefan Schulz, and Macdonald Christie. The Role of Phosphorylation Sites in Desensitization of μ-Opioid Receptor. *Mol Pharmacol*, page mol.115.098244, May 2015.

[155] Stefanie Blättermann, Lucas Peters, Philipp Aaron Ottersbach, Andreas Bock, Viktoria Konya, C David Weaver, Angel Gonzalez, Ralf Schröder, Rahul Tyagi, Petra Luschnig, Jürgen Gäb, Stephanie Hennen, Trond Ulven, Leonardo Pardo, Klaus Mohr, Michael Gütschow, Akos Heinemann, and Evi Kostenis. A biased ligand for OXE-R uncouples Gα and G$\beta\gamma$ signaling within a heterotrimer. *Nat Chem Biol*, 8(7):631–638, July 2012.

[156] Gayathri Swaminath, Yang Xiang, Tae Weon Lee, Jacqueline Steenhuis, Charles Parnot, and Brian K Kobilka. Sequential binding of agonists to the beta2 adrenoceptor. Kinetic evidence for intermediate conformational states. *J Biol Chem*, 279(1):686–691, January 2004.

[157] Jeffrey J Liu, Reto Horst, Vsevolod Katritch, Raymond C Stevens, and Kurt Wüthrich. Biased signaling pathways in β2-adrenergic receptor characterized by 19F-NMR. *Science*, 335 (6072):1106–1110, March 2012.

[158] Rie Nygaard, Yaozhong Zou, Ron O Dror, Thomas J Mildorf, Daniel H Arlow, Aashish Manglik, Albert C Pan, Corey W Liu, Juan José Fung, Michael P Bokoch, Foon Sun Thian, Tong Sun Kobilka, David E Shaw, Luciano Mueller, R Scott Prosser, and Brian K Kobilka. The dynamic process of β(2)-adrenergic receptor activation. *Cell*, 152(3):532–542, January 2013.

[159] Xavier Deupi and Brian K Kobilka. Energy landscapes as a tool to integrate GPCR structure, dynamics, and function. *Physiology (Bethesda, Md.)*, 25(5):293–303, October 2010.

[160] Karen J Gregory, Nathan E Hall, Andrew B Tobin, Patrick M Sexton, and Arthur Christopoulos. Identification of orthosteric and allosteric site mutations in M2 muscarinic acetylcholine receptors that contribute to ligand-selective signaling bias. *Journal of Biological Chemistry*, 285(10):7459–7474, March 2010.

[161] Katherine W Figueroa, Michael T Griffin, and Frederick J Ehlert. Selectivity of agonists for the active state of M1 to M4 muscarinic receptor subtypes. *The Journal of pharmacology and experimental therapeutics*, 328(1):331–342, January 2009.

[162] Michael T Griffin, Katherine W Figueroa, Sarah Liller, and Frederick J Ehlert. Estimation of agonist activity at G protein-coupled receptors: analysis of M2 muscarinic receptor signaling through Gi/o,Gs, and G15. *Journal of Pharmacology and Experimental Therapeutics*, 321(3):1193–1207, June 2007.

[163] Terry Kenakin. Functional selectivity through protean and biased agonism: who steers the ship? *Mol Pharmacol*, 72(6):1393–1401, December 2007.

[164] James Whyte Black and Paul Leff. Operational models of pharmacological agonism. *Proceedings of the Royal Society of London. Series B, Biological sciences*, 220(1219):141–162, December 1983.

[165] S Rajagopal, S Ahn, D H Rominger, W Gowen-MacDonald, C M Lam, S M DeWire, J D Violin, and Robert J Lefkowitz. Quantifying Ligand Bias at Seven-Transmembrane Receptors. *Mol Pharmacol*, 80(3):367–377, August 2011.

[166] Terry Kenakin, Christian Watson, Vanessa Muniz-Medina, Arthur Christopoulos, and Steven Novick. A Simple Method for Quantifying Functional Selectivity and Agonist Bias. *ACS Chemical Neuroscience*, 3(3):193–203, March 2012.

[167] Terry Kenakin and Arthur Christopoulos. Measurements of ligand bias and functional affinity. *Nature reviews. Drug discovery*, 12(6):483–483, June 2013.

[168] Sudarshan Rajagopal. Quantifying biased agonism: understanding the links between affinity and efficacy. *Nature reviews. Drug discovery*, 12(6):483–483, June 2013.

[169] James W Wisler, Kunhong Xiao, Alex R B Thomsen, and Robert J Lefkowitz. Recent developments in biased agonism. *Current opinion in cell biology*, 27:18–24, April 2014.

[170] Keshava Rajagopal, Erin J Whalen, Jonathan D Violin, Jonathan A Stiber, Paul B Rosenberg, Richard T Premont, Thomas M Coffman, Howard A Rockman, and Robert J Lefkowitz. beta-arrestin2-mediated inotropic effects of the angiotensin II type 1A receptor in isolated cardiac myocytes. *Proc Natl Acad Sci U S A*, 103(44):16284–16289, 2006.

[171] Guido Boerrigter, Michael W Lark, Erin J Whalen, David G Soergel, Jonathan D Violin, and John C Burnett. Cardiorenal actions of TRV120027, a novel ß-arrestin-biased ligand at the angiotensin II type I receptor, in healthy and heart failure canines: a novel therapeutic strategy for acute heart failure. *Circulation. Heart failure*, 4(6):770–778, November 2011.

[172] G Michael Felker, Javed Butler, Sean P Collins, Gad Cotter, Beth A Davison, Justin A Ezekowitz, Gerasimos Filippatos, Phillip D Levy, Marco Metra, Piotr Ponikowski, David G Soergel, John R Teerlink, Jonathan D Violin, Adriaan A Voors, and Peter S Pang. Heart Failure Therapeutics on the Basis of a Biased Ligand of the Angiotensin-2 Type 1 Receptor. *JACC: Heart Failure*, 3(3):193–201, March 2015.

[173] L M Bohn, Robert J Lefkowitz, R R Gainetdinov, and K Peppel. Enhanced morphine analgesia in mice lacking β-arrestin 2. *Science*, 286(2495):2495–2498, 1999.

[174] Kirsten M Raehal, Julia K L Walker, and Laura M Bohn. Morphine side effects in beta-arrestin 2 knockout mice. *Journal of Pharmacology and Experimental Therapeutics*, 314(3):1195–1201, September 2005.

[175] Scott M DeWire, Dennis S Yamashita, David H Rominger, Guodong Liu, Conrad L Cowan, Thomas M Graczyk, Xiao-Tao

Chen, Philip M Pitis, Dimitar Gotchev, Catherine Yuan, Michael Koblish, Michael W Lark, and Jonathan D Violin. A G protein-biased ligand at the μ-opioid receptor is potently analgesic with reduced gastrointestinal and respiratory dysfunction compared with morphine. *The Journal of pharmacology and experimental therapeutics*, 344(3):708–717, March 2013.

[176] R Medzhitov, P PrestonHurlburt, and C A Janeway. A human homologue of the Drosophila Toll protein signals activation of adaptive immunity. *Nature*, 388(6640):394–397, 1997.

[177] Sky W Brubaker, Kevin S Bonham, Ivan Zanoni, and Jonathan C Kagan. Innate Immune Pattern Recognition: A Cell Biological Perspective. *Annual Review of Immunology*, 33(1):257–290, March 2015.

[178] R Shimazu, S Akashi, H Ogata, Y Nagai, K Fukudome, K Miyake, and M Kimoto. MD-2, a molecule that confers lipopolysaccharide responsiveness on Toll-like receptor 4. *Journal of Experimental Medicine*, 189(11):1777–1782, 1999.

[179] Fabio Re and Jack L Strominger. Monomeric recombinant MD-2 binds toll-like receptor 4 tightly and confers lipopolysaccharide responsiveness. *J Biol Chem*, 277(26):23427–23432, June 2002.

[180] Taro Kawai and Shizuo Akira. The role of pattern-recognition receptors in innate immunity: update on Toll-like receptors. *Nature Publishing Group*, 11(5):373–384, May 2010.

[181] Masahiro Yamamoto, Shintaro Sato, Hiroaki Hemmi, Hideki Sanjo, Satoshi Uematsu, Tsuneyasu Kaisho, Katsuaki Hoshino, Osamu Takeuchi, Masaya Kobayashi, Takashi Fujita, Kiyoshi Takeda, and Shizuo Akira. Essential role for TIRAP in activation of the signalling cascade shared by TLR2 and TLR4. *Nature*, 420(6913):324–329, November 2002.

[182] Irit Nachtigall, Andrey Tamarkin, Sascha Tafelski, Andreas Weimann, Andreas Rothbart, Susanne Heim, Klaus D Wernecke, and Claudia Spies. Polymorphisms of the toll-like receptor 2 and 4 genes are associated with faster progression and a more severe course of sepsis in critically ill patients. *The Journal of international medical research*, 42(1):93–110, February 2014.

[183] E Lorenz, J P Mira, K L Frees, and D A Schwartz. Relevance of mutations in the TLR4 receptor in patients with gram-negative septic shock. *Archives of internal medicine*, 162(9):1028–1032, 2002.

[184] Nicolas WJ Schröder and Ralf R Schumann. Single nucleotide polymorphisms of Toll-like receptors and susceptibility to infec-

tious disease. *The Lancet Infectious Diseases*, 5(3):156–164, March 2005.

[185] Flobert Y Tanga, Nancy Nutile-McMenemy, and Joyce A DeLeo. The CNS role of Toll-like receptor 4 in innate neuroimmunity and painful neuropathy. *Proc Natl Acad Sci U S A*, 102(16):5856–5861, April 2005.

[186] Mark R Hutchinson, Yingning Zhang, Kimberley Brown, Benjamen D Coats, Mitesh Shridhar, Paige W Sholar, Sonica J Patel, Nicole Y Crysdale, Jacqueline A Harrison, Steven F Maier, Kenner C Rice, and Linda R Watkins. Non-stereoselective reversal of neuropathic pain by naloxone and naltrexone: involvement of toll-like receptor 4 (TLR4). *Eur J Neurosci*, 28(1):20–29, July 2008.

[187] S S Lewis, Mark R Hutchinson, N Rezvani, L C Loram, Y Zhang, S F Maier, K C Rice, and L R Watkins. Evidence that intrathecal morphine-3-glucuronide may cause pain enhancement via toll-like receptor 4/MD-2 and interleukin-1beta. *Neuroscience*, 165 (2):569–583, January 2010.

[188] X Wang, L C Loram, K Ramos, A J de Jesus, J Thomas, K Cheng, A Reddy, A A Somogyi, Mark R Hutchinson, L R Watkins, and H Yin. Morphine activates neuroinflammation in a manner parallel to endotoxin. 109(16):6325–6330, April 2012.

[189] Mark R Hutchinson, Yingning Zhang, Mitesh Shridhar, John H Evans, Madison M Buchanan, Tina X Zhao, Peter F Slivka, Benjamen D Coats, Niloofar Rezvani, Julie Wieseler, Travis S Hughes, Kyle E Landgraf, Stefanie Chan, Stephanie Fong, Simon Phipps, Joseph J Falke, Leslie A Leinwand, Steven F Maier, Hang Yin, Kenner C Rice, and Linda R Watkins. Evidence that opioids may have toll-like receptor 4 and MD-2 effects. *Brain Behav Immun*, 24(1):83–95, January 2010.

[190] C Stevens, S Aravind, S Das, and R Davis. Pharmacological characterization of LPS and opioid interactions at the toll-like receptor 4. *Br J Pharmacol*, 168(6):1421–1429, March 2013.

[191] Phil Skolnick, Hirsch Davis, Derrick Arnelle, and Daniel Deaver. Translational potential of naloxone and naltrexone as TLR4 antagonists. *Trends Pharmacol Sci*, 35(9):431–432, September 2014.

[192] Naomi Misawa, A K M Kafi, Mitsuru Hattori, Kenji Miura, Kenji Masuda, and Takeaki Ozawa. Rapid and high-sensitivity cell-based assays of protein-protein interactions using split click beetle luciferase complementation: an approach to the study of G-protein-coupled receptors. *Analytical chemistry*, 82(6):2552–2560, March 2010.

[193] Caroline A Schneider, Wayne S Rasband, and Kevin W Eliceiri. NIH Image to ImageJ: 25 years of image analysis. *Nat Methods*, 9(7):671–675, July 2012.

[194] Johannes Schindelin, Curtis T Rueden, Mark C Hiner, and Kevin W Eliceiri. The ImageJ ecosystem: An open platform for biomedical image analysis. *Molecular reproduction and development*, 82(7-8):518–529, July 2015.

[195] Johannes Schindelin, Ignacio Arganda-Carreras, Erwin Frise, Verena Kaynig, Mark Longair, Tobias Pietzsch, Stephan Preibisch, Curtis Rueden, Stephan Saalfeld, Benjamin Schmid, Jean-Yves Tinevez, Daniel James White, Volker Hartenstein, Kevin Eliceiri, Pavel Tomancak, and Albert Cardona. Fiji: an open-source platform for biological-image analysis. *Nat Methods*, 9(7):676–682, July 2012.

[196] Joachim Goedhart, Laura van Weeren, Merel J W Adjobo-Hermans, Ies Elzenaar, Mark A Hink, and Theodorus W J Gadella. Quantitative co-expression of proteins at the single cell level - application to a multimeric FRET sensor. *PLoS One*, 6(11):e27321, 2011.

[197] Nadine Frölich, Christian Dees, Christian Paetz, Xuan Ren, Martin J Lohse, Viacheslav O Nikolaev, and Meinhart H Zenk. Distinct pharmacological properties of morphine metabolites at G(i)-protein and β-arrestin signaling pathways activated by the human μ-opioid receptor. *Biochemical pharmacology*, 81(10):1248–1254, May 2011.

[198] Y Yu, L Zhang, X Yin, H Sun, G R Uhl, and J B Wang. Mu opioid receptor phosphorylation, desensitization, and ligand efficacy. *J Biol Chem*, 272(46):28869–28874, November 1997.

[199] P A Zaki, D E Keith, G A Brine, F I Carroll, and C J Evans. Ligand-induced changes in surface mu-opioid receptor number: Relationship to G protein activation? *Journal of Pharmacology and Experimental Therapeutics*, 292(3):1127–1134, March 2000.

[200] M J Clark, Mary J Clark, Cheryse A Furman, Timra D Gilson, and John R Traynor. Comparison of the relative efficacy and potency of mu-opioid agonists to activate Galpha(i/o) proteins containing a pertussis toxin-insensitive mutation. *Journal of Pharmacology and Experimental Therapeutics*, 317(2):858–864, May 2006.

[201] Jamie McPherson, Guadalupe Rivero, Myma Baptist, Javier Llorente, Suleiman Al-Sabah, Cornelius Krasel, William L

Dewey, Chris P Bailey, Elizabeth M Rosethorne, Steven J Charlton, Graeme Henderson, and Eamonn Kelly. μ-opioid receptors: correlation of agonist efficacy for signalling with ability to activate internalization. *Mol Pharmacol*, 78(4):756–766, October 2010.

[202] Paola Molinari, Vanessa Vezzi, Maria Sbraccia, Cristina Grò, Daniela Riitano, Caterina Ambrosio, Ida Casella, and Tommaso Costa. Morphine-like opiates selectively antagonize receptor-arrestin interactions. *Journal of Biological Chemistry*, 285(17): 12522–12535, April 2010.

[203] Peng Huang, George B Kehner, Alan Cowan, and Lee-Yuan Liu-Chen. Comparison of Pharmacological Activities of Buprenorphine and Norbuprenorphine: Norbuprenorphine Is a Potent Opioid Agonist. *Journal of Pharmacology and Experimental Therapeutics*, 297(2):688–695, May 2001.

[204] Donna A Volpe, Grainne A McMahon Tobin, R Daniel Mellon, Aspandiar G Katki, Robert J Parker, Thomas Colatsky, Timothy J Kropp, and S Leigh Verbois. Uniform assessment and ranking of opioid μ receptor binding constants for selected opioid drugs. *Regulatory toxicology and pharmacology : RTP*, 59(3): 385–390, April 2011.

[205] Sarah A Nickolls, Alison Waterfield, Rachael E Williams, and Ross A Kinloch. Understanding the effect of different assay formats on agonist parameters: a study using the μ-opioid receptor. *Journal of biomolecular screening*, 16(7):706–716, August 2011.

[206] C Sternini, M Spann, B Anton, D E Keith, N W Bunnett, M von-Zastrow, C Evans, and N C Brecha. Agonist-selective endocytosis of mu opioid receptor by neurons in vivo. *Proc Natl Acad Sci U S A*, 93(17):9241–9246, 1996.

[207] D E Keith, S R Murray, P A Zaki, P C Chu, D V Lissin, L Kang, C J Evans, and M von Zastrow. Morphine activates opioid receptors without causing their rapid internalization. *J Biol Chem*, 271(32):19021–19024, August 1996.

[208] L M Bohn, L A Dykstra, Robert J Lefkowitz, M G Caron, and L S Barak. Relative opioid efficacy is determined by the complements of the G protein-coupled receptor desensitization machinery. *Mol Pharmacol*, 66(1):106–112, July 2004.

[209] Georgina L Thompson, J Robert Lane, Thomas Coudrat, Patrick M Sexton, Arthur Christopoulos, and Meritxell Canals. Biased Agonism of Endogenous Opioid Peptides at the μ-Opioid Receptor. *Mol Pharmacol*, 88(2):335–346, August 2015.

[210] Sascha Just, Susann Illing, Michelle Trester-Zedlitz, Elaine K Lau, Sarah J Kotowski, Elke Miess, Anika Mann, Christian Doll, Jonathan C Trinidad, Alma L Burlingame, Mark von Zastrow, and Stefan Schulz. Differentiation of Opioid Drug Effects by Hierarchical Multi-Site Phosphorylation. *Mol Pharmacol*, 83(3): 633–639, March 2013.

[211] David Winpenny, Mellissa Clark, and Darren Cawkill. Biased ligand quantification in drug discovery: from theory to high throughput screening to identify New biased μ opioid receptor agonists. *Br J Pharmacol*, pages n/a–n/a, January 2016.

[212] Yuting Li, Xing Liu, Chang Liu, Jiuhong Kang, Jingyu Yang, Gang Pei, and Chunfu Wu. Improvement of morphine-mediated analgesia by inhibition of β-arrestin2 expression in mice periaqueductal gray matter. *International journal of molecular sciences*, 10(3):954–963, March 2009.

[213] C H Yang, H W Huang, K H Chen, Y S Chen, S M Sheen-Chen, and C R Lin. Antinociceptive potentiation and attenuation of tolerance by intrathecal β-arrestin 2 small interfering RNA in rats. *British Journal of Anaesthesia*, 107(5):774–781, November 2011.

[214] C E Groer, K Tidgewell, R A Moyer, W W Harding, R B Rothman, T E Prisinzano, and L M Bohn. An Opioid Agonist that Does Not Induce μ-Opioid Receptor—Arrestin Interactions or Receptor Internalization. *Mol Pharmacol*, 71(2):549–557, February 2007.

[215] David G Soergel, Ruth Ann Subach, Nancy Burnham, Michael W Lark, Ian E James, Brian M Sadler, Franck Skobieranda, Jonathan D Violin, and Lynn R Webster. Biased agonism of the μ-opioid receptor by TRV130 increases analgesia and reduces on-target adverse effects versus morphine: A randomized, double-blind, placebo-controlled, crossover study in healthy volunteers. *Pain*, 155(9):1829–1835, September 2014.

[216] X Fan, J Zhang, X Zhang, W Yue, and L Ma. Acute and chronic morphine treatments and morphine withdrawal differentially regulate GRK2 and GRK5 gene expression in rat brain. *Neuropharmacology*, 43(5):809–816, October 2002.

[217] Cullen L Schmid, Nicole M Kennedy, Nicolette C Ross, Kimberly M Lovell, Zhizhou Yue, Jenny Morgenweck, Michael D Cameron, Thomas D Bannister, and Laura M Bohn. Bias Factor and Therapeutic Window Correlate to Predict Safer Opioid Analgesics. *Cell*, 171(5):1165–1175.e13, November 2017.

[218] Mark R Hutchinson, A L Northcutt, T Hiranita, X Wang, S S Lewis, J Thomas, K van Steeg, T A Kopajtic, L C Loram, C Sfregola, E Galer, N E Miles, S T Bland, J Amat, R R Rozeske, T Maslanik, T R Chapman, K A Strand, M Fleshner, R K Bachtell, A A Somogyi, H Yin, J L Katz, K C Rice, S F Maier, and L R Watkins. Opioid activation of toll-like receptor 4 contributes to drug reinforcement. *J Neurosci*, 32(33):11187–11200, August 2012.

[219] X Wang, Y Zhang, Y Peng, Mark R Hutchinson, K C Rice, H Yin, and L R Watkins. Pharmacological characterization of the opioid inactive isomers (+)-naltrexone and (+)-naloxone as Toll-like receptor 4 antagonists. *Br J Pharmacol*, November 2015.

[220] Linda R Watkins, Xiaohui Wang, Sanam Mustafa, and Mark R Hutchinson. In vivo veritas: (+)-Naltrexone's actions define translational importance: A letter in response to Skolnick et al. 'Translational potential of naloxone and naltrexone as TLR4 antagonists'. *Trends Pharmacol Sci*, 35(9):432–433, September 2014.

[221] Jakobus van Unen, Anette D Stumpf, Benedikt Schmid, Nathalie R Reinhard, Peter L Hordijk, Carsten Hoffmann, Theodorus W J Gadella, and Joachim Goedhart. A New Generation of FRET Sensors for Robust Measurement of Gαi1, Gαi2 and Gαi3 Activation Kinetics in Single Cells. *PLoS One*, 11(1): e0146789, 2016.

[222] Edward L Stahl, Lei Zhou, Frederick J Ehlert, and Laura M Bohn. A novel method for analyzing extremely biased agonism at G protein-coupled receptors. *Mol Pharmacol*, 87(5):866–877, May 2015.

AFFIDAVIT

I hereby confirm that my thesis entitled "Molecular Signaling Mechanisms at the μ-Opioid Receptor " is the result of my own work. I did not receive any help or support from commercial consultants. All sources and/or materials applied are listed and specified in the thesis.
Furthermore, I confirm that this thesis has not yet been submitted as part of another examination process neither in identical nor in similar form.

Hiermit erkläre ich an Eides statt, die Dissertation "Molekulare Signalmechanismen am μ-Opioidrezeptor " eigenständig, d.h. insbesondere selbstständig und ohne Hilfe eines kommerziellen Promotionsberaters angefertigt und keine anderen als die von mir angegebenen Quellen und Hilfsmittel verwendet zu haben.
Ich erkläre weiterhin, dass die Dissertation weder in gleicher noch in ähnlicher Form bereits in einem anderen Prüfungsverfahren vorgelegen hat.

Würzburg, September 2018

Dr. med. Benedikt Schmid